# Optimized resource allocation and user/cell association for future dense networks

Duc Thang Ha

université PARIS-SACLAY

UNIVERSITÉ PARIS SUD
Comprendre le monde, construire l'avenir

NNT : 2019SACLS290

Thèse de doctorat

# Allocation de ressources et association utilisateur/cellule optimisées pour les futurs réseaux denses

Thèse de doctorat de l'Université Paris-Saclay
préparée à l'Université Paris-Sud

École doctorale n°580 Sciences et technologies de l'information et de la communication (STIC)
Spécialité de doctorat : Réseaux, information et communications

Thèse présentée et soutenue à Orsay, le 30-9-2019, par

**DUC THANG HA**

Composition du Jury :

| | |
|---|---|
| Xavier Lagrange<br>Professeur, IMT Atlantique (Département Systèmes Réseaux, Cybersécurité et Droit du numérique / IRISA Adopnet) | Président |
| Nadjib Ait Saadi<br>Professeur, Engineering School ESIEE Paris (Laboratory of Computer Science Gaspard-Monge - LIGM / CNRS) | Rapporteur |
| Mylène Pischella<br>Maître de conférences, Conservatoire National des Arts et Métiers - CNAM (Electronics, Control Engineering and Systems department (EASY) & CEDRIC/LAETITIA) | Rapporteur |
| Megumi Kaneko<br>Associate Professor, National Institute of Informatics - NII Tokyo (Information Systems Architecture Science Research Division) | Examinateur |
| Lila Boukhatem<br>Maître de Conférences, Université Paris-Sud (Laboratoire de Recherche en Informatique - LRI) | Directeur de thèse |
| Steven Martin<br>Professeur des Universités, Université Paris-Sud (Laboratoire de Recherche en Informatique - LRI) | Co-directeur de thèse |

# Contents

# List of Tables

# List of Figures

# Acronyms

**ABUC** Adaptive Beamforming and User Clustering.

**BBU** Baseband Unit.

**BF** Beamforming.

**CapEx** Capital Expenditure.

**CPRI** Common Public Radio Interface.

**CRAN** Cloud Radio Access Network.

**CRRA** Cooperative Radio Resource Allocation.

**CSI** Channel State Information.

**D2D** Devices-to-Devices.

**DQL** Deep Q-learning.

**DRL** Deep reinforcement learning.

**EE** Energy Efficiency.

**H-CRAN** Heterogeneous-Cloud Radio Access Network.

**HPN** High Power Node.

**IC** Interference Collaboration.

**IoT** Internet of Things.

**LPN** Low Power Node.

**LS-CSSP** Large-Scale Cooperative Spatial Signal Processing.

**LSCP** Large-scale Collaborative processing.

**LSTM** Long Short Term Memory.

**MABUC** Mobility-Aware Beamforming and User Clustering.

**MIMO** Multiple-Input-Multiple-Output.

**MINLP** Mixed Integer Nonlinear Programming.

**OpEx** Operating Expense.

**POMDP** Partially observable Markov decision process.

**QoS** Quality of Service.

**RL** Reinforcement Learning.

**RRH** Remote Radio Head.

**SE** Spectral Efficiency.

**UE** User Equipment.

**WMMSE** Weighted Minimum Mean Square Error.

**WSR** Weighted Sum-rate.

**ZFBF** Zero-Forcing Beamforming.

# Abstract

Recently, mobile operators have been challenged by a tremendous growth in mobile data traffic. In such a context, Cloud Radio Access Network (CRAN) has been considered as a novel architecture for future wireless networks. The radio frequency signals from geographically distributed antennas are collected by Remote Radio Heads (RRHs) and transmitted to the cloud-centralized Baseband Units (BBUs) pool through fronthaul links. This centralized architecture enables a global optimization of joint baseband signal processing and radio resource management functions for all RRHs and users.

At the same time, Heterogeneous Networks (HetNets) have emerged as another core feature for 5G network to enhance the capacity/coverage while saving energy consumption. Small cells deployment helps to shorten the wireless links to end-users and thereby improving the link quality in terms of spectrum efficiency (SE) as well as energy efficiency (EE). Therefore, combining both cloud computing and HetNet advantages results in the so-called Heterogeneous-Cloud Radio Access Networks (H-CRAN) which is regarded as one of the most promising network architectures to meet 5G and beyond system requirements.

In this context, we address the crucial issue of beamforming and user-to-RRH association (user clustering) in the downlink of H-CRANs. We formulate this problem as a sum-rate maximization problem under the assumption of mobility and CSI (Channel State Information) imperfectness. Our main challenge is to design a framework that can achieve sum-rate maximization while, unlike other traditional reference solutions, being able to alleviate the computational complexity, CSI feedback and reassociation signaling costs under various mobility environments. Such gain helps in reducing the control and feedback overhead and in turn improve the uplink throughput.

Our study begins by proposing a simple yet effective algorithm baptized Hybrid algorithm that periodically activates dynamic and static clustering schemes to balance between the optimality of the beamforming and association solutions while being aware of practical system constraints (complexity and signaling overhead). Hybrid algorithm considers time dimension of the allocation and scheduling process rather than its optimality (or suboptimality) for the sole current scheduling frame. Moreover, we provide a cost analysis of the algorithm in terms of several parameters to better comprehend the trade-off among the numerous dimensions involved in the allocation process.

The second key contribution of our thesis is to tackle the beamforming and clustering problem from a mobility perspective. Two enhanced variants of the Hybrid algorithm are proposed: ABUC (Adaptve Beamforming and User Clustering), a mobility-aware version that is fit to the distinctive features of channel variations, and MABUC (Mobility-Aware Beamforming and User Clustering), an advanced version of the algorithm that tunes dynamically the feedback scheduling parameters (CSI feedback type and periodicity) in accordance with individual user velocity. MABUC algorithm achieves a targeted sum-rate performance while supporting the complexity and CSI signaling costs to a minimum.

In our last contribution, we propose to go further in the optimization of the CSI feedback scheduling parameters. To do so, we take leverage of reinforcement learning (RL) tool to optimize on-the-fly the feedback scheduling parameters according to each user mobility profile. More specifically, we propose two RL models, one based on Q-learning and a second based on Deep Q-learning algorithm formulated as a POMDP (Partially observable Markov decision process). Simulation results show the effectiveness of our proposed framework, as it enables to select the best feedback parameters tailored to each user mobility profile, even in the difficult case where each user has a different mobility profile.

**Keywords**: 5G, H-CRAN, beamforming, user-to-cell association, imperfect CSI, mobility, reinforcement learning.

# Résumé

Depuis plusieurs années, les opérateurs de téléphonie mobile sont confrontés à une croissance considérable du trafic de données mobiles. Dans un tel contexte, la technologie Cloud Radio Access Network (CRAN) qui intègre les solutions de Cloud Computing aux réseaux d'accès radio est considérée comme une nouvelle architecture pour les futures générations de réseaux 5G. Dans un réseau CRAN, les signaux des utilisateurs sont collectés par des antennes géographiquement réparties appelées Remote Radio Heads (RRH) et transmis à une unité de traitement centralisée dans le cloud (BBU : Baseband Unit) via des liaisons fronthaul. L'approche CRAN permet une optimisation globale des fonctions de traitement en bande de base du signal et de la gestion des ressources radio pour l'ensemble des RRH et des utilisateurs.

Parallèlement, les réseaux hétérogènes (HetNets) ont été proposés pour augmenter efficacement la capacité et la couverture du réseau 5G tout en réduisant la consommation énergétique. Les réseaux HetNets préconisent le déploiement dense de petites cellules au plus proche des utilisateurs afin d'améliorer la qualité de la liaison et par conséquent l'efficacité spectrale (ES) et l'efficacité énergétique (EE). En combinant les avantages du Cloud avec ceux des réseaux HetNets, le concept de réseaux H-CRAN (Heterogeneous Cloud Radio Access Networks) est né et est considéré comme l'une des architectures les plus prometteuses pour répondre aux exigences des futures systèmes de télécommunications.

C'est dans ce contexte complexe que s'inscrivent nos travaux de thèse. Plus particulièrement, nous abordons le problème important de l'optimisation jointe de l'association utilisateur-RRH (appelée aussi clustering) et de la solution de beamforming sur la liaison descendante d'un système H-CRAN. Nous formulons le problème comme un problème de maximisation du débit total du système sous des contraintes de mobilité et d'imperfection de CSI (Channel State Information).

Notre principal défi consiste à concevoir une solution capable de maximiser le débit tout en permettant, contrairement aux autres solutions de référence, de réduire la complexité de calcul, et les coûts de signalisation et de feedback CSI dans divers environnements où la mobilité utilisateur est prise en compte.

Notre étude commence par proposer un algorithme simple mais efficace, baptisé algorithme Hybride, qui active périodiquement des schémas de clustering dynamiques et statiques pour aboutir à un compromis satisfaisant entre optimalité du beamforming et de l'association utilisateur-RRH (offerte par le clustering dynamique) et le coût en complexité et signalisation CSI et réassociation (réduites grâce au clustering statique). L'originalité de l'algorithme Hybride, comparé aux autres solutions de la littérature, réside aussi dans sa prise en compte de la dimension temporelle du processus d'allocation (Clustering et beamforming) sur plusieurs trames successives plutôt que son optimalité (ou sous-optimalité) pour la seule trame d'ordonnancement courante. De plus, nous développons une analyse des coûts de l'algorithme en fonction de plusieurs critères (complexité et signalisation) afin de mieux appréhender le compromis entre les nombreux paramètres impliqués.

La deuxième contribution de la thèse s'intéresse au problème de beamforming et de clustering sous la perspective de la mobilité utilisateur. Deux variantes améliorées de l'algorithme Hybride sont proposées : ABUC (Adaptive Beamforming et User Clustering), une version adaptée à la mobilité des utilisateurs et aux variations du canal radio, et MABUC (Mobility-Aware Beamforming et User Clustering), une version améliorée qui règle dynamiquement les paramètres de feedback du CSI (périodicité et type de CSI) en fonction de la vitesse de l'utilisateur. L'algorithme MABUC offre de très bonnes performances en termes de débit cible tout en réduisant efficacement la complexité et les coûts de signalisation CSI.

Dans la dernière contribution de la thèse, nous approfondissons l'étude en explorant l'optimisation automatique des paramètres d'ordonnancement du CSI. Pour ce faire, nous exploitons l'outil de l'apprentissage par renforcement (Reinforcement Learning - RL) afin d'optimiser à la volée les paramètres de feedback CSI (périodicité et type) en fonction du profil de mobilité individuelle des utilisateurs. Plus spécifiquement, nous proposons deux modèles d'apprentissage par renforcement. Le premier modèle basé sur un algorithme de type Q-learning a permis de démontrer l'efficacité de l'approche dans un scénario à taille réduite. Le second modèle, plus scalable car basé sur une approche de type Deep Q-learning,

a été formulé sous la forme d'un processus de type POMDP (Partially observable Markov decision process). Les résultats de la simulation montrent l'efficacité des solutions proposées qui permettent de sélectionner les paramètres de feedback les plus adaptés à chaque profil de mobilité utilisateur, même dans le cas complexe où chaque utilisateur possède un profil de mobilité différent et variable dans le temps.

**Keywords**: 5G, H-CRAN, beamforming, association utilisateur-cellule, imperfection de CSI, mobilité, apprentissage par renforcement.

# Chapter 1

# Introduction

## 1.1 Background

Next generation of mobile and wireless communications system (5G) is transforming the way people communicate and extending the boundaries of the wireless industry. 5G will move beyond networks that are purpose-built for mobile broadband alone, toward systems that connect far more different types of devices at different speeds. The Internet of Things (IoT) is one of the primary contributors to global mobile traffic growth and this progression will lead to a huge mobile and wireless traffic volume predicted to increase a thousand-fold over the next decade [GJ15]. Besides sustaining the tremendous growth of the traffic load, 5G system is designed to fulfill diverse application requirements: far more stringent latency and reliability levels are expected to be necessary to support applications related to healthcare, security, logistics, automotive applications, or mission-critical control; Network scalability and flexibility are required to support a large number of devices with very low complexity and to enable long battery lifetimes [OBB+14].

In such a context, Cloud Radio Access Network (CRAN) has been considered as a novel network architecture for modern wireless networks. In a CRAN system, all Baseband Units (BBUs) are shifted into the cloud to constitute a centralized processing pool. The radio frequency signals from geographically distributed antennas are collected by Remote Radio Heads (RRHs) and transmitted to the cloud platform through fronthaul links [AoCHC15]. This centralized architecture

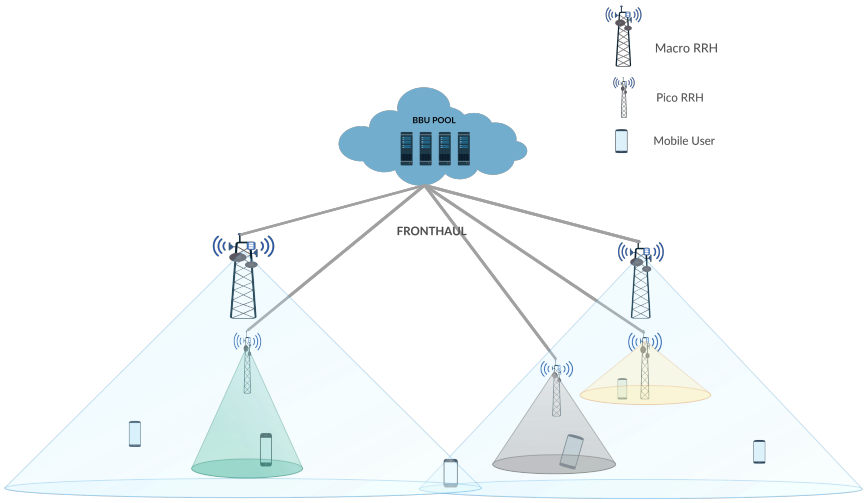


Figure 1.1: H-CRAN system model

enables a global optimization of joint baseband signal processing and radio resource management functions for all RRHs and users. However, such benefits come at the expense of large bandwidth demands on fronthaul links, as well as significant computational complexity burden at the BBUs side.

At the same time, Heterogeneous Networks (HetNets) have emerged as another core feature for 5G network to enhance the capacity/coverage while saving energy consumption. HetNets are constituted by conventional macro cells and overlaying small cells. With small cells deployment, wireless links to end-users become shorter, thereby improving the link quality in terms of spectrum efficiency (SE) as well as energy efficiency (EE). Therefore, combining both cloud computing and HetNet advantages results in the so-called Heterogeneous-Cloud Radio Access Networks (H-CRAN) depicted in Fig. 1.1 and which is regarded as one of the most promising network architectures to meet 5G system requirements [PLZW15].

## 1.2 Problem statement

In this thesis, we address the resource allocation issue which is formulated as a sum-rate maximization problem in the downlink of H-CRAN. We specifically focus on the problem of joint beamforming and user clustering optimization.

The beamforming techniques are based on the definition of a highly directive pattern in a desired transmission direction, depending on the network operation conditions and the network transmitting necessities. In wireless communications, beamforming helps to increase the signal power at the intended user and reduce interference to non-intended users. A high signal power is achieved by transmitting the same data signal from all antennas, but with different amplitudes and phases, both can be expressed in a complex vector called beamforming vector. As one vector is assigned to each user and can be matched to its channel, we can solve jointly the optimal beamforming problem with the user-to-RRH association by determining the non-zero beamforming vector.

The goal of this thesis is to optimize the user-to-RRH association with sum-rate maximization, that is to find the best configuration of user-to-RRH links with the corresponding beamforming weights such that the system sum-rate is maximized. This problem is usually formulated as a non-convex problem, that requires a nearly-optimal method to be solved.

In fact, the technical challenges of 5G H-CRAN have been pointed out in a number of works, in particular regarding resource allocation, interference management and fronthaul constraint alleviation [PLJ+14, DDD+15, MZC+17]. Specifically, the heterogeneous feature of access points in H-CRAN generalizes the problem of beamforming and user-to-RRH association compared to its CRAN counterpart. Many studies solved the scheduling problem by jointly optimizing the beamforming and user clustering in order to maximize network performance such as sum-rate, SE and EE [HYA13, RGIG15, DY14, DY15, PYXP16]. However, these solutions generate a large amount of control signaling and Channel State Information (CSI) overhead. CSI refers to known channel properties of a communication link and describes the reception quality of a signal propagating from the transmitter to the receiver and represents the combined effect of, for example, scattering, fading, and power decay with distance. Furthermore, most of these works did not consider the influence of user mobility and the resulting time-varying wireless environment over the long-term scheduling performance.

Therefore, our main challenge in the H-CRAN resource allocation problem is to design a framework that can achieve the targeted sum-rate maximization

while, unlike other traditional reference solutions, being able to alleviate the control and signaling costs. The proposed solution needs to reduce the required computational complexity, amount of CSI feedback and re-association signaling overhead over the long-term allocation process. Furthermore, the impact of the realistic channel variations due to different users mobilities is also an important issue. In mobility environments, the traditional solutions proposed in the literature for fixed users environments are no longer effective due to the strong stochastic characteristic and the non-deterministic variables of the network. For that reason, we aim at developing novel, effective and adaptive algorithms able to tackle the dynamics of such complex systems.

## 1.3 Research objectives and contributions

In order to cope with the above-mentioned challenges, we aim in this thesis to explore the joint beamforming and user clustering issue in the downlink of H-CRANs. The objective is to investigate the trade-off between system performance expressed in terms of sum-rate against the cost incurred during the scheduling, beamforming and clustering process. We propose a new class of algorithms that balance the different trade-off levels between the performance gains and the incurred costs in terms of computational complexity, CSI feedback overhead and user-to-RRH reassociation signaling overhead. Besides, these algorithms need to be adaptive and scalable under various mobility environments.

Following the aforementioned challenges, the contributions of the present thesis can be summarized as follows:

**- A thorough analysis on performance-cost trade-off of joint beamforming and user clustering problem in Cloud Radio Access Networks**

Our first contribution is a simple yet effective algorithm baptized Hybrid algorithm that addresses the beamforming and user clustering problem in H-CRAN. This mechanism periodically activates dynamic and static clustering schemes to balance between the optimality of the beamforming and association solutions while being aware of practical system constraints (complexity and signaling overhead). Another originality of our algorithm is that it foresees the time dimension of the allocation and scheduling process rather than its optimality (or sub-optimality) for the sole current scheduling frame. Moreover, we provide a cost

analysis of the algorithm in terms of several parameters to better comprehend the trade-off among the numerous parameters involved in the allocation process.

**- Advanced Mobility-Aware Algorithms**

Another key contribution of our thesis is to tackle the beamforming and clustering problem from a mobility perspective. For that purspose, we propose ABUC (Adaptive Beamforming and User Clustering), an enhanced version of the Hybrid algorithm that is aware of users mobility behavior. The derived extensive mobility analysis allowed us to design MABUC (Mobility-Aware Beamforming and User Clustering) an extended version of ABUC which based on the mobility profile of users (mainly velocity) selects the best CSI feedback strategy and periodicity to achieve the targeted sum-rate performance while ensuring the minimum possible cost (complexity and CSI signaling). MABUC algorithm takes into account the user mobility by using a CSI estimation model which can improve the algorithm performance compared to reference schemes. Our proposed algorithm has the benefit to meet the targeted sum-rate performance while being aware and adaptive to practical system constraints such as mobility, complexity and signaling costs.

**- A deep reinforcement learning for resource allocation in H-CRAN**

In our last contribution, we design a reinforcement learning framework which enables the proposed ABUC algorithm to optimize its scheduling parameters on-the-fly, given each user mobility profile. Different to ABUC algorithm which parameters, i.e. period $T$ and CSI feedback strategy, are fixed during the whole scheduling process or MABUC algorithm, which adopts its parameters based on a scenario dependant empirical analysis, this Q-learning framework enables to activate in real-time dynamic and static clustering schemes under different CSI feedback strategies adaptively depending on the individual user mobility profile. To do that, we formulate the optimization problem as a Q-learning model in which an agent learns from the environment to wisely select the optimal feedback parameters, i.e. period T and CSI feeedback type.

## 1.4 Thesis Outline

The outline of this thesis is organized as follows:

Chapter 1 firstly introduces the background of CRAN/H-CRAN, and then illustrates the motivations, problem statements, research objectives and main contributions of this thesis.

Chapter 2 presents the state-of-the-art for this research. In this chapter, we introduce the paradigm, characteristics and technical issues related to CRAN and H-CRAN. We then provide a literature review of the most relevant research works dealing with radio resource allocation problems in CRAN/H-CRAN. Finally, we propose a taxonomy of these works based on their main features in terms of performance objective and methodology which simplifies the discussion about their main advantages and limitations.

Chapter 3 reveals our first contribution, a hybrid user clustering and beamforming algorithm aiming at weighted sum-rate (WSR) maximization. At first, we introduce some background on beamforming and user scheduling. Then, we survey some research works which dealt with the joint beamforming and user clustering problem, the key issue in our thesis. Next, we detail two main reference clustering solutions (dynamic and static clusterings) on which our strategy relies on. Then, we elaborate the features of our proposed Hybrid algorithm and present a cost analysis that expresses the algorithms' costs in terms of computational complexity, CSI feedback overhead and user-to-RRH re-association signalling.

Chapter 4 scrutinizes the effect of users mobility on our beamforming and user clustering solutions. First, we introduce a CSI estimation model which allows to take into account user mobility (velocity). Then, we introduce ABUC, a mobility-aware version of the Hybrid algorithm that is tailored to the distinctive features of channel variations. Through extensive simulations, we derive empirically the best parameter values of the algorithm according to the users velocity. Then, we propose MABUC, an enhanced version of the scheme which, based on the previous empirical study, automatically selects the best CSI periodicity and feedback strategy to achieve a targeted sum-rate performance while maintaining the complexity and CSI signaling costs to a minimum.

Chapter 5 proposes to go further in the optimization of the scheduling parameters. To do so, we take leverage of reinforcement learning (RL) tool to optimize on-the-fly the feedback scheduling parameters according to each user mobility profile. Indeed, reinforcement learning is especially suited for dealing with such intricate long-term resource allocation optimization, under dynamically varying wireless environments. At first, we introduce some basics on deep reinforcement

learning and Q-learning approach. Then, we show how we apply the Q-learning strategy to ABUC algorithm to dynamically select on-the-fly the best CSI feedback parameters tailored to each user mobility profile. Next, we motivate the development of a new framework for ABUC based on Deep Q-learning. We present the new formulation of the problem as a POMDP (Partially observable Markov decision process) and detail the features of ABUC's Deep Q-learning framework.

Chapter 6 summarizes the thesis and provides potential directions for future research.

# Chapter 2

# State of the Art

In this chapter, we introduce some backgrounds on CRANs and H-CRANs, followed by an overview of their technical and research issues and associated solutions proposed in the literature. In addition, we particularly focus on the joint beamforming and user clustering problem and detail the most relevant algorithms proposed in this context.

## 2.1 CRAN/ H-CRAN motivations

The great success of mobile communications in the recent decades brings billions of user equipments (UE) and devices into networks to demand high bandwidth connections. Following the breakthrough of multiple-input-multiple-output (MIMO) technology to approach the Shannon limit in the past decades, the next generation of mobile communications rely on all the recent advances in air-interface transmission.

Motivated by the potential significant benefits, CRANs have been advocated by both mobile operators (e.g., Orange, NTT DoCoMo, Telefonica, and China Mobile) and equipment vendors (e.g., Cisco, Intel, IBM, Huawei, ZTE, Ericsson, and so on) [PSL+16]. CRAN encompasses many features such as: centralized processing, collaborative radio, real-time cloud computing, and power efficient infrastructure. It aims at reducing the number of cell sites while maintaining similar coverage, and reducing capital expenditures and operating expenses (CapEx, OpEx) while offering better services [WZHW15]. This architecture is a foremost combination of emerging technologies from both the wireless network and the

information technology industries that has the potential to improve spectral efficiency (SE) and energy efficiency (EE) based on the centralized cloud principle of sharing storage and computing resources via virtualization.

The wireless industry and research community are still working on improving the key features of CRANs, including the reduced cost, high EE and SE and forward and backward compatibility. In particular, CRANs can reduce the cost of the deployment owing to the possibility to substitute full-fledged dense BSs with RRHs. The RRH deployment results in reducing the construction space and saving energy consumption of dense BSs. In [11], a quantitative analysis of the cost was presented in CRANs, and it was shown that CRANs can lead to a CapEx reduction of 10% to 15% per kilometer comparing with traditional long term evolution (LTE) networks. Meanwhile, CRANs enable the flexible allocation of scarce radio and computing resources across all RRHs centrally processed by the same BBU pool, which reaps statistical multiplexing gains due to the load balance of adjacent RRHs for the un-uniformly traffic distribution. Furthermore, CRANs simplify the cellular network upgrading and maintenance due to the centralized architecture. At the BBU pool, baseband processing can be implemented using software radio technology based on open IT architectures, making the system upgrading to different standards possible without hardware upgrades. With CRANs, mobile operators can quickly deploy RRHs to expand and make upgrades to their cellular network. Mobile operators only need to install new RRHs and connect them to the BBU pool in order to expand the network coverage or split the cell to improve SE.

In addition, the HetNet architecture materializes the concept of small cells and has been proved to further increase system capacity [DMW+11]. In HetNets, besides the Macrocells formed by the existing eNodeBs, there are heterogeneous small cell networks (e.g. femto or pico cells to underlay or overlay the Macrocells). The motivation of such architecture is to increase the spatial spectrum reuse and increase the whole network efficiency. For this reason, the use of very dense and low-power-small-cells with highly spacial spectrum reuse is a promising way to handle the tremendous amount of devices [BLM+14]. However, even though densely deployed small cells can provide shorter transmission distance

and more efficient spatial reuse, it also introduces additional inter-cell interference problems and extra management issues. To compensate such defects, H-CRANs have been proposed on top of CRANs [HHLC15]. To overcome the technical challenges in HetNets, H-CRANs are presented as 5G RANs [PLJ+14] which are fully backward compatible with different kinds of CRANs and HetNets. They have been proposed as a solution to alleviate the burden on fronthaul encountered in CRAN and to provide ubiquitous coverage. Another motivation is to embed the cloud computing technology into HetNets to realize the large-scale cooperative signal processing and networking functionalities, and thus SE and EE performances are substantially improved beyond existing HetNets and CRANs.

## 2.2 CRAN/H-CRAN architectures

In this section, we highlight the main architectural features of CRAN and H-CRAN and their advantages with a particular emphasis on their overall improvement of system capacity and efficiency [LCWW12].

### 2.2.1 Cloud RAN

The evolution of cellular BSs in mobile communication systems is shown in Fig. 2.1. In 1G and 2G cellular networks, radio and baseband processing functionality are integrated inside a BS. While in 3G and 4G cellular networks, a BS is divided into a RRH and a BBU. In this BS architecture, the location of the BBU can be far from the RRH for a low site rental and the convenience of maintenance. In beyond 4G, BBUs are migrated into a BBU pool, which is virtualized and shared by different cell sites, and RRHs are connected to the BBU pool via fronthaul links, resulting in a generic CRAN architecture.

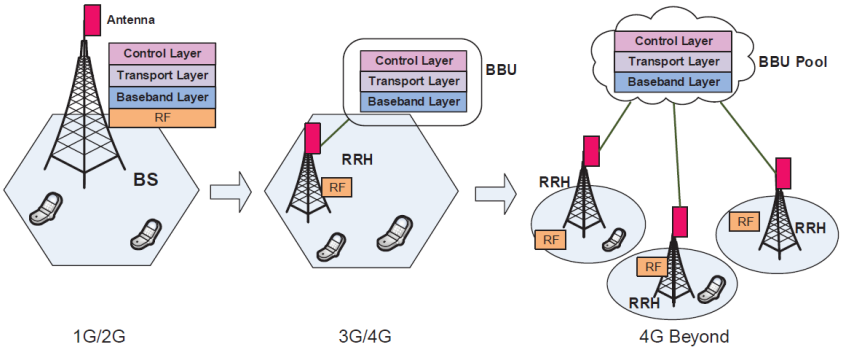


Figure 2.1: CRAN architecture evolution

The concept of CRAN was first proposed in [LSZ+10] and described in details in [Mob11]. CRAN is based on the "Cloudification" or, in other words, the migration of baseband processing from standalone BSs to a cloud data center composed of a pool of virtual BSs (BBUs). Thanks to this centralized network architecture, computation resources are virtualized in CRAN; they are aggregated on a pool level and flexibly allocated on demand. This constitues the fundamental and basic feature of CRAN. Within this cloud data center, BBUs collaborate: they work together in a large BBU pool to share and exchange network information such as signalling, traffic information and channel state information of mobile users in the system. Hence, by performing a proper load balancing between BBUs, the CRAN can adapt itself to non-uniform traffic during the day, allowing efficient utilization of baseband resources and better interference management across multiple cells [TCP+15].

In a typical CRAN as shown in Fig. 2.2, the traditional BS is decoupled into two parts: distributed RRHs, and BBUs clustered as a BBU pool in a centralized location. The functional split options may divide different functions between RRH and BBU. RRHs with radio frequency functions support high capacity in hot spots, while the virtualized BBU pool provides large-scale collaborative processing (LSCP), cooperative radio resource allocation (CRRA), and intelligent networking. The BBU pool communicates with RRHs via common public radio interface (CPRI) protocol, which supports a constant bit rate and bidirectional digitized inphase and quadrature (I/Q) transmission, and includes specifications for control plane and data plane [EAN11].

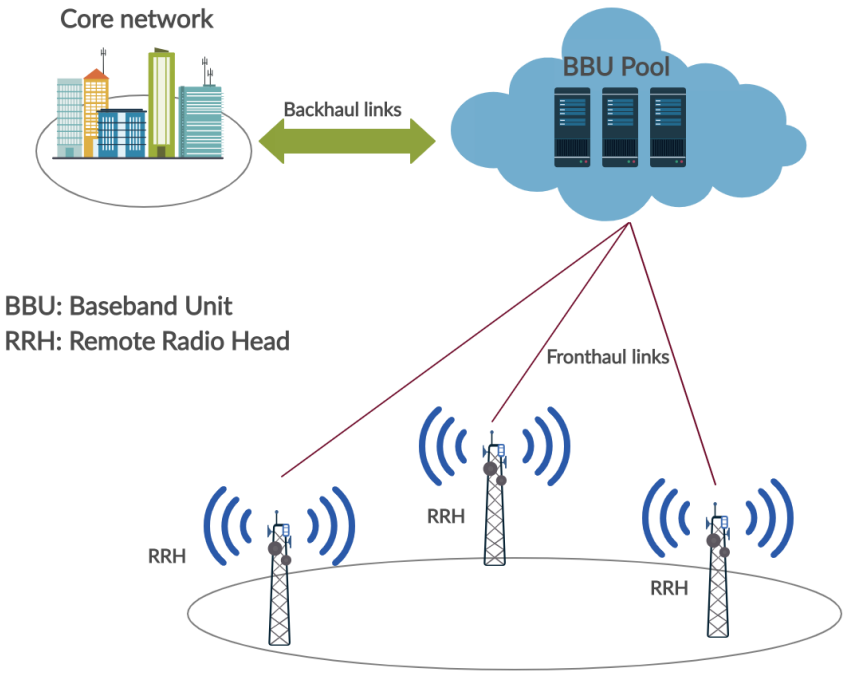


Figure 2.2: Traditional CRAN system

The design of CRAN allows fewer BBUs to be needed compared to the traditional architecture, CRAN has also the potential to decrease the cost of network operation by reducing power and energy consumption. New BBUs can be added and upgraded easily, thereby improving scalability and easing network maintenance [CCY+15].

### 2.2.2 Heterogeneous CRAN

To increase the capacity of cellular networks in dense areas with high traffic demands, low power nodes (LPNs, e.g., small cells such as pico or femto cells) serving for the pure "data-only" services with high capacity are identified as the main key components in HetNets [PLW+11]. The H-CRAN system has essentially the same architecture as CRAN. In H-CRAN, fronthaul is mainly used for data transfer [GH17]. The centralized control functions and signallings are no more achieved by BBU pool and are transferred to specific components denoted as high power nodes (HPNs, e.g., macro or micro base stations), which were previously used in heterogeneous networks. The link between the BBU pool and HPNs is called in

this case backhaul [PLZW15].

Similarly with the traditional CRAN, H-CRANs include a large number of RRHs with low energy consumption and which are coordinated with each other through the centralized BBU pool to achieve high cooperative gains. However, different from CRANs, H-CRANs are proposed as a cost-efficient solution by incorporating the cloud computing into HetNets. The motivation behind H-CRANs is to enhance the capabilities of HPNs with massive multiple antenna techniques and simplify the LPNs while connecting them to a "baseband signal processing cloud" with high speed optical fibers or RF (Radio Frequency) links [DDR+15]. As such, the baseband data processing as well as the radio resource control for LPNs are moved to the cloud server so as to take advantage of the cloud computing capabilities [PLJ+14].

### 2.2.3 CRAN/H-CRAN features

#### 2.2.3.1 Advantages

Among the main reasons to adopt CRAN is the benefit brought by cooperative signal processing, load balancing, and scheduling throughout traffic-aware selected BSs in the BBU pool [MKGM+15]. Consequently, the channel and user information given by each connected RRH-BBU link can help in reducing the interference. Specifically, the supported functionalities at the BBU pool are ensured by intercell interference coordination, CSI, Coordinated MultiPoint (CoMP) [PBS+12], and joint multicell processing [NGM15]. Moreover, the coordination at the BBU pool can optimize the use of power per operation by enabling massive MIMO [PCB15] or CoMP concepts [IHD+14].

Cloud RAN is much more than centralising baseband processing in one location and using the fibre optical cables to connect to remote radio heads located at the cell sites. More importantly, Cloud RAN is an attempt at decoupling the hardware and software platforms of wireless base stations. From a network and hardware point of view, the BBU pool is equipped with cloud resources. The involved resources could be allocated dynamically and managed efficiently with respect to dynamic traffic scheduling and the radio channel variation. It also provides configurable cloud capabilities, which makes the network management, maintenance, and scalability easier with its high elasticity.

CRAN architecture also helps to achieve higher system capacity with lower power consumption as the RRHs are deployed closer to UEs. Furthermore, the cost of network expansion to ensure seamless coverage taking into account the transition between the RAN technologies relies on densely deploying inexpensive RRHs [SRB+15].

The use of H-CRAN beyond CRAN has been beneficial to serve disadvantaged users placed at the cell edge of HPNs. As a better coverage is provided, and unnecessary handover is avoided with the existent infrastructure. Besides, H-CRAN was proposed to alleviate the fronthaul constraints and complexity in CRAN by alleviating the amount of information conveyed in the fronthaul. Lightening RRHs functionalities also opens ways to more functionalities such as high-speed data transmission with numerous related services. Moreover, HPN and BBU signallings help to manage the inter-tier interference between LPNs and HPNs.

#### 2.2.3.2 Drawbacks

Despite their numerous benefits, CRANs suffer from unescapable drawbacks such as fronthaul capacity limitions, complexity, security, etc.

Fronthaul links between BBUs and RRUs are required to have high bandwidth capability with low delay and cost requirements. Indeed, in the fully centralized approach which is the most adopted structure in CRAN, the fronthaul link requires a huge communication capacity as it carries all the IQ data between the RRHs and BBU [Sal16]. Another drawback is the high cost of optical fabric which increases the capital expenditures of cellular providers [AoCHC15].

Another significant challenge in CRAN is the security challenge in terms of user privacy and trusted parties. As resources are shared between BBUs, breaking user privacy and accessing assumingly secured data is a possibility, especially in such distributed architecture [TZY17].

## 2.3 Radio resource allocation in CRAN/H-CRAN

A large number of research works have been carried out in the literature, to address the radio resource allocation (RA) problem in CRANs and H-CRANs [LAL16, PLZW15, PLZW15, DDD+15, DYTB11]. Most of them have tackled the downlink

resource allocation when emphasizing on one or several aspects such interference management, coordinated multi-point transmissions, beamforming, energy efficiency, complexity, etc. In the following, we present some relevant works and organize them based on their most predominant optimization objective.

### 2.3.1 Interference management

HetNets are incorporated into CRAN to increase the capacity of cellular networks in dense areas with high traffic demands. In such systems, the received interference at a user consists mainly of two parts, namely the intra-tier interference from the BSs/users in the same tier the user is associated with, and the inter-tier interference from BSs/users belong to the other tier. However, it is in underlaid deployments in which the base stations of the two tiers reuse the same spectral resources that the interference management is more tricky as it requires inter-tier coordination. Hence, it is critical to suppress interferences through advanced RA and signal processing techniques to fully unleash the potential gains of HetNets, such as adopting the advanced coordinated multi-point (CoMP) transmission and reception technique to suppress both intra-tier and inter-tier interferences. In H-CRAN, since the baseband processing is centralized at the BBU pool, the cooperative processing techniques for interference mitigation can be leveraged [PLZW15].

One of the well known technique for interference suppression is Large-Scale Cooperative Spatial Signal Processing (LS-CSSP). As shown in [IHD+14], the distributed LS-CSSP has good potential to strengthen uplink signal and suppress inter-RRH interference, whose gain can reach $40-100\%$ in the weak coverage area. In [CRZK17], the authors present the flexible and scalable 5G H-CRAN architecture and focus on radio resource management (RRM) and an interference mitigation massive MIMO precoding scheme. In conventional networks, a base station is only able to collect the local CSI through the backhaul of its own served users. Thus it can not access to the CSI of the nearby interfered victim users. To overcome this issue, a two-tier interference-free hybrid precoding scheme is proposed with a flexible CSI acquisition process that allows to collect the CSI of the users connected to all RRHs in H-CRAN. By performing precoding within the null-space of the neighboring victim users, the proposed scheme limited the interference impact that could degrade the system performance.

In [MZC+17], the authors consider the interference management when D2D communication is incorporated into H-CRAN. With D2D communications, proximity users in a cellular network can communicate directly with each other without going through the BS. Therefore, the interference between the D2D users and macro-cell users is much more difficult to comprehend. The sub-channels allocation to multiple D2D pairs and the RRH users (RUEs) is investigated and the authors propose that the sub-channel that has been pre-allocated to a macro-cell user (MUE) can be reused for throughput improvement. The overall throughput and the number of admitted users is maximized and the users quality of service (QoS) is guaranteed. Such a resource allocation problem is formulated as a mixed integer nonlinear programming (MINLP) problem which is NP-hard and has been transformed into a many-to-one matching game. The proposed matching game has been proved to reach a stable matching with a low computational complexity.

In [PXH+15], an inter-tier interference mitigation method is proposed by a contract-based interference coordination framework. An optimal contract design that maximizes the rate-based utility is derived when perfect CSI is acquired at both BBU Pool and macro-RRHs. Furthermore, contract optimization when only partial CSI can be obtained from practical channel estimation is addressed as well. Monte Carlo simulations are provided to confirm the analysis, and the simulation results show that the proposed framework can significantly increase the transmission data rates over baseline algorithms, thus demonstrating the effectiveness of the proposed contract-based solution.

In [PXC+15], inter-tier interference suppression techniques are considered in the context of collaborative processing and cooperative radio resource allocation (CRRA). Closed-form expressions for the overall outage probabilities, system capacities, and average bit error rates under these two schemes are derived. Furthermore, CRRA optimization models based on Interference Collaboration (IC) and Beamforming (BF) are presented to maximize the users sum rates via power allocation, which is solved with convex optimization. Simulation results demonstrate that the derived expressions for these performance metrics for IC and BF are accurate, and the relative performance between IC and BF schemes depends on system parameters such as the number of antennas at the MBS, the number of RRHs, and the target signal-to-interference-plus-noise ratio threshold.

Most of these mentioned papers consider the ideal case of interference coordination in which accurate CSIs are assumed for all transmitters and receivers. However, this assumption is non-trivial especially in view of the overwhelming signalling overhead and the inevitable existence of CSI distortion in practical systems [BG06]. Therefore, in order to deal with realistic scenarios, not only the impact of imperfect CSI but also channel estimation techniques should be considered when examining interference coordination in H-CRANs.

### 2.3.2 Complexity management

The computational complexity of RAN functions is one of the main obstacles for the introduction of cloud computing principles into mobile networks radio access. Computational limitations in mobile wireless networks have a significant impact on the real-time network performance. This implies the need for a mechanism which estimates the computational load of the aggregated cells and assures that the computational resources are sufficient.

In [CJL+14], a cost-effective architecture for CRAN is presented for a scalable wireless access network which satisfies green radio constraints at the same time. The authors focused on the SE and EE of CRAN implementation in HetNet. The SE improvements was achieved by cooperative transmission among RRHs. Moreover, to improve EE, a simplified pre-coding scheme is proposed to reduce the power consumption incurred by the cooperation computational complexity.

In [RMVT15], the authors have developed a framework which solves the user resource allocation problem under the assumption of limited computational resources in a centralized cloud platform. The underlying optimization problem is solved with an adapted water-filling approach, making it feasible to fulfill the strict timing requirements of the wireless access. Furthermore, an intuitive complexity-cut-off approach is proposed to deliver near-to-optimal results as well.

In [VTR14], the authors consider the interplay between computational efficiency and data throughput that is fundamental to CRAN. The concept of computational outage in mobile networks is introduced and applied to the analysis of complexity constrained dense CRAN networks. The same authors consider in [RTV15] the computational requirements of a centralized RAN with the goal of illuminating the benefits of pooling computational resources. Several new performance metrics are defined, including the computational outage probability,

complexity outage, computational gain, computational diversity, and especially the complexity-rate trade-off. Using the developed metrics, it is shown that centralizing the computing resources of CRAN may provide a higher throughput per computational resource as compared with the local processing.

There are several techniques to reduce the computational complexity. In [MAA18], to tackle both complexity and latency problems, a MapReduce framework and fast matrix algorithms are proposed. Two levels of complexity reduction are given: the MapReduce framework minimizes the complexity from $O(N^3)$ to $O((N/k)^3)$, where N is the total number of RRHs and k is the number of RRHs per group, given that the processing of RRHs is divided into parallel groups. The second approach using the algorithms of fast matrix inversion reduces the computation complexity from $O((N/k)^3)$ to $O((N/k)^2.807)$. In [ARN+17], the authors address a joint user association, admission and power allocation problem that maximizes the throughput and number of users accommodated by the H-CRAN. An outer approximation approach (OAA) is given based on linear programming that simplifies the NP-Hard nature of the problem. The OAA guarantees a convergence after a finite number of computations.

We can conclude that the computational complexity is an important design constraint especially in the context of cloud computing and should be considered in any resource allocation solution design.

### 2.3.3 Fronthaul constrained resource allocation

The fronthaul capacity constraints have great impact on CRAN performance, and the scale size of RRHs accessing the same BBU pool is limited and could not be too large due to the implementation complexity [PLZW15]. This limitation often leads to the problem of RRH clustering when the scheduler task is to derive the optimal user-to-RRH association that optimizes the system performance under limited fronthaul capacity. To overcome the problems related to the non-ideal fronthaul, several cooperative processing and resource allocation strategies have been proposed.

In [DDD+15], resource allocation solutions for H-CRAN are investigated, and different schemes are proposed, namely, coordinated scheduling and multicloud association. In the coordinated scheduling, the main issue is to maximize the network-wide utility subject to user connectivity constraints. The search space

is exponentially large and makes such exhaustive search clearly infeasible. Then, the authors proposed a graph-theoretical-based approach to solve the problem. In addition, multicloud H-CRAN is proposed to overcome the main limitations of single cloud RAN such as the distance separating BSs in the network and also the computation burden when connecting multiple BSs to the same cloud.

In H-CRANs architecture, users can benefit from the coverage diversity provided by several heterogeneous nodes leading to a user-centric architecture [DDD+15]. Determining the optimal user-to-RRH association that offers the best performance becomes a combinatorial optimization problem of high complexity. Exhaustive search is infeasible for any reasonably sized network, even with very powerful processors at the cloud. Consequently, this problem has been addressed in many research works [SZL13] [DYTB11] [PSSS13]. The problem is equivalent to the joint beamforming and user-to-RRH clustering problem which by solving the sparse beamforming issue indirectly decides which users should be served by which RRHs.

In [PYP14], the authors studied the user clustering problem and evaluated the appropriate number of associated RRHs per user to balance the throughput gain and implementation cost. In [HYA13], the advantages of small cells clustering is evaluated in a dense heterogeneous network for downlink MIMO. It is shown that by giving reasonable cluster sizes, each cluster can form a virtual MIMO network wherein users are separated via spatial multiplexing using jointly designed downlink beamforming vectors. In [RGIG15] [DY14], a Weighted Minimum Mean Square Error (WMMSE) method is used for solving joint beamforming and user clustering problems for sum-rate maximization. In [RGIG15], the authors implemented a greedy RRH clustering algorithm and compared it to two transmit precoding schemes, Zero-Forcing Beamforming (ZFBF) and WMMSE-based coordinated beamforming. They showed that WMMSE outperforms other reference beamforming approaches. In [DY14], the WSR maximization problem is solved using similar WMMSE approach under dynamic and static user clusterings. It is shown that dynamic clustering significantly improves the system performance over other naive clustering schemes, while static clustering also achieves substantial performance gain. Due to the lack of convergence guarantee for the algorithm in [DY14], the same authors propose a new algorithm in [DY15] which is proved to converge to a local optimum. Different to previous works, whose aim is to solve the weighted sum rate maximization problem with backhaul constraints in

CRANs, the paper [PYXP16] applies the generalized WMMSE approach to solve the average weighted energy efficiency (EE) utility objective function with each RRH's transmit power, individual fronthaul capacity, and inter-tier interference constraints.

## 2.4 Discussion

In this section, we discuss and provide a taxonomy of most relevant literatures addressing resource allocation related issue in CRAN/H-CRAN. The main distintive features of the research works are given in the Table 2.1.

From the table, we can observe that most research works are interested in optimizing the system throughput or weighted sumrate. This is motivated by the fact that the throughput requirements are stringent in 5G system. The optimization problem is usually coupled with RRH transmit power constraint and limited fronthaul capacity. Most of the problems are formulated as non-convex problems and solved using convex transformations and nearly-optimal methods. Several papers analysed the algorithmic complexity analysis [HYA13, DY14, PYXP16, DDD$^+$15, MAA18] while others [RTV15, VTR14, RMVT15] consider the computational complexity as the objective function but only for the uplink case.

However, the majority of these works did not fully consider the required computational complexity and the incurred signaling costs over a long-term scheduling process. In particular, such beamforming techniques rely on accurate CSI feedback for all user-to-RRH links, which may create excessive burden on fronthaul links. Moreover, most of these works ignored the costs in terms of computational complexity at the BBU side and user-to-RRH re-association signalling during successive scheduling frames. Indeed, the complexity of optimal solutions may be bearable when applied once for a given time frame, but such complexity would be unbearable when completed on the long-term scheduling process. To the best of our knowledge, there are very limited works considering the time-dimension and the induced complexity and signaling costs in their user clustering and beamforming design problems.

In addition, almost all works accepted the assumption of CSI perfection, which is clearly unrealistic as it creates a tremendous burden on the fronthaul link [AWA11].

| [REF] | Objective Function | Constraints | Problem Formulation | Proposed algorithm/ solution |
|---|---|---|---|---|
| [MZC+17] | Overall throughput and the number of admitted D2D users | Interference | MINLP problem | Matching game, constrained-DA algorithm |
| [PXC+15] | RRH-accessed users' sum rates | Interference, QoS, transmit power | Non-convex problem | Lagrange Dual Decomposition Method |
| [PXH+15] | Rate-based utility | Interference, incomplete CSI, transmit power | Non-convex problem | Contract-based game theory |
| [CJL+14] | Sum throughput | Transmit power | Convex problem | Water-filling algorithm |
| [ARN+17] | Max Throughput and number of users | Transmit power, Qos | MINLP problem | Outer Approximation Algorithm |
| [DDD+15] | Network-wide utility | User connectivity constraints | Discrete mapping problem | Graph-theoretical-based algorithm |
| [SZL13] | Network power consumption | QoS, RRH transmit power | Second-order cone programming (SOCP) problem | Branch-and-bound method |
| [PSSS13] | Weighted sum-rate | Power and backhaul capacity | Multivariate Compression Problem | Majorization Minimization (MM) algorithm |
| [DY14, DY15] | Weighted sum-rate | Fronthaul capacity and RRH transmit power | Non-convex problem | WMMSE method |
| [DY15] | Weighted sum-rate and power | RRH transmit power, QoS | SOCP problem | WMMSE method |
| [PYXP16] | Weighted energy efficiency | Interference, fronthaul capacity, transmit power | Non-convex problem | Lyapunov framework, WMMSE method |

Table 2.1: Taxonomy table of most relevant radio resource-allocation-related research works

Very few papers put the CSI acquisition and CSI imperfection into the optimization problem constraints [CRZK17, MAA18]. Moreover, almost all papers were agnostic to users' mobility behavior and its impact on the performance metrics of the designed solutions. Given the above discussion, we focus in this thesis on developing novel user clustering and beamforming solutions that meet computational complexity and intended feedback costs constraints insuring their applicability in practical systems. Such solutions should provide a good balance between antagonistic parameters (such as throughput, energy consumption, computational complexity, signalling,...) on the long-term scheduling process while being aware of user mobility. These objectives constitute the key research goals of this PhD thesis.

# Chapter 3

# Performance-Cost Trade-off Investigation on Joint Sparse Beamforming and Scheduling Problem for Downlink Cloud Radio Access Network

## 3.1 Introduction

The centralized architecture of H-CRAN enables a global optimization of joint baseband signal processing and radio resource management functions for all RRHs and users. However, how H-CRAN may be deployed for 5G is still not straightforward, as the fronthaul constraints (such as capacity, delay, etc) have an important impact on worsening the performance, and the scale size of RRHs accessing the same BBU pool is limited and could not be too large due to the implementation complexity. So far, many works have focused on investigating approaches for maximizing the global system performance while being aware of fronthaul constraints [PLZW15, DDD$^+$15, DYTB11, SZL13, PYP14, HYA13, RGIG15, DY14]. In particular, several approaches focused on radio resource allocation optimization problems is strongly related to key techniques in H-CRAN such as beamforming

and user clustering, i.e., user-to-RRH association.

### 3.1.1 Background on beamforming and scheduling

Beamforming or spatial filtering is a signal processing technique used in sensor arrays for directional signal transmission or reception. In wireless communications, the goal is to increase the signal power at the intended user and reduce interference to non-intended users. A high signal power is achieved by transmitting the same data signal from all antennas, but with different amplitudes and phases, both can be expressed in a complex vector $\mathbf{w}_{lk}$. As one beamforming vector is assigned to each user and can be matched to its channel, we can solve jointly the optimal beamforming problem with the user-to-RRH association by determining the non-zero beamforming vector.

Fig. 3.1 illustrates an example of a user $k$ clustering configuration with user-to-RRH associations determined by the derived $\mathbf{w}_{lk}$ beamforming vector variables. The joint problem of beamforming and user clustering is to determine the optimal serving RRH clusters for each user and the corresponding beamforming vector variables that maximize the overall system performance.

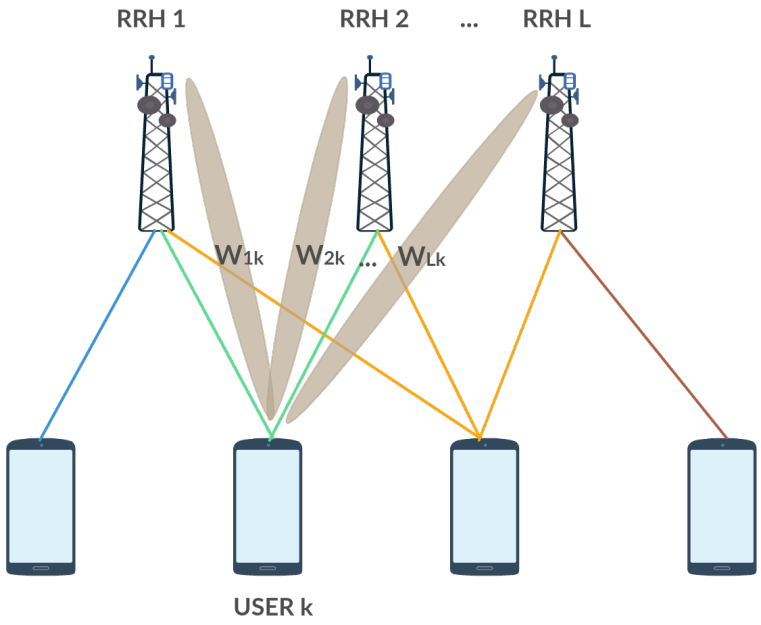


Figure 3.1: Illustration of joint beamforming and user clustering in CRAN system

Most of the state-of-the-art aimed at increasing various metrics such as throughput, spectral efficiency or energy efficiency while alleviating the fronthaul constraints. Many studies have focused on the user clustering problem [PYP14, HYA13, PYP14]. The objective is to evaluate the appropriate cluster size, i.e. number of associated RRHs serving each user to balance throughput gain and implementation cost. The work in [PYP14] shows that the ergodic capacity gain from the RRH density is larger than that from the number of antennas per RRH, which indicates that the association number should not be bigger than a small number of RRHs per user to balance the performance gain and the implementation cost.

The joint beamforming and user clustering problem had been tackled in several works [RGIG15, DY14]. The well-known Weighted Minimum Mean Square Error (WMMSE) method is usually used to solve the problems expressed by different objective functions for sum-rate maximization or power minimization. In [DY14], the weighted sum-rate (WSR) maximization problem is considered under dynamic and static user clusterings in which the initial RRH clusters are allowed to be updated (dynamic clustering) or maintained fixed (static clustering) during each scheduling frame. Due to the lack of convergence guarantee for the non-convex algorithm in [DY14], the same authors propose a new algorithm in [DY15] which is proved to converge to a local optimum with a fixed user clustering.

Such beamforming techniques rely on accurate CSI feedback for all user-to-RRH links, which may create excessive burden on the fronthaul links. However, most of these previous works did not fully consider the required computational complexity and the incurred signaling costs over a long-term scheduling process. In [DY14], it is shown that dynamic clustering significantly improves the system performance over other naive clustering schemes, while static clustering also achieves subtantial performance gain. But the difference between these two approaches of clustering in terms of CSI overhead and complexity have not been studied or analyzed so far.

In this chapter, we aim to explore the joint beamforming and user clustering issue in downlink H-CRAN and analyze the different trade-off levels between the performance gains and the incurred costs in terms of computational complexity, CSI feedback overhead and user-to-RRH re-association signaling overhead. We consider two main constraints: the capacity constraint and transmit power limitation of the fronthaul. Latency is one of the main constraints for the fronthaul in a H-CRAN architecture, this parameter determines the maximum length for

the optical link between RRH and BBU. However, we assume in this work that the latency is negligible in all transport links including the fronthaul.

More specifically, we propose an algorithm that periodically activates dynamic and static clustering schemes to balance between the optimality of the beamforming and association solutions while being aware of practical system constraints (complexity and signaling overhead). Moreover, we provide an analysis of each type of costs to better comprehend the trade-off among the numerous dimensions involved in the allocation process.

Our first goal is to propose a new effective algorithm which is able to achieve maximum performance while being aware of practical system constraints such as complexity and signaling overhead. To do this, firstly, we study the effect of different clustering schemes, i.e. dynamic and static schemes on the performance and complexity of the algorithms. Second, based on this analysis and to better comprehend the trade-off process, we propose a simple algorithm, we baptize Hybrid algorithm, which periodically activates dynamic and static schemes to manage the clustering process. The Hybrid algorithm strategy tries to balance between the solution optimality and complexity and signaling costs. More specifically, the proposed algorithm implements a periodic dynamic/static clustering in which a dynamic clustering is executed periodically (every T frames) and a static algorithm is used in the frames between two successive periods. The complexity reduction is obtained as the static algorithm relies on the same clustering obtained by the previous dynamic iteration.

The rest of this chapter is structured as follows: Section 3.2 presents the system model and Section 3.2 details the problem formulation and reference schemes. Next, we describe in Section 3.4 our proposed Hybrid algorithm and its cost analysis in section 3.5. The simulation results are presented in section 3.6. Finally, Section 3.7 concludes the chapter.

## 3.2 System Model

We consider the H-CRAN model in [DY14] which consists of a BBU Pool, $L$ macro and pico RRHs and $K$ users. Each RRH and user is equipped with $M$ and $N$ antennas, respectively, and users are randomly located in the service area.

Let $\mathbb{L} = \{1,2,...,L\}$ and $\mathbb{K} = \{1,2,...,K\}$ be the sets of RRHs and of users, respectively. The propagation channel from RRHs to the $k^{th}$ user is denoted as $\mathbf{H}_k \in \mathbb{C}^{N\times ML}, \forall k \in \mathbb{K}$ which includes the path loss and Rayleigh fading effects.

$$\mathbf{H}_k = \left[\mathbf{H}_{1k}^1,...\mathbf{H}_{1k}^M,\dots\mathbf{H}_{lk}^1,...\mathbf{H}_{lk}^M,\dots\mathbf{H}_{Lk}^1,...\mathbf{H}_{Lk}^M\right],$$

where $\mathbf{H}_{1k}^m$ of size $N \times 1$.

We focus on the downlink transmission with linear beamforming technique. It is worth noting here, that compared to other existing works which deal with Resource Block (RB) allocation in OFDMA-based CRANs/H-CRANs, we assume here that all resource blocks are shared by all RRHs and that the interference among RRHs is handled by beamforming.

In order to represent the RRH cluster and transmit beamformer in a compact form, we denote a network-wide beamforming matrix $\mathbf{w}_k \in \mathbb{C}^{ML\times 1}$ as the transmit beamforming vector from all RRHs to the $k^{th}$ user.

$$\mathbf{w}_k = \left[\mathbf{w}_{1k}^H,\cdots,\mathbf{w}_{lk}^H,\cdots,\mathbf{w}_{Lk}^H\right]^H,$$

where $\mathbf{w}_{lk} \in \mathbb{C}^{M\times 1}$. We suppose that RRH $l$ is not part of user $k$'s serving cluster, then the corresponding beamformer block $w_k^l$ is set to 0. Since each user is expected to be served by only a small number of RRHs, the network-wide beamforming vector wk is group sparse. Here, we assume that all the $L$ RRHs can potentially serve each scheduled user in order to simplify the notations.

Let $s_k \in \mathbb{C}$ be the encoded information symbol for user $k$ with $\mathbb{E}\left[|s_k|^2\right] = 1$. $x$ and $y_k$ denote the transmit signal from all the RRHs and received signal at the user k in the downlink beamforming transmission, respectively. With linear transmit beamforming scheme at the RRHs. The received signal at user $k$, $\mathbf{y}_k \in \mathbb{C}^{N\times 1}$, is expressed as

$$\mathbf{y}_k = \mathbf{H}_k\mathbf{w}_k s_k + \mathbf{H}_k \sum_{j=1, j\neq k}^{K} \mathbf{w}_j s_j + \mathbf{n}_k,$$

where $\mathbf{n}_k \sim \mathscr{CN}(\mathbf{0}, \sigma_k^2\mathbf{I}_N)$ is the additive white Gaussian noise and $\mathbf{I}_N$ is the identity matrix of size $N \times N$. The first term is the desired signal to user $k$ and the second term is the interference.

The Signal-to-Interference-plus-Noise Ratio (SINR) at user $k$ can be expressed

as

$$SINR_k = \frac{\|\mathbf{u}_k^H \mathbf{H}_k \mathbf{w}_k\|^2}{\sum_{j=1, j\neq k}^{K} \|\mathbf{u}_k^H \mathbf{H}_j \mathbf{w}_j\|^2 + \sigma_k^2 \|\mathbf{u}_k\|_2^2}, \tag{3.1}$$

where $\mathbf{u}_k \in \mathbb{C}^{N\times 1}$ is the receive beamforming vector of user $k$.

The achievable rate of user k is given by

$$r_k = \log_2(1 + \mathbf{w}_k^H \mathbf{H}_k^H (\sum_{j=1, j\neq k}^{K} \mathbf{H}_k \mathbf{w}_j \mathbf{w}_j^H \mathbf{H}_k^H + \sigma_k^2 \mathbf{I}_N)^{-1} \mathbf{H}_k \mathbf{w}_k). \tag{3.2}$$

Note that the rate expression 3.2 can also account for the user scheduling operation. A user k is scheduled, i.e. $R_k$ is nonzero, if and only if its beamformer vector $w_k$ is nonzero. Therefore, the user scheduling, RRH clustering and beamforming design for the downlink H-CRAN is unified within this single task of determining the sparse beamforming vector $w_k$ for each user.

## 3.3 Problem Formulation and Reference Schemes

### 3.3.1 Weighted Sumrate Maximization Problem Formulation

In this chapter, we propose a joint dynamic clustering, user scheduling and beamforming design strategy for the downlink H-CRAN. The proposed algorithm designs a group sparse beamforming vector $w_k$ for each user in each scheduling slot. A beamforming vector for each user is optimized where the nonzero entries in the beamforming vector correspond to the user's serving cluster. In fact, since each user is expected to be served by only a small number of RRHs, the network-wide beamforming vector wk is group ***sparse***.

We assume that the BBU Pool has access to global CSI for designing the sparse beamforming vector $w_k$. Once $w_k$ is determined, the BBU Pool transmits user $k$'s message, along with the beamforming coefficients, to those RRHs corresponding to the nonzero entries in $w_k$ through the fronthaul links. We also assume that the channels are slow varying and only consider the fronthaul consumption due to the user data sharing and ignore the fronthaul required for sharing CSI and

delivering beamforming coefficients.

We focus on the following WSR maximization problem that aims at maximizing the WSR of all users in the network under the fronthaul link capacity contraints and per-RRH power constraints. This problem is formulated as,

$$\begin{aligned} \max_{\{\mathbf{w}_{lk}, l\in\mathbb{L}, k\in\mathbb{K}\}} \quad & \textstyle\sum_{k=1}^{K} \alpha_k r_k & (1) \\ \text{s.t.} \quad & P_l = \sum_{k=1}^{K} \|\mathbf{w}_{lk}\|_2^2 \le P_l^{max} & (1a) \\ & \sum_{k=1}^{K} 1\{\|\mathbf{w}_{lk}\|_2^2\} r_k \le C_l^{max} & (1b) \end{aligned} \tag{P1}$$

where $\alpha_k$ is the scheduling priority weight associated with user $k$.

In (P1), the first constraint $(1a)$ corresponds to the transmit power constraint of RRH $l$, i.e., $P_l$ should be smaller than the maximum transmit power $P_l^{max}$. The second constraint $(1b)$ expresses that the sum-rate of users connected to RRH $l$ should be smaller than its fronthaul link capacity $C_l^{max}$. Intuitively, the fronthaul consumption at the $l-th$ RRH is the accumulated data rates of the users served by RRH $l$. So, we can characterize whether or not user $k$ is served by RRH l using the indicator function and cast the per-RRH fronthaul constraint as (1b).

We can see that the fronthaul capacity constraint (1b) is a function of both the cluster size and the user rate, where in addition the user rate is a function of user scheduling and beamforming operation. This observation provides us with different degrees of freedom in controlling the fronthaul consumption depending on whether the RRH clustering is dynamic or fixed in different user scheduling time slots.

Specifically, in the case where the serving cluster for each user is fixed, or equivalently the set of users associated with each RRH is predetermined, the fronthaul consumption at RRH $l$ is also equal to the accumulated data rates of users associated with RRH $l$, which can be formulated as

$$\sum_{k=1}^{K_l} r_k \le C_l^{max} \tag{3.3}$$

where $K_l$ denotes the size of fixed subset of users associated with RRH $l$. Note

that in equation 3.3, in each time-frequency slot, only the subset of users scheduled to be served have nonzero rates. So in 3.3, summing over the set of users associated with RRH $l$ is equivalent to summing over the set of scheduled users.

Problem (P1) is a non-convex Mixed-Integer Non-Linear Programming (MINLP) proven to be NP-hard [DY15], and hence cannot be solved in polynomial time.

### 3.3.2 Reference Schemes

#### 3.3.2.1 Dynamic Clustering Algorithm

The conventional WSR maximization in problem (P1) is a well-known non-convex optimization problem, for which finding the global optimal solution is already quite challenging even without the additional mixed discrete and continuous fronthaul constraint (1b). In this section, we present a weighted minimum mean square error (WMMSE) approach that had been used in several previous works [DY14, RGIG15].

It was shown in [DY14, RGIG15] that this WSR optimization problem is equivalent to a WMMSE problem with variables $\mathbf{w}_k$, $\mathbf{u}_k$ and $\rho_k$ defined below while being convex with respect to each of the variables. This enables to resolve the WMMSE problem through the block coordinate descent method by iteratively optimizing over each variable [RHL13] while keeping the others fixed.

We observe that the indicator function in (1b) can also be equivalently expressed as an $l0$-norm of a scalar. The $l0$-norm is the number of nonzero entries in a vector. So it reduces to an indicator function in the scalar case. This equivalent expression allows to approximate a non-convex $l0$-norm optimization objective by a convex reweighted $l0$-norm, i.e.

$$\|x\|_0 \approx \sum_i \beta_i |x_i| \tag{3.4}$$

where $x_i$ denotes the $i$-th component in the vector $x$ and $\beta_i$ is the weight associated with $x_i$. In particular, we can reformulate the fronthaul constraint (1b) as:

$$\sum_{k=1}^{K} \beta_{lk} \hat{r}_k \|\mathbf{w}_{lk}\|_2^2 \leq C_l^{max} \tag{3.5}$$

where $\beta_{lk}$ is a constant weight associated to RRH $l$ and user $k$ and is updated iteratively according to

$$\beta_{lk} = \frac{1}{\|\mathbf{w}_{lk}\|_2^2 + \tau}, \forall k, l, \tag{3.6}$$

where $\tau$ is a small constant regularization factor and $\|\mathbf{w}_{lk}\|_2^2$ is taken from the previous iteration. This heuristic weight updating rule (3.6) is motivated by the fact that by choosing $\beta_{lk}$ to be inversely proportional to the transmit power level $\|\mathbf{w}_{lk}\|_2^2$, those RRHs with lower transmit power to user k would have higher weights and would be forced to further reduce its transmit power and encouraged to drop out of the BS cluster eventually. Note that not only the BS cluster formation, but also the user scheduling can be controlled through $\|\mathbf{w}_{lk}\|_2^2$ since the user $k$ is scheduled if and only if there exists at least one RRH $l \in \mathbb{L}$ such that $\|\mathbf{w}_{lk}\|_2^2 \neq 0$.

However, even with the above approximation, the optimization problem (P1) with the fronthaul constraint (1b) replaced by 3.5 is still difficult to deal with, due to the fact that the rate $R_k$ appears in both the objective function and the constraints. To address this difficulty, it is proposed to solve the problem (P1) iteratively with fixed rate $\hat{r}k$ in equation 3.5 obtained from the previous iteration. Under fixed $\beta_{lk}$ and $\hat{r}k$, problem (P1) now reduces to

$$\begin{aligned} \max_{\{\mathbf{w}_{lk}, l\in\mathbb{L}, k\in\mathbb{K}\}} \quad & \textstyle\sum_{k=1}^{K} \alpha_k r_k & (2) \\ \text{s.t.} \quad & P_l = \sum_{k=1}^{K} \|\mathbf{w}_{lk}\|_2^2 \leq P_l^{max} & (2a) \\ & \sum_{k=1}^{K} \beta_{lk} \hat{r}_k \|\mathbf{w}_{lk}\|_2^2 \leq C_l^{max} & (2b) \end{aligned} \tag{P2}$$

Although the approximated problem (P2) is still nonconvex, it can be reformulated as an equivalent WMMSE problem and use the block coordinate descent method to reach its stationary point. It is already proven in [SRLH11] that (P2) can be solved by finding the optimal beamformer $\mathbf{w}_k$ under fixed $\mathbf{u}_k$ and $\rho_k$ in the following equivalent Quadratically Constrained Quadratic Programming (QCQP) problem:

$$\begin{aligned} \min_{\{\mathbf{w}_{lk}, l\in\mathbb{L}, k\in\mathbb{K}\}} \quad & \textstyle\sum_k \mathbf{w}_k^H (\sum_j \alpha_j \rho_j \mathbf{H}_j^H \mathbf{u}_j \mathbf{u}_j^H \mathbf{H}_j) \mathbf{w}_k \\ & -2\textstyle\sum_k \alpha_k \rho_k Re\{\mathbf{u}_k^H \mathbf{H}_k \mathbf{w}_k\} \qquad (3) \\ \text{s.t.} \quad & \sum_{k=1}^{K} \|\mathbf{w}_{lk}\|_2^2 \le P_l^{max} \qquad (3a) \\ & \sum_{k=1}^{K} \beta_{lk} \hat{r}_k \|\mathbf{w}_{lk}\|_2^2 \le C_l^{max} \qquad (3b) \end{aligned} \tag{P3}$$

In QCQP problem (P3), $\hat{r}_k$ is the achievable rate from the previous iteration. We define $e_k$ as the corresponding Mean Square Error (MSE),

$$e_k = \mathbf{u}_k^H \Big( \sum_{j=1, j\neq k}^{K} \mathbf{H}_k \mathbf{w}_j \mathbf{w}_j^H \mathbf{H}_k^H + \sigma_k^2 \mathbf{I}_N \Big) \mathbf{u}_k - 2Re\{\mathbf{u}_k^H \mathbf{H}_k \mathbf{w}_k\} + 1, \tag{3.7}$$

and $\rho_k$ is the MSE weight for user $k$,

$$\rho_k = e_k^{-1}. \tag{3.8}$$

$\mathbf{u}_k$ is the optimal receive beamforming vector under fixed $\mathbf{w}_k$ and $\rho_k$,

$$\mathbf{u}_k = \Big( \sum_{j=1, j\neq k}^{K} \mathbf{H}_k \mathbf{w}_j \mathbf{w}_j^H \mathbf{H}_k^H + \sigma_k^2 \mathbf{I}_N \Big)^{-1} \mathbf{H}_k \mathbf{w}_k. \tag{3.9}$$

Finally, the derived problem (P3) can be resolved using the Algorithm 1 given below [RHL13].

**Algorithm 1:** Dynamic Algorithm

initialize frame $\beta_{lk}, \hat{r}_k, \mathbf{w}_k, \forall(l,k)$
**repeat**
1) Fix $\mathbf{w}_k$ and compute the MMSE receiver $\mathbf{u}_k$ and the corresponding MSE $e_k$ according to (3.9) and (3.7)
2) Update MSE weight $\rho_k$ according to (3.8)
3) Find the optimal transmit beamformer $\mathbf{w}_k$ under fixed $\mathbf{u}_k$ and $\rho_k$, by solving problem (P3)
4) Compute the achievable rate $r_k$
5) Update $\hat{r}_k = r_k$ and $\beta_{kl}$ according to (3.6)
**until** *convergence*

**Remark:** *To achieve the optimal performance, Algorithm 1 solves the beamforming problem by considering all possible user to RRH links, i.e.,* $\mathbf{w}_k$ *is of size* $LM$ *in each scheduling frame, for each user* $k$*. The beamforming solution implicitly resolves the clustering problem since the user to RRH associations are updated according to the solution* $\mathbf{w}_k$*, i.e., the assignment of each link is identified by a non-zero element of the beamforming vector. This case, where* $\mathbf{w}_k$ *is of size* $LM$*, is referred as the* ***dynamic clustering algorithm****.*

*However, this global optimization requires intractable computational complexity and tremendous amounts of signaling and CSI overheads. Therefore, an alternative approach is to limit the computational burden by reducing the considered user to RRH links, i.e.,* $\mathbf{w}_k$ *would be of size* $L_k$ *where* $L_k \leq L$ *for each user* $k$*, at the expense of reduced sum-rate performance. This approach is referred as the* ***static clustering algorithm****.*

#### 3.3.2.2 Static Clustering Algorithm

In the previous section, RRH clustering is dynamically determined in each time-frequency slot together with the beamforming vector and user scheduling in a joint fashion. However, dynamic RRH clustering may incur significant signaling overhead in practice as new RRH-user associations need to be established continuously over time. In this section, we discuss static clustering schemes, where the RRH clusters only need to be updated at much larger time scale, typically only when user locations change.

As discussed previously, fronthaul consumption under static clustering can still be controlled by jointly optimizing the user scheduling and beamforming. In this section, the authors in [SRLH11] proposed to adapt the sparse beamforming algorithm presented in previous section to jointly schedule the users and design the beamforming vectors under per-RRH fronthaul constraints while assuming that the RRH clustering is fixed.

Different to dynamic algorithm, in static scheduling, only a fixed subset of RRHs in each cluster is considered, i.e. $l \in \mathbb{L}_k$, where $\mathbb{L}_k$ is the fixed cluster of RRHs serving user $k$. Likewise, $\mathbb{K}_l$ is defined as the subset of users associated with RRH $l$. The WSR maximization problem (P1) can now be re-formulated as

$$\begin{aligned} \max_{\{\mathbf{w}_{lk}, l\in\mathbb{L}_k, k\in\mathbb{K}\}} \quad & \sum_{k=1}^{K} \alpha_k r_k & (4) \\ \text{s.t.} \quad & P_l = \sum_{k\in\mathbb{K}_l} \|\mathbf{w}_{lk}\|_2^2 \le P_l^{max} & (4a) \\ & \sum_{k\in\mathbb{K}_l} r_k \le C_l^{max} & (4b) \end{aligned} \tag{P4}$$

We can see that problem (P4) is much simplified as compared to problem (P1), as the constraints (4a) and (4b) consider only a fixed subset of users $\mathbb{K}_l$, while the variable $\mathbf{w}_{lk}$ covers only the beamforming vectors from a subset of RRHs to each user since $\mathbf{w}_{lk} = 0$ for $l \notin \mathbb{L}_k$. Therefore, problem (P4) can be solved by applying a method similar to that of dynamic algorithm but under fixed $\mathbb{L}_k$ instead of $\mathbb{L}$.

The WSR problem under static clustering can be resolved by Algorithm 2 given below [RHL13]. The variables $\mathbf{w}_k^{\mathbb{L}_k}$ and $\mathbf{H}_k^{\mathbb{L}_k}$ denote the beamforming vector and the channel matrix to user $k$ from the RRHs of its fixed cluster $\mathbb{L}_k$, respectively. They have the same size as $\mathbf{w}_k$ and $\mathbf{H}_k$, respectively, by only their elements corresponding to RRHs within their cluster $\mathbb{L}_k$ are non-zeros.

**Algorithm 2:** Static Algorithm

initialize frame $\mathbb{L}_k, \beta_k, \hat{r}_k, \mathbf{w}_k, \forall k$
**repeat**
1) Compute (3.7), (3.8), (3.9) by replacing $\mathbf{w}_k$ and $\mathbf{H}_k$ by $\mathbf{w}_k^{\mathbb{L}_k}$ and $\mathbf{H}_k^{\mathbb{L}_k}$, respectively
2) Fix $\mathbb{L}_k$ during the whole process
3) Call Dynamic Algorithm to solve (P4) under fixed $\mathbb{L}_k$
**until** *convergence*

It is worth noting that both dynamic and static algorithms implement user scheduling operation implicitly by optimizing the beamforming vectors for all the users in the entire network but only selecting those users with nonzero beamforming vectors to be served. This is in contrast to the conventional user scheduling approach, where typically a subset of users are pre-selected and only the beamforming vectors corresponding to those pre-selected users are optimized. The simulation results presented by the authors in [DY15] showed that the proposed algorithms are able to achieve better performance by scheduling the users implicitly, although the performance gain comes at a complexity cost.

We also note that both algorithms require global CSI at the BBU Pool in order

to schedule the users and to design beamformers accordingly, which may lead to tremendous amount of channel quality information overhead. Therefore, another goal we seek in our research work is to address the impact of CSI overhead on the system performance of H-CRAN under a more realistic model.

## 3.4 Proposed Hybrid Beamforming and User Clustering Algorithm

### 3.4.1 Reducing algorithm complexity

This section introduces our first contribution: A Hybrid beamforming and user clustering algorithm which leverages the advantages of both previously introduced dynamic and static clusterings, i.e., the performance optimality and cost reduction. As shown in the previous section, static clustering reduces the computational complexity as well as the number of signaling messages needed to update the user-to-RRH associations. However, this may degrade the achievable throughput performance compared to the dynamic optimal solution.

So far, several research works have focused on optimizing the system performance over each scheduling frame. However, to our knowledge, there have been no studies investigating the effects of these algorithms over a long-term process. Indeed, the time dimension of these optimization mechanisms has been ignored, and their feasibility in real and practical systems may be really costly. Our aim is to balance the performance and the complexity cost over a long-term optimization process while taking into account the network and user dynamics.

In the Hybrid algorithm, we propose to alternate dynamic and static clustering approaches in a periodic way. We define a period $T$ and apply the dynamic algorithm at each $T$ scheduled frames, while in the intermediate frames, a static algorithm is executed using the cluster subsets obtained from the previous dynamic frame. Note that we refer to the frames where we apply the dynamic algorithm as *dynamic frames*, and the frames where the static algorithm is applied as *static frames*. Our approach has the benefit to consider the temporal dimension of the allocation process which means that rather than focusing on finding an optimal solution for a given frame $t$, and repeating this process for each successive frame $(t+1, t+2, \ldots)$, we prefer considering the allocation optimization on

a longer observation time window to better consider the dynamics of the system parameters and their correlation over time. The motivation behind this hybrid approach lies in the fact that performing the optimal dynamic algorithm in each frame is not only computationally expensive but also unnecessary and resource wasteful whenever the channel, user and network states stay more or less stable over few successive frames.

Fig. 3.2 illustrates the principles of the Hybrid algorithm over a simple example where the period T is fixed to 3. In the intermediate frames $(t_1, t_2, t'_1, t'_2, \ldots)$, a static algorithm is executed using the cluster subsets obtained from the previous dynamic frames $(t_0, t'_0, \ldots)$. By doing so, we can narrow down the performance gap with the optimal dynamic solution, while reducing the required computational complexity, CSI feedback and re-association signaling overhead over the long-term allocation process. It is worth noting here that in the static intermediate frames, while the cluster subsets remain fixed, the optimal beamforming vectors are updated upon receiving new CSI feedback information.

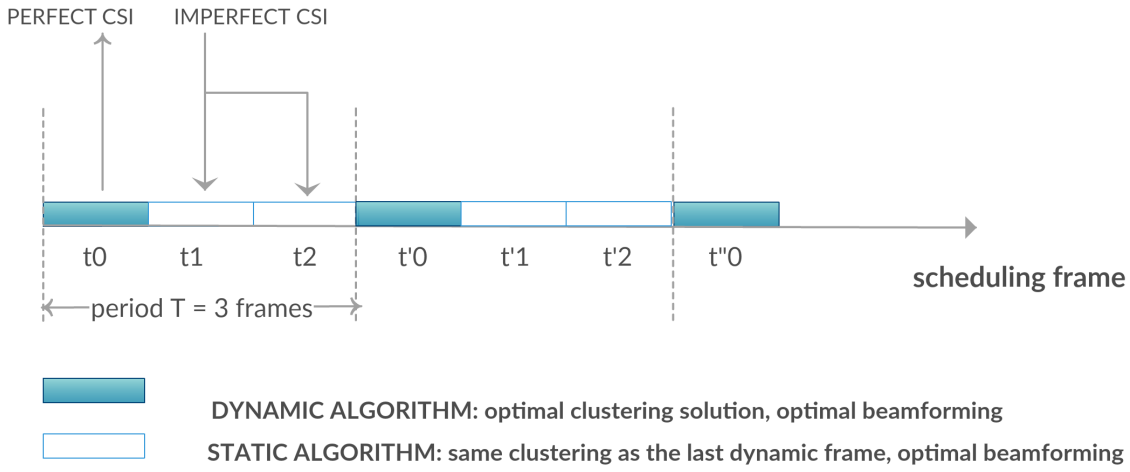


Figure 3.2: Hybrid algorithm with $T = 3$

The Hybrid algorithm allows to reduce three main cost metrics: amount of CSI overhead, user-to-RRH association signaling and computational complexity.

- **CSI overhead**: in this chapter, we consider 2 types of CSI feedback: perfect (full) CSI and imperfect CSI. Most of the literature assumes perfect CSI available at the BBU pool for each scheduling frame, where the full information of CSI is available without any delay or loss. Such an assumption is hardly

justified in real systems as it creates a tremendous burden on the fronthaul links. By limiting the number of RRHs serving each user, the static approach enables to reduce the amount of CSI feedback as CSI information is required only for the channels linking the user to a subset $\mathbb{L}_k$ of RRHs instead of all RRHs $\mathbb{L}$. Moreover, to enable additional CSI overhead savings, we propose to assume imperfect CSI at the BBU pool, where the CSIs are fed back with a delay (outdated CSI) or using an estimation method. In this chapter, we generated the imperfect CSI using an estimation error model that will be detailed in section 3.6.1. More precisely, we rely on a full and perfect CSI in dynamic frames, i.e., every $T$ frames so that the derived optimal solution is based on perfect knowledge of the instantaneous channels. For static frames, imperfect CSI is assumed which means that the algorithm will use the latest CSI fed back during the previous dynamic frame.

- **User-to-RRH association**: in the Hybrid algorithm, the user-to-RRH associations are optimized every $T$ frames, while the cluster subsets are fixed and kept stable for every intermediate static frame. By doing so, the number of re-association messages exchanged between the BBU pool, RRHs and users can be significantly reduced compared to the pure dynamic strategy in which the re-association messages are exchanged every scheduling frame.

- **Computational complexity**: a natural consequence of the Hybrid solution is to reduce the required computational complexity by making use of static clustering in intermediate frames. Indeed, a major source of complexity is the size of each beamforming vector $\mathbf{w}_k$ which is significantly reduced in the static frames compared to dynamic ones.

The main goal of the optimization process will be to maximize the period $T$ in order to minimize the above costs, while maintaining the performance degradation under acceptable limits. The details of the Hybrid clustering algorithm are summarized in Algorithm 3. The convergence time is assumed reached once the difference of the sum-rate between 2 successive frames does not exceed 1% in 20 consecutive frames.

**Algorithm 3:** Proposed Hybrid Clustering Algorithm with imperfect CSI

```
initialize frame t = 0, period T ;
repeat
    if mod(t,T) = 0 then
        Get perfect CSI H_k(t) for all users k ;
        Call Dynamic Algorithm ;
    else
        Use imperfect CSI H_k(δT) at t = δT + mod(t,T), for all users k;
        Call Static Algorithm ;
    Set clustering solution as the initial clusters for frame t+1 ;
    Move to next frame;
until convergence;
```

## 3.5 Cost analysis of the proposed Hybrid algorithm

In this section, we elaborate a cost analysis of the Hybrid algorithm in terms of the previously mentioned cost parameters.

### 3.5.1 CSI overhead

We consider two cases for CSI feedback for the proposed Hybrid algorithm. In the Full/Perfect CSI case, the CSI is fed back by every user to each of their serving RRH for every frame. While in the Imperfect CSI case, CSIs are returned only for dynamic frames, i.e., every $T$ frames, and used for all successive intermediate static frames. Based on these considerations, we can easily derive the amount of CSI overhead for each period $T$ in each of the following cases to be considered in the numerical evaluations:

- Dynamic algorithm with Full CSI:

$$O_{dyn}^{fcsi} = KLMNT, \tag{3.10}$$

- Hybrid algorithm with Full CSI:

$$O_{hybrid}^{fcsi} = \sum_{k}(L + (T-1)L_k)MN, \tag{3.11}$$

- Hybrid algorithm with Imperfect CSI:

$$O_{hybrid}^{icsi} = KLMN. \tag{3.12}$$

We recall here that M and N are the number of antennas per RRH and user, respectively. L is total number of RRHs and K is total number of users.

### 3.5.2 User-to-RRH re-association overhead

Signaling overhead is generally neglected in most of the related works, although it may be a serious issue in practical systems, especially for the dynamic clustering strategy as it continuously updates the user-to-RRH associations for each scheduling frame. In this work, we consider the total number of signaling messages generated by the re-association process following the derived beamforming and clustering solutions. More specifically, we denote by $S$ the amount of this signaling cost. Re-associations are counted for all newly established user-to-RRH links, or for released links between two successive frames. A simple calculation of the re-association cost $S$ averaged over all frames $I$ is given as follows:

$$S = \frac{1}{I} \sum_{i} \sum_{k} S_k^i \tag{3.13}$$

where $S_k^i$ is the re-association cost of user $k$ at frame $i$ and which can be expressed as

$$S_k^i = (|\{L_k^i \cup L_k^{i-1}\}| - |\{L_k^i \cap L_k^{i-1}\}|), \tag{3.14}$$

where $L_k^i$ is the number of RRHs serving user $k$ at frame $i$.

### 3.5.3 Computational complexity

As in [DY14], we assume a typical network model where $K > L > M > N$. In the proposed Hybrid algorithm, the complexity required for dynamic frames is given as $O(K^4L^3M^3)$ [DY14]. For static frames, the complexity of the algorithm is dominated by problem (P3). By solving the problem via interior point method, the

complexity of this problem will be similar to that of a linear program. The complexity in practice is in order of $n^2 m$ (assuming $m \geq n$), in which $n$ is the dimension of the solution and $m$ is the dimension of the constraint. In our problem, the total number of variables $\mathbf{w}_k$ and $R_k$ is $(\sum_{k=1}^{K} L_k M + K)$, while the largest dimension of constraints is given by (2b), i.e., $K \sum_{k=1}^{K} L_k M$. Thus, the complexity of static frames may be expressed as

$$O((\sum_{k=1}^{K} L_k M + K)^2 (K \sum_{k=1}^{K} L_k M)), \tag{3.15}$$

whose dominating term is given by

$$O(K^3 \sum_{k=1}^{K} L_k M). \tag{3.16}$$

## 3.6 Simulation Results

In this section, we numerically evaluate the performance of the proposed Hybrid clustering algorithm. We consider a 7-cell wrapped around two-tier H-CRAN. Each cell is a regular hexagon with a single macro-RRH located at the center and 3 pico-RRHs equally separated in space as illustrated in Fig. (3.3). The number of mobile users is varied between 5 and 30 per macro cell (corresponding to 35 and 210 users in the whole system). The users are randomly generated in the cell coverage. The fronthaul constraints for macro-RRH and pico-RRH are 683.1 Mbps and 106.5 Mbps, respectively, these values are typical ones as used in the baseline scheme considered in [DY15].

The simulations are realized using Matlab environment. We use CVX as the specific tool for convex optimization solver. The results are averaged over 20 random generations of channel matrix for two tier H-CRAN. An example of a generated cellular network is presented in Fig. 3.3.

The other parameter settings are presented in Table 3.1.

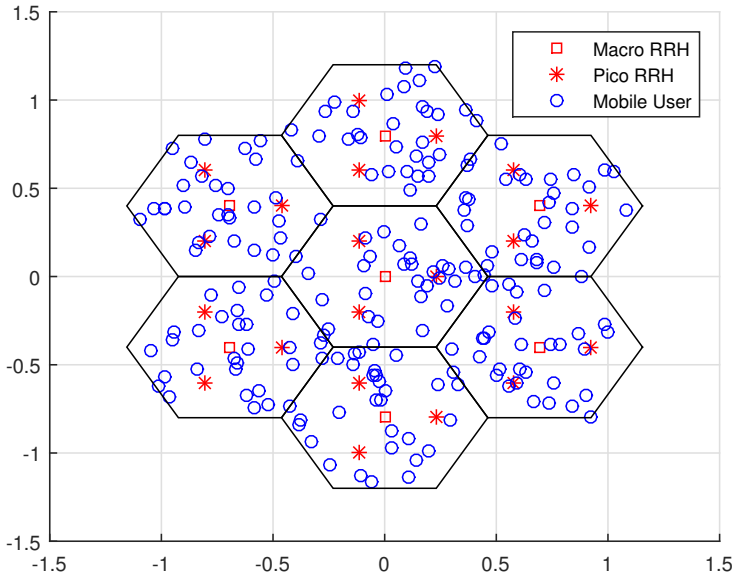


Figure 3.3: 7-cell wrapped around two-tier heterogeneous network with 30 users/cell

| Simulation parameters | |
|---|---|
| Cellular layout | Hexagonal 7-cell wrapped-around |
| Channel bandwidth | 10MHz |
| Intercell distance | 0.8km |
| Number of macro RRHs, pico RRHs, users per macro cell | (7,21,5-30) |
| TX power for macro/pico RRH | (43, 30) dBm |
| Antenna gain | 15 dBi |
| Background noise | -169 dBm/Hz |
| Path-loss from macro RRH to user | 128.1 + 37.6 log10(d) |
| Path-loss from pico RRH to user | 140.7 + 36.7 log10(d) |
| Rayleigh small scale fading | 0 dB |
| Log-normal shadowing | 8 dB |
| CSI error variance | -20 dB |

Table 3.1: Parameter settings for simulations

### 3.6.1 Hybrid algorithm performance

To take into account the temporal dimension of the allocation process, we consider the channel correlations between successive frames within a given period. We take the following correlation model [LSDL07] in which the channel at frame $i+1$ is expressed as $\mathbf{H}_k(i+1) = \mathbf{H}_k(i) + e(i)$. $e(i)$ is a complex Gaussian random variable with zero mean and variance $\sigma_h^2$, independent of $\mathbf{H}_k(i)$.

In Fig. 3.4, we show the average sum-rate convergence of reference dynamic and static algorithms and the proposed Hybrid algorithm with periods $T = 2$ and $T = 3$. Moreover, as setting $T \geq 4$ induced excessive sum-rate degradation compared to baseline algorithms, we choose to limit the appropriate period values to $T = 2$ and $T = 3$. We evaluate the performance with equal priority weights $\alpha_k = 1$ for every user k. Note that the fairness may be taken into account by varying $\alpha_k$. As we can see, the dynamic algorithm outperforms the static one, while the proposed Hybrid algorithm with $T = 2$ and $T = 3$ approaches the optimal sum-rate performance of the dynamic algorithm. As expected, the smaller the period, the closer the proposed solution to the optimal case. As the period increases, the Hybrid algorithm derives a solution based on a more outdated initial clustering. But still, the deterioration of the proposed algorithm is limited (6.4 % for $T = 2$ and 9.1% for $T = 3$) compared to that of the static algorithm (30 %).

In Fig. 3.5, we observe the sum-rate performance as a function of the number of users per macro cell. We can see that the proposed Hybrid algorithm with perfect CSI for $T = 2$ (red line) always achieves the closer performance to the dynamic optimal solution, while the Hybrid algorithm with imperfect CSI (green line) presents a quite considerable throughput degradation to the perfect CSI case.

It is also worth noting that the proposed method with $T = 3$ with perfect CSI (cyan line) behaves better than with T=2 and imperfect CSI (green line). With $T = 3$ and imperfect CSI, the proposed method is also outperformed by the static algorithm with perfect CSI. These observations prove that the proposed CSI estimation method is not enough accurate to achieve a good performance in case of imperfect CSI, the main reason is that the value of random error variable $e_i$ does not give a smooth correlation between the channels of successive frames. Therefore, it is crucial to find a much more advanced method of CSI estimation in the our next developments.

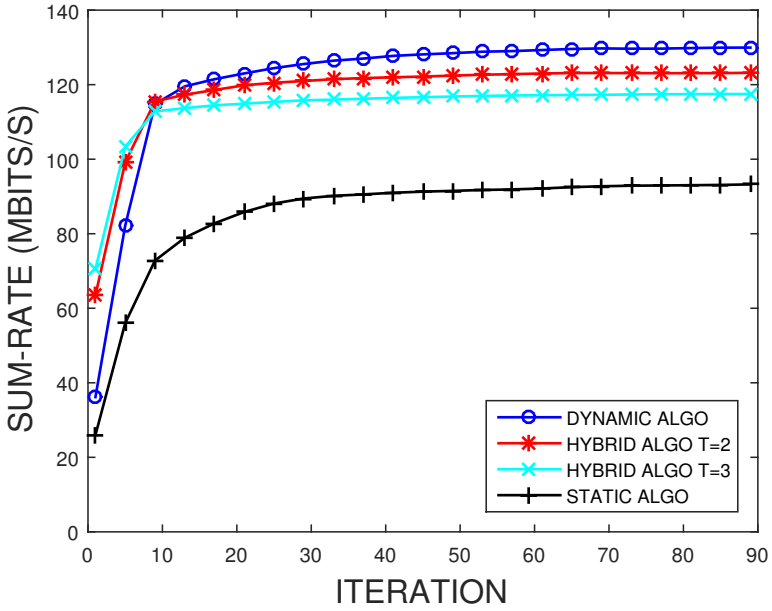


Figure 3.4: Average sum-rate convergence against number of iterations

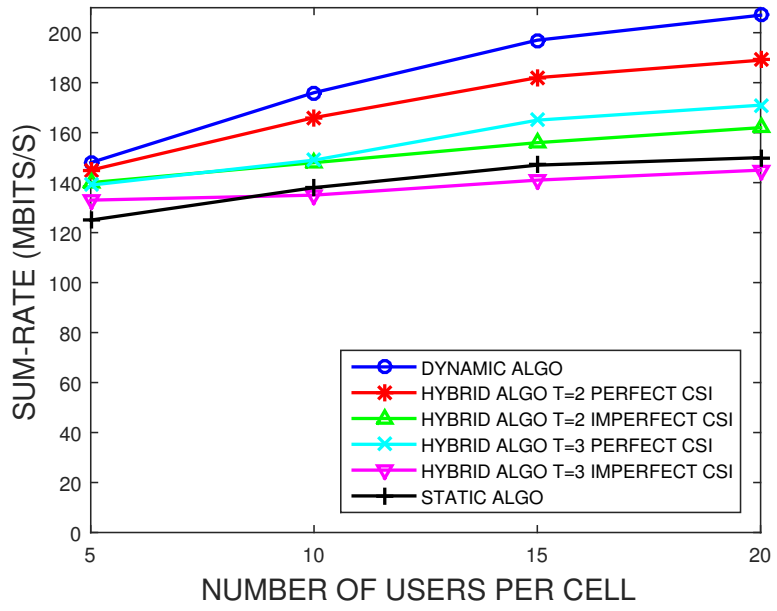


Figure 3.5: Sum-rate performance as function of the number of users per macro cell

In Fig. 3.6, we plot the cumulative distribution function of per user data rates for all the algorithms with Perfect CSI. The Hybrid algorithm shows almost similar performance as the dynamic algorithm. The user rate at the 50-th percentile reaches about 98% and 99% of the optimal performance with $T = 2$ and $T = 3$, respectively. The performance of the static algorithm is the lowest: about 81% of the optimal performance at 50-th percentile.

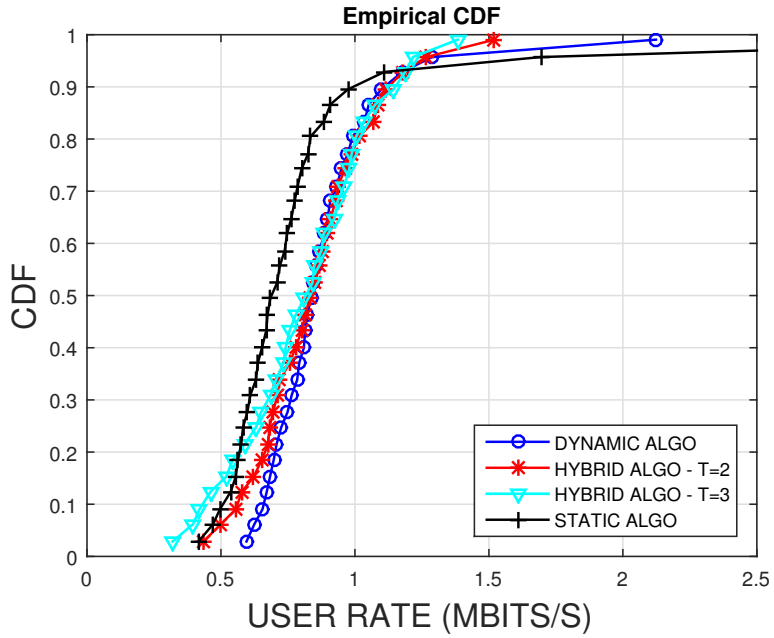


Figure 3.6: Cumulative distribution function of user data rate

To evaluate the cost reduction achieved by our proposed algorithm, we first plot in Fig. 3.7 the amount of CSI feedback overhead as a function of the number of users per macro cell. We observe that the Hybrid algorithm with perfect CSI provides an important reduction in CSI overhead compared to the dynamic scheme (43-48% for T=2 and 63-66% for T=3). This comes from the reduction of the required CSIs to be fed back owing to smaller cluster sizes in intermediate static frames. Moreover, the performance in terms of CSI overhead can be further improved by employing imperfect CSI instead of perfect CSI.

Furthermore, the Hybrid algorithm enables a significant reduction of the number of user-to-RRH association messages. For example, for the case of 20 users per macro cell, from the simulation results, we obtain $S_{Dyn} = 1057$ for the dynamic

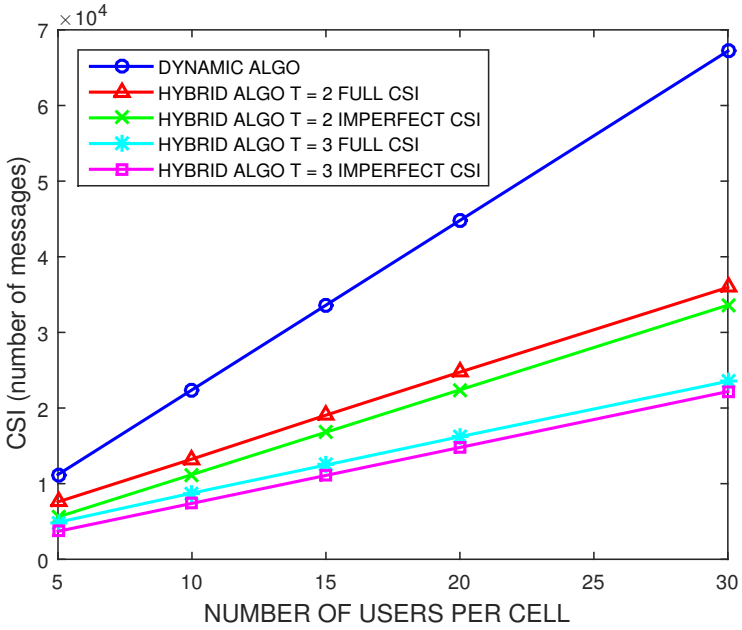


Figure 3.7: CSI overhead as function of the number of users per macro cell

scheme, $S_{Hybrid} = 483$ for the proposed scheme with $T = 2$ and $S_{Hybrid} = 273$ with $T = 3$, resulting into 54.3% and 74% reduction, respectively.

| Number of users/cell | 10 | 15 | 20 | 30 |
|---|---|---|---|---|
| Dynamic algo | $4.2 \times 10^{12}$ | $2.1 \times 10^{13}$ | $6.7 \times 10^{13}$ | $3.4 \times 10^{14}$ |
| Hybrid algo T=2 | $5.4 \times 10^{7}$ | $2.0 \times 10^{8}$ | $4.7 \times 10^{8}$ | $1.8 \times 10^{9}$ |
| Hybrid algo T=3 | $5.1 \times 10^{7}$ | $1.9 \times 10^{8}$ | $4.4 \times 10^{8}$ | $1.7 \times 10^{9}$ |

Table 3.2: Computational complexity as function of the number of users per macro cell

Finally, in Table 3.2, we show the computational complexity gain obtained by our proposed algorithm with $T = 2$ and $T = 3$ when compared to the dynamic solution. The results prove that our scheme reduces drastically the complexity mainly thanks to the smaller cluster sizes $L_k$ per user $k$ used in intermediate static frames. From the complexity formula presented in Section 3.5.3, we can easily observe that the reduction in complexity is proportional to the period $T$.

Comparing the degradation rate of sum-rate performance to the gain in terms of user-association messages, CSI overhead and algorithm complexity, we can certainly assert that the proposed Hybrid clustering can ensure a good agreement for the performance-cost trade-off. The appropriate tuning of the algorithm's

parameters such as period $T$ and type of CSI will play an important role on the global system performance. Our next objective is to go further in the analysis to better comprehend the correlation between all the involved parameters and their effect on the targeted performance metrics while being aware of all system dynamics.

## 3.7 Conclusion

In this chapter, we presented our first contribution: the Hybrid beamforming and user clustering algorithm. Our algorithm's periodic activation of dynamic and static clustering strategies leverages both the optimality of the dynamic solution and the low-complexity of its static counterpart. The key benefit of the proposed Hybrid algorithm is to take into account the temporal dimension of the allocation process while being aware of practical system operation metrics. The numerical results show that the proposed solution narrows significantly the performance gap with the optimal dynamic solution, while considerably reducing the required computational complexity, CSI feedback and re-association signaling overhead when considering the user scheduling process over several frames.

However, in this first contribution we manually varied the value of the period as our primary goal was to analyze and observe the impact of such parameter. Our ultimate objective is to enhance this algorithm to tune and adapt dynamically the value of T based on the user and network dynamics such as user channels, user mobility, user/RRH densities, etc.

# Chapter 4

# An Advanced Mobility-Aware Algorithm for Joint Beamforming and Clustering in Heterogeneous Cloud Radio Access Networks

## 4.1 Introduction

The emergence of the Internet of Things (IoT) applications bring a tremendous number of communicating mobile users. This forward momentum won't lead only to a massive mobile and wireless data traffic but also a problem of mobility management [GJ15]. In addition, when migrating from traditional macrocell deployment to HetNet environments, recent studies have demonstrated that mobility becomes more challenging, due to potentially more exigent interference conditions, small cells coverage appearing and disappearing more frequently with UE devices movements [BMSP12, LGX12].

Therefore, the problem of beamforming and clustering that we consider in this thesis becomes much more complex due to two main reasons: Firstly, as the user moves, its serving RRH cluster also changes quickly, which requires more CSI overhead to update the association; Secondly, the system performance such as sum-rate will be strongly impacted by the mobility, which should influence optimal performance-cost trade-off for a larger time-scale optimization perspective.

To alleviate the problem of control signaling and CSI overhead costs, we have proposed in the previous chapter [TBKM17] a hybrid user clustering and beamforming algorithm for weighted sum-rate maximization. This hybrid scheme is able to leverage the advantages of both dynamic and static user clusterings in H-CRAN, where the dynamic clustering performs optimally at the expense of maximum signaling overhead, while static clustering performs worse but drastically reduces the amount of overhead. The proposed Hybrid algorithm was shown to achieve a good performance compared to dynamic clustering, while greatly reducing the required computational complexity, amount of CSI feedback and reassociation signaling. However, in this first work we did not consider any user mobility issues.

Our objective in this chapter is two-fold: first, we aim to consider and analyze the impact of more realistic channel variations due to different user velocities on the Hybrid algorithm behavior. Second, based on this analysis we plan to develop a new version of the Hybrid algorithm which takes into account the mobility dynamics of users and tries to take the best decision on parameters tuning to achieve the best performance. More particularly, we consider in this chapter a different optimization problem. Namely, we propose a heuristic algorithm for minimizing a cost function in terms of computational complexity and CSI overhead for a given targeted sum-rate reflecting a minimum Quality-of-Service (QoS) requirement.

The rest of this chapter is structured as follows: Section 4.2 describes the system model, the problem formulation and gives the reference schemes. Next, we describe in Section 4.3 our proposed mobility-aware algorithm and conduct its cost analysis in section 4.4. The simulation results are presented in section 4.5. Finally, Section 4.6 concludes the chapter.

## 4.2 System model and problem formulation

### 4.2.1 System model

We consider the same H-CRAN model presented in the previous chapter and which consists of one BBU Pool, $L$ macro and pico RRHs and $K$ users. Each RRH and user is equipped with $M$ and $N$ antennas, respectively, and users are randomly located in the network area.

We recall that $\mathbb{L} = \{1,2,...,L\}$ and $\mathbb{K} = \{1,2,...,K\}$ are the sets of RRHs and of users, respectively. The propagation channel from RRHs to the $k^{th}$ user is denoted as $\mathbf{H}_k \in \mathbb{C}^{N\times ML}, \forall k \in \mathbb{K}$ which includes the path loss and Rayleigh fading effects.

We denote by $h_{n,q}$, the $(n,q)-th$ element of matrix $\mathbf{H}_k$, where $q = (l-1)M + m, l \in [1,L], m \in [1,M]$. Hence, $h_{n,q}$ is the channel gain between the $m$-th antenna of the $l$-th RRH and the $n$-th antenna of user $k$. Given the user mobility profile, channel correlations will be assumed between the consecutive scheduling frames, as detailed in next Section 4.2.2.

Let $\mathbf{w}_k \in \mathbb{C}^{ML\times 1}$ be the transmit beamforming vector from all RRHs to the $k^{th}$ user,

$$\mathbf{w}_k = \left[\mathbf{w}_{1k}^H, \cdots, \mathbf{w}_{lk}^H, \cdots, \mathbf{w}_{Lk}^H\right]^H,$$

where $\mathbf{w}_{lk} \in \mathbb{C}^{M\times 1}$.

Let $s_k \in \mathbb{C}$ be the encoded information symbol for user $k$ with $\mathbb{E}\left[|s_k|^2\right] = 1$. The received signal at user $k$, $\mathbf{y}_k \in \mathbb{C}^{N\times 1}$, is expressed as

$$\mathbf{y}_k = \mathbf{H}_k\mathbf{w}_k s_k + \mathbf{H}_k \sum_{j=1, j\neq k}^{K} \mathbf{w}_j s_j + \mathbf{n}_k,$$

where $\mathbf{n}_k \sim \mathscr{CN}(\mathbf{0}, \sigma_k^2\mathbf{I}_N)$ is the additive white Gaussian noise and $\mathbf{I}_N$ is the identity matrix of size $N \times N$.

The SINR at user $k$ can be expressed as

$$SINR_k = \frac{|\mathbf{u}_k^H\mathbf{H}_k\mathbf{w}_k|^2}{\sum\limits_{j=1, j\neq k}^{K} |\mathbf{u}_k^H\mathbf{H}_j\mathbf{w}_j|^2 + \sigma_k^2\|\mathbf{u}_k\|_2^2}, \tag{4.1}$$

where $\mathbf{u}_k \in \mathbb{C}^{N\times 1}$ is the receive beamforming vector of user $k$.

The achievable rate of user k is given by

$$r_k = \log_2(1 + \mathbf{w}_k^H\mathbf{H}_k^H(\sum_{j=1, j\neq k}^{K} \mathbf{H}_k\mathbf{w}_j\mathbf{w}_j^H\mathbf{H}_k^H + \sigma_k^2\mathbf{I}_N)^{-1}\mathbf{H}_k\mathbf{w}_k). \tag{4.2}$$

### 4.2.2 CSI estimation in mobile environment

In this chapter, we aim to extend our Hybrid algorithm by designing an advanced mobility-aware version of the solution which can dynamically adapt the algorithm's parameters to the changes of users mobility and hence the channel conditions.

Clearly, we expect a strong relation between the user's velocity and the dynamic scheduling frequency. More precisely, when the mobility is high, the fast changing channel conditions require frequent CSI acquisitions to better optimize the beamforming and clustering allocation and this results in selecting a smaller period $T$. Conversely, when mobility is low, $T$ could be larger to achieve gains in terms of CSI feedback and re-association signaling provided that the CSI information is not too outdated.

To cope with the outdated CSI problem, we propose to use a CSI estimation model based on the user's mobility. The proposed approach is based on [MSKS12] for modeling the estimated CSI matrix $\hat{\mathbf{H}}_k \in \mathbb{C}^{N \times ML}, \forall k \in \mathbb{K}$. We denote by $\hat{h}_{n,q}$, the $(n,q)-th$ element of matrix $\hat{\mathbf{H}}_k$, where $q = (l-1)M + m$. Hence, $\hat{h}_{n,q}$ is the estimated channel gain between the $m$-th antenna of the $l$-th RRH and the $n$-th antenna of user $k$, which is estimated as

$$\hat{h}_{n,q} = \lambda_v h_{n,q} + (\sqrt{1-\lambda_v^2})\beta_{n,q}, \tag{4.3}$$

In (4.3), $\beta_{n,q} \sim \mathscr{CN}(0, F_{lk})$ where $F_{lk}$ is the large-scale fading of the downlink channel from RRH $l$ to user $k$, $\lambda$ is the correlation coefficient between $\hat{h}_{n,q}$ and $h_{n,q}$ which is expressed as

$$\lambda = J_0(2\pi f_{d,lk} T_{d,l}), \tag{4.4}$$

where $J_0(.)$ is the zeroth order Bessel function, $T_{d,l}$ is the fronthaul delay of the RRH $l$ and $f_{d,lk}$ is the maximum Doppler frequency of the channel between the RRH $l$ and user $k$. If the user moves at speed $v$ (m/s), then the maximum Doppler frequency is calculated as $f_d = \frac{vf}{c}$, where $f$ is the carrier frequency in Hertz and $c$ is the speed of light. Therefore, we can express $\lambda$ as function of $v$,

$$\lambda_v = J_0\left(\frac{2\pi f T_{d,l}}{c} v\right), \tag{4.5}$$

This mobility-aware CSI estimation approach allows to save CSI feedback in the static frames but at the risk of a possible degradation in throughput compared to the case where perfect and full CSI is available. Such degradation will depend on CSI variations and hence on users mobility.

### 4.2.3 Problem formulation and reference schemes

In this first part of this chapter, we focus on the same weighted sum-rate maximization problem (P1) that have been presented in the previous chapter and which is formulated as follows,

$$\begin{aligned} \max_{\{\mathbf{w}_{lk}, l\in\mathbb{L}, k\in\mathbb{K}\}} \quad & \textstyle\sum_{k=1}^{K} \alpha_k r_k & (1) \\ \text{s.t.} \quad & P_l = \sum_{k=1}^{K} \|\mathbf{w}_{lk}\|_2^2 \leq P_l^{max}, \forall l \in \mathbb{L} & (1a) \\ & \sum_{k=1}^{K} 1\{\|\mathbf{w}_{lk}\|_2^2\} r_k \leq C_l^{max}, \forall l \in \mathbb{L} & (1b) \end{aligned} \tag{P1}$$

Compared to the previous chapter, the rate $r_k$ in problem (P1) is a function of user velocity as it is a function of the channel. Therefore, the solution of (P1) will be clearly affected by the mobility.

As in the previous chapter, we rely on two reference schemes namely the dynamic and static clusterings which were described in chapter 3 [DY14] [DY15].

## 4.3 Proposed Adaptive Beamforming and User Clustering (ABUC) Algorithm

ABUC is based on the hybrid clustering concept that we introduced in the previous chapter and in which we proposed to alternate dynamic and static clustering approaches in a periodic way. The goal of ABUC algorithm is to enable a high weighted sum-rate performance, while reducing the induced costs in terms of CSI feedback and signaling overhead, given channel time-variations. Compared to the previous chapter, in this work, we extend our algorithm to cope with different types of user mobility profiles. In consequence, the CSI estimation method is also improved as it is tailored to time-varying channels reflecting user mobility.

In practical H-CRAN, due to the delayed feedback, partial information or estimation error of CSI, the obtained channel is not perfect. Indeed, the imperfection in CSI has been proven to have a significant impact on the system performance [AAD+16]. Therefore, we will extend the proposed algorithms in the previous chapter to solve the joint beamforming and clustering problem in the presence of different CSI feedback strategies during the scheduling process, namely: Full CSI, Partial CSI and Estimated CSI which are defined as follows:

- *Full CSI:* CSIs are assumed to be perfect at each frame and can be fully used in all scheduling frames.
- *Partial CSI [RL14, PEW+18]:* perfect CSIs are only known at dynamic frames (each period $T$), while at intermediate frames the channel gains are set equal to the last Full CSI received in the previous dynamic frame.
- *Estimated CSI [MSKS12]:* perfect CSIs are only known at dynamic frames (each period $T$) and at each intermediate frame CSIs are estimated according to the model given by Eq. (4.3).

Note that unlike Partial and Estimated CSI approaches, the Full CSI assumption is impractical in real systems due to the fronthaul delays and the signaling burden, which justifies our assumption of imperfect CSI knowledge at the BBU pool.

Combining these CSI feedback strategies and the periodicity $T$ results into the following variants of the proposed ABUC algorithm:

- *($T$, Full CSI)*: Full CSI fedback every frame for beamforming; dynamic clustering optimization every $T$ frames,
- *($T$, Partial CSI)*: CSI fedback every $T$ frames, reused in all intermediate frames for beamforming; dynamic clustering optimization every $T$ frames,
- *($T$, Estimated CSI)*: CSI fedback every $T$ frames, estimated for all intermediate frames for beamforming; dynamic clustering optimization every $T$ frames.

Based on these considerations, we can derive the amount of CSI overhead for each period $T$ in each of the following cases to be considered in the numerical evaluations:

- Dynamic algorithm with Full CSI:

$$O^{f}_{dyn} = KLMNT, \tag{4.6}$$

- ABUC algorithm with Full CSI:

$$O^{f}_{ABUC} = \sum_{k}(L + (T-1)L_k)MN, \tag{4.7}$$

- ABUC algorithm with Partial CSI and Estimated CSI:

$$O^{p,e}_{ABUC} = KLMN. \tag{4.8}$$

The detailed description of the proposed ABUC algorithm is given in Algorithm 4.

**Algorithm 4:** Proposed ABUC Scheme with different types of CSI

initialize frame t = 0, user velocity $v$

**repeat**

  **if** $t \mod T = 0$ **then**

    Get perfect CSI $\mathbf{H}_k(t)$ for all users $k$

    Call Dynamic Algorithm

  **else**

    **if** *Full CSI* **then**

      Get perfect CSI $\mathbf{H}_k(t)$ for all users $k$

    **else if** *Partial CSI* **then**

      Use imperfect CSI $\hat{\mathbf{H}}_k(t) = \mathbf{H}_k(t - \mod(t, T))$, for all users $k$

    **else**

      Estimate CSI $\hat{\mathbf{H}}_k(t)$ following (4.3) for all users $k$

    Call Static Algorithm

  Set clustering solution as the initial clusters for frame t+1

  Move to next frame

**until** *convergence*

| Simulation parameters | |
|---|---|
| Cellular layout | Hexagonal 7-cell wrapped-around two-tier model |
| Channel bandwidth | 10MHz |
| Intercell distance | 0.8km |
| TX power for macro/pico RRH | (43, 30) dBm |
| Antenna gain | 15 dBi |
| Background noise | -169 dBm/Hz |
| Path-loss from macro RRH to user | 128.1 + 37.6 log10(d) |
| Path-loss from pico RRH to user | 140.7 + 36.7 log10(d) |
| Log-normal shadowing | 8 dB |
| CSI error variance | -20 dB |
| User priority weights $\alpha_k$ | 1 $\forall k$ |

Table 4.1: Parameter settings for simulations

## 4.4 Numerical Results of ABUC algorithm

In this section, we numerically evaluate the performance of the proposed ABUC algorithm. We consider a 7-cell wrapped around two-tier H-CRAN. Each cell has a single macro-RRH and 3 pico-RRHs equally separated in space. The number of mobile users is varied between 5 and 20 per macro-cell, uniformly distributed over the coverage area. We assume a Random Waypoint model to represent users' movements, in which each user move to a random direction with fixed velocity during every scheduling frame. The fronthaul constraints for macro-RRH and pico-RRH are 683.1 Mbps and 106.5 Mbps, respectively [DY15]. All channels undergo Rayleigh small scale fading and log-normal shadowing. The other parameter settings are presented in Table 4.1.

To evaluate the performance of the proposed ABUC algorithm and its behavior with regards to user mobility, we consider different mobility profiles represented by the parameter $\lambda$ which is a function of velocity. In equation (4.5), we set the carrier frequency $f$ and the fronthaul delay $T_{dl}$ for all RRH $l$ as 900 MHz and 2 ms [3GP14], respectively.

The algorithms are executed on Matlab environment during a time period randomly selected. To guarantee a good confidence interval, we ploted a average of 30 experiments representing different random initial positions of users and channel realizations.

### 4.4.1 ABUC algorithm performance

To evaluate the performance of the proposed ABUC algorithm and its behavior with regards to user mobility, we consider different mobility profiles represented by the parameter $\lambda$ which is a function of velocity. In equation (4.5), we set the carrier frequency $f$ and the fronthaul delay $T_{dl}$ for all RRH $l$ as 900 MHz and 2 ms [3GP14], respectively.

The performance of ABUC algorithm is compared to two baseline schemes, namely dynamic and static algorithms with Full CSI as in [DY14, DY15]. Note that considering Full CSI for static and dynamic algorithms guarantees their best sum-rate performance. For ABUC scheme, we varied both CSI feedback strategy and the period value $T$. We focus on three representative types of mobility profiles: low, medium and high mobility with fixed velocities of 6 km/h, 36 km/h and 72 km/h, respectively.

#### 4.4.1.1 Sum-rate performance

In Fig. 4.1, we show the average sum-rate convergence of reference dynamic and static algorithms for $K = 10$ users per macrocell, and the proposed ABUC algorithm with periods $T = 2$ and $T = 3$ for all CSI feedback strategies. It is worth noting that ABUC with $T = 1$ is equivalent to the dynamic algorithm with Full CSI. As we can observe in the figure, the dynamic algorithm outperforms the static one, while ABUC algorithm with Full CSI is closer to the optimal sum-rate performance of the dynamic algorithm. As expected, the larger the period, the lower the performance of our proposed solution since it uses a more outdated clustering solution (derived in the last dynamic frame). In addition, ABUC scheme with Estimated CSI shows a very close performance to ABUC with Full CSI case under low mobility (see Fig. 4.1 (a)). However, its performance degrades with higher velocities as the Estimated CSI quality looses accuracy as shown in Figs. 4.1 (b),(c). Under high mobility, Fig. 4.1 (c) shows that the Estimated CSI strategy degrades even below the Partial CSI scheme. This behavior will be further discussed in the next subsection.

Fig. 4.2 evaluates the sum-rate performance as a function of the number of users per macro cell and their mobility profile. We can observe the same tendency in performance with the increasing number of users. ABUC algorithm with

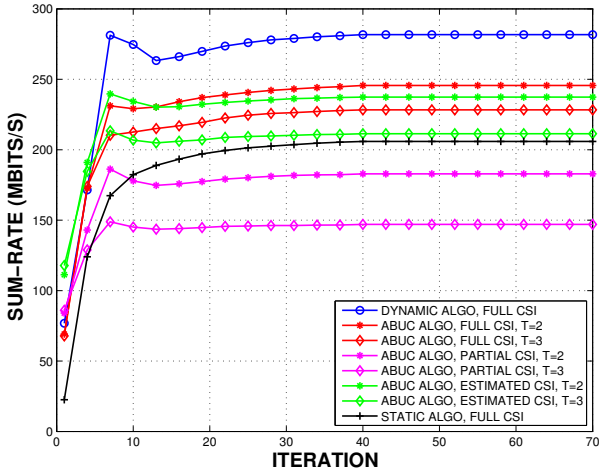


(a) Low mobility (6 km/h)

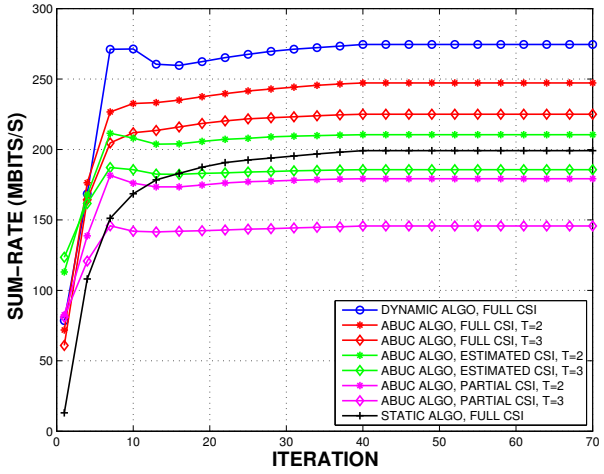


(b) Medium mobility (36 km/h)

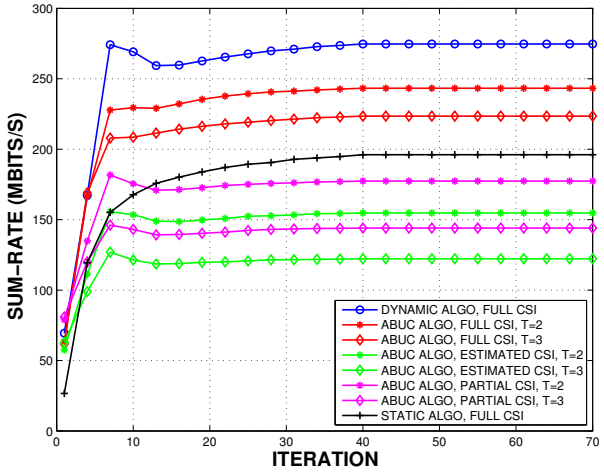


(c) High mobility (72 km/h)

Figure 4.1: Average sum-rate convergence against number of iterations

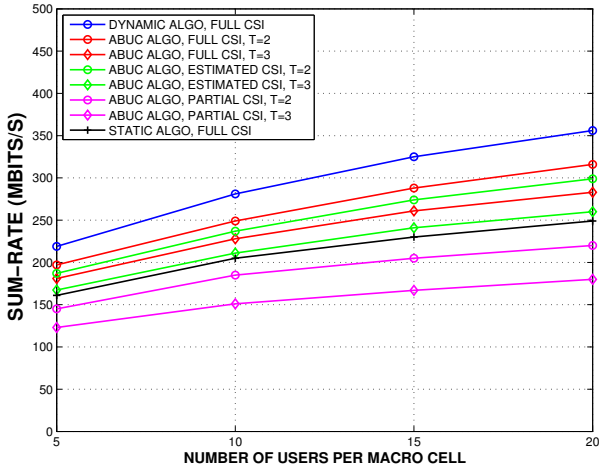


(a) Low mobility (6 km/h)

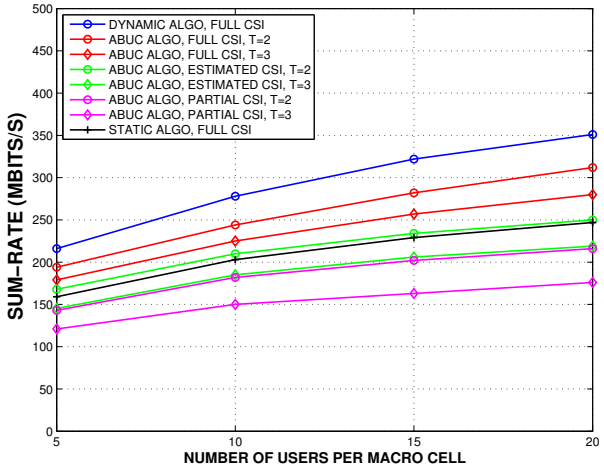


(b) Medium mobility (36 km/h)

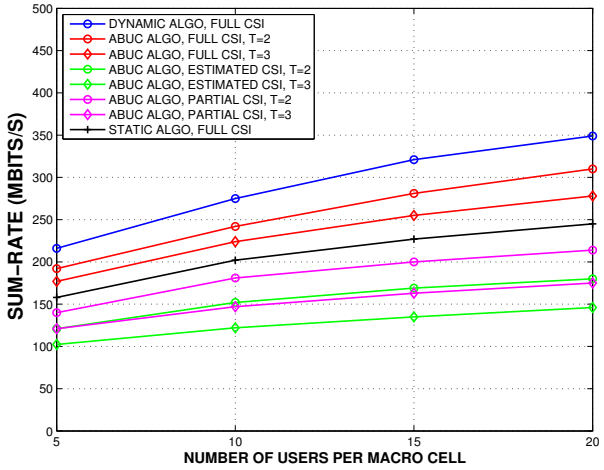


(c) High mobility (72 km/h)

Figure 4.2: Sum-rate performance as function of the number of users per macro cell

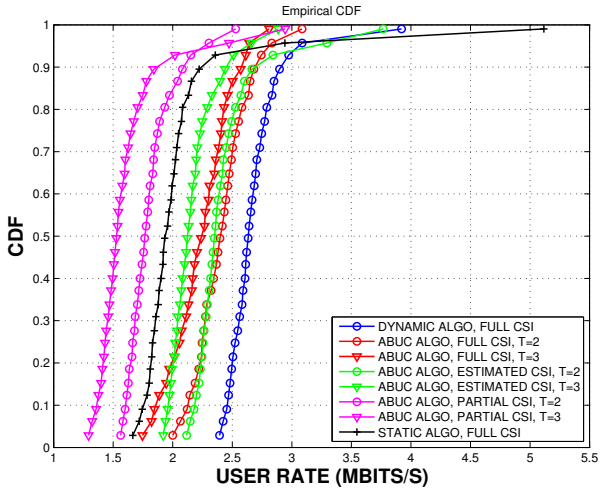


(a) Low mobility (6 km/h)

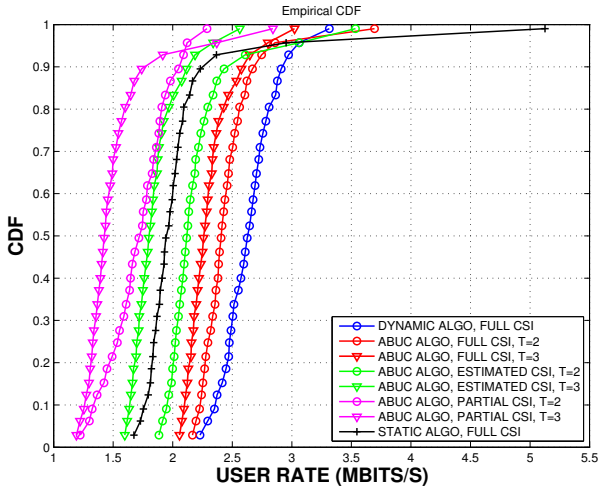


(b) Medium mobility (36 km/h)

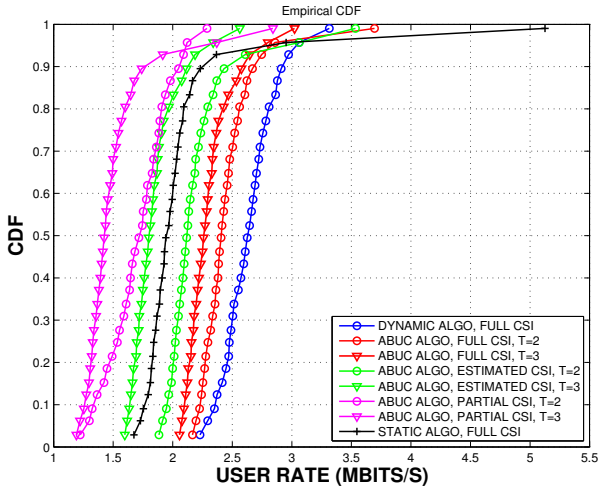


(c) High mobility (72 km/h)

Figure 4.3: Cumulative distribution function of user data rate

Full CSI offers a close performance to the dynamic optimal solution for all mobility scenarios. Again, ABUC with Estimated CSI exhibits a good performance for lower mobility while Partial CSI outperforms it for high mobility. From these figures, we can also observe the effect of period $T$ on the sum-rate: ABUC with $T = 3$ and Full CSI behaves better than with T=2 and Partial CSI. With $T = 3$ and Partial CSI, the proposed method is outperformed by the static algorithm with full (perfect) CSI, showing the importance of accurate CSIs.

In Fig. 4.3, we plot the cumulative distribution function (CDF) of per user data rates for proposed ABUC variants and baseline dynamic and static algorithms. We notice that the ABUC algorithm shows a near performance to the dynamic algorithm in case of Full CSI, i.e. it reaches up to 91.3% and 86.8% of the optimal performance with $T = 2$ and $T = 3$ at the 50-th percentile, respectively, for low mobility scenario. We can also point out that in this case of low mobility the behavior of the proposed ABUC with Estimated CSI which tends to allocate more resources to low CSI quality users unlike the ABUC with Full CSI dynamic algorithm which concentrates the resources towards best CSI users to maximize the global sum-rate.

#### 4.4.1.2 Cost performance

Another important part of the analysis concerns the costs induced by all the compared schemes. We first plot in Fig. 4.4 the amount of generated CSI feedback overhead as a function of the number of users. We can see that all variants of ABUC algorithm provide an important reduction in CSI overhead compared to the dynamic scheme (43-48% for T=2 and 63-66% for T=3). For the ABUC Full CSI case, this gain comes from smaller cluster sizes ($L_k \leq L$ in equation (4.7)) in intermediate static frames. Moreover, the performance in terms of CSI overhead can be significantly improved by employing Partial CSI or Estimated CSI instead of Full CSI. Note that the amount of CSI feedback for partial and Estimated CSI is equal as shown in equation (4.8).

Furthermore, ABUC algorithm enables a large reduction of the number of user-to-RRH association messages. We plot in Fig. 4.5 the re-association cost of ABUC algorithm compared to the dynamic one for the three mobility profiles and different user loads (10 and 20 users per macro cell). In this figure, we observe a significant reduction of re-association messages for ABUC scheme compared to

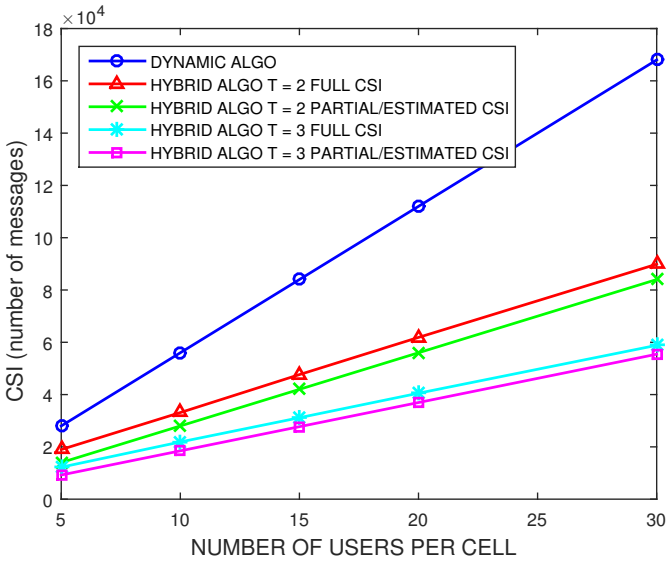


Figure 4.4: CSI overhead as function of the number of users per macro cell

the dynamic one, which is even more under high user load. Note that as shown in section 4.3, the re-association cost of the proposed algorithm depends only on period $T$ and is unaffected by the CSI feedback strategy. With $T = 2$ and $T = 3$ ABUC achieves 54.3% and 74% reduction compared to the dynamic scheme, respectively. In addition, the results show that the mobility acts on the generated re-association messages as high user mobility requires more frequent changes of serving RRHs over successive scheduling frames. However, this increase in re-association cost is marginal proving the robustness of the proposed schemes against varying user loads and velocities.

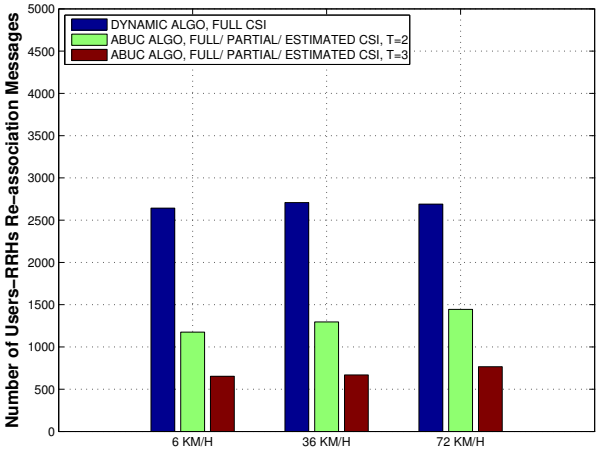


(a) 10 users/macro cell

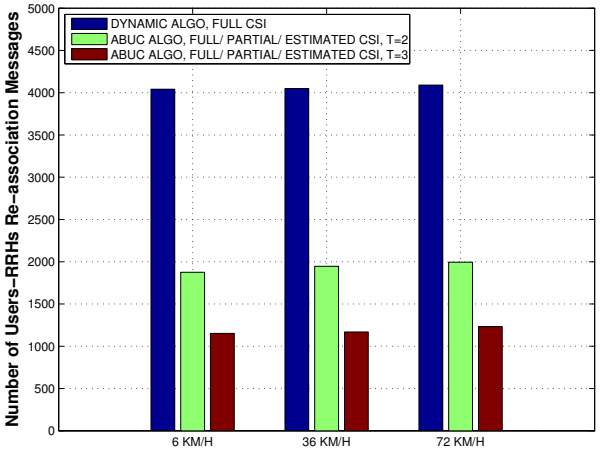


(b) 20 users/macro cell

Figure 4.5: Re-association cost as function of number of users per macro cell

#### 4.4.1.3 Complexity performance

We represent in Table 4.2 the computational complexity of ABUC algorithm compared to dynamic algorithm. We can see that ABUC with both values of T drastically decreases the computation complexity owing mainly to the smaller cluster sizes $L_k$ used in intermediate static frames. Note that we can also observe that the reduction in complexity for ABUC is proportional to the period T.

| Number of users/macro cell | 10 | 20 | 30 |
|---|---|---|---|
| Dynamic algo | $4.2 \times 10^{12}$ | $6.7 \times 10^{13}$ | $3.4 \times 10^{14}$ |
| ABUC algo T=2 | $5.4 \times 10^{7}$ | $4.7 \times 10^{8}$ | $1.8 \times 10^{9}$ |
| ABUC algo T=3 | $5.1 \times 10^{7}$ | $4.4 \times 10^{8}$ | $1.7 \times 10^{9}$ |

Table 4.2: Computational complexity as function of the number of users per macro cell

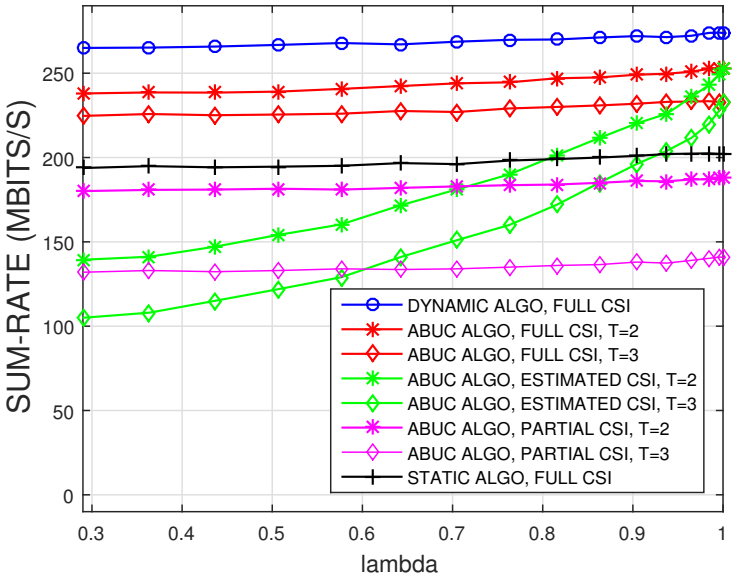


Figure 4.6: Sum-rate performance against lambda

### 4.4.2 Performance-cost tradeoff analysis: a mobility perspective

In this section, we discuss the performance-cost tradeoff under different mobility conditions. To characterize the different variants of ABUC algorithm, we define the parameters $(T, f)$, where $T$ is the period of dynamic frames, and $f$ is the CSI feedback strategy used for intermediate frames, i.e., $T \in \{2,3\}$ and $f$ may be chosen among Full CSI, Partial CSI and Estimated CSI.

Fig. 4.6 summarizes the sum-rate behavior of all algorithms against users velocities represented by the correlation coefficient $\lambda$ (Equation (4.3)). As we can see, $\lambda$ approaching 1 corresponds to the fixed users scenario and hence the Estimated CSI is very close to the real channel state, explaining why our ABUC scheme with Estimated CSI closely approaches its performance with Full CSI. On the other end, when $\lambda$ tends to 0, the user velocity is very high leading to

very dynamic channel variations. This can be observed on the performance of ABUC with Estimated CSI which degrades even lower than the case with Partial CSI given the poor quality of the CSI estimation. In addition, we observe that unlike ABUC with full and Partial CSI strategies, the performance of ABUC with Estimated CSI is strongly dependent on user mobility. In light of these considerations and the performance tendencies noticeable in Fig. 4.6, we identify three mobility regions: low mobility, medium mobility and high mobility corresponding to the velocity and $\lambda$ ranges (0-18 km/h ; $0.96 \leq \lambda \leq 1$), (18-54 km/h ; $0.7 \leq \lambda \leq 0.96$), ($v \geq 54$ km/h ; $\lambda \leq 0.6$), respectively. For each range of velocity, we can deduce the most suitable algorithm with its parameters $(T, f)$ that can balance the trade-off between sum-rate performance and the generated costs.

- *Low mobility scenario*: from Fig. 4.6, ABUC scheme with Estimated CSI for both values of $T$ ($T = 2$ and $T = 3$) closely approaches ABUC sum-rate performance with Full CSI, while largely reducing the CSI feedback overhead and re-association costs compared to the baseline dynamic algorithm (as shown in Fig. 4.4 and Fig. 4.5). In addition, Fig. 4.3a reveals that ABUC with estimated and Full CSI achieve similar user fairness levels for each $T$. Moreover, regarding the computational complexity, we can see in Table 2 that ABUC with both values of $T$ drastically decreases the computation complexity owing mainly to the smaller cluster sizes $L_k$ used in intermediate static frames. Note that we can also observe that the reduction in complexity for ABUC is proportional to the period $T$. Therefore, we can conclude that ABUC with ($T = 3$ ; Estimated CSI) provides the best trade-off for low mobility users.
- *Medium mobility scenario*: for medium velocities, ABUC with Estimated CSI looses some performance compared to Full CSI but still outperforms Partial CSI case and performs close to baseline static algorithm with Full CSI. Here again, considering the balance between the loss of sum-rate performance and the gain in complexity and signaling costs (Fig. 4.4 and Fig. 4.5), we can infer that ABUC with ($T = 2$ ; Estimated CSI) provides the best trade-off performance for medium mobility. However, if the system can afford a higher overhead consumption, ABUC with ($T = 2$ ; Full CSI) offers the best sum-rate performance.
- *High mobility scenario*: In high mobility environments, it is clear that the

Estimated CSI becomes obsolete and hence ABUC with Estimated CSI has no more benefits. As a consequence, ABUC with ($T = 2$ ; Partial CSI) is preferred as the best option to realize the sum-rate and cost trade-off.

## 4.5 Advanced Mobility - Aware Joint Beamforming and User Clustering scheme

### 4.5.1 MABUC Algorithm Description

In this second part of this chapter, we introduce MABUC (Mobility - Aware Joint Beamforming and User Clustering). MABUC algorithm inherits the dynamic behavior of ABUC and the hybrid schemes [TBKM17, TBKNT19] by alternating dynamic and static clustering approaches in a periodic way. However, the key and novel idea in MABUC is to select the best value of $T$ period dynamically based on the network dynamics and users mobility, rather than maintaining it always fixed. In this chapter, we consider different user mobility profiles noted $u \in \mathbb{U}$ corresponding to different ranges of users' velocities (for example vehicular mobility profile, pedestrian mobility profile, etc.). As such, each profile may be represented by a range of channel correlation coefficients, denoted by $(\lambda_u^1, \lambda_u^2)$ with $\lambda_u^i \in (0,1)$. Note that we still consider three CSI feedback strategies: full CSI, partial CSI and estimated CSI as described in the previous section.

Specifically, the algorithm to be applied in each frame $t$ for a given user $k$ of profile $u$ will use a couple of parameters $(T_u, f_u)$, in which $T_u$ is the period identifying the dynamic frames (where the dynamic algorithm is called) and $f_u$ is the CSI feedback strategy used for intermediate frames. The choice of these parameters will impact the performance gain as well as the CSI signaling cost related to the users belonging to profile $u$.

Let $\mathbb{T}$ and $\mathbb{F}$ denote the set of possible values of $T$ and CSI feedback schemes, respectively.

$$\mathbb{T} = \{T_1, \ldots, T_p, \ldots, T_P\}$$

$$\mathbb{F} = \{f_1, \ldots, f_q, \ldots, f_Q\}$$

where $P \in \mathbb{N}$ and $Q$ represents the set of all possible CSI feedback strategies as

those detailed in section 4.3.

Obviously, the users who belong to a given profile $u$ will have their own parameters $(T_u, f_u)$ which will condition their induced throughput performance and signaling cost. We can formulate $(T_u, f_u)$ selection problem for users of profile $u$ as the following optimization problem:

$$\begin{aligned} \min_{(T_u, f_u)} \quad & C_u(T_u, f_u) && (5) \\ \text{s.t.} \quad & \sum_{k \in u, u \in \mathbb{U}} r_k(T_u, f_u) \geq R^{target} && (5a) \end{aligned} \tag{P5}$$

where $R^{target}$ denotes the sum-rate target for each scheduling process which can correspond to an actual mobile data demand. $C_u$ denotes the cost induced by the use of the clustering and beamforming algorithm using $(T_u, f_u)$ parameters for users of profile $u$. The objective function in (5) is the cost generated by the selection of $(T_u, f_u)$ in the joint beamforming and clustering algorithm for users of profile $u$, while the constraint (5a) ensures that the total sum-rate of users of profile $u$ reaches the targeted sum-rate.

It is worth noticing that when considering practical systems features we can limit the size of sets $P$ and $Q$: we maintain the same 3 CSI feedback strategies (namely full CSI, partial CSI and estimated CSI, as described in section 4.3), and may limit the period $T_u$ up to $T = 3$ frames due to the significant loss of sum-rate performance for longer periods [HBKM18]. Given the mathematical intractability of problem (P5), we propose to solve it by a heuristic based on the empirical analysis detailed in section 4.4.2.

Based on the algorithm costs analysis previously presented in section 4.3 [TBKM17], we can express the cost $C_u(T_u, f_u)$ as

$$C_u(T_u, f_u) = \mu \times CP(T_u, f_u) + \sqrt{1 - \mu^2} \times CS(T_u, f_u)^2 \tag{4.9}$$

In equation (4.9), $CP(T_u, f_u)$ is the computational complexity for the beamforming and clustering algorithm using $(T_u, f_u)$, $CS(T_u, f_u)$ denotes the amount of CSI overhead induced when using period $T_u$ and $\mu$ is a weighting factor, $0 < \mu < 1$. From the results of complexity analysis given in section 3.5.3 [TBKM17], we have

$$CP(T_u, f_u) = O(K^4 L^3 M^3) + (T_u - 1) O(K^3 \sum_{k=1}^{K} L_k M) + C_{est} \tag{4.10}$$

in which the first term is the complexity of the dynamic algorithm, the second corresponds to the complexity of the static algorithm which is executed in $(T_u - 1)$ frames and $C_{est}$ denotes the computational cost for CSI estimation in the case of estimated CSI and equals zero otherwise. Note that $C_{est}$ may be negligible compared to the other terms in (4.10).

In addition, $CS(T_u, f_u)$, the amount of CSI overhead for each period $T_u$, can be derived in each of the following cases as:

- full CSI: $CS^f(T_u, Full) = \sum_k (L + (T_u - 1)L_k)MN$,
- partial CSI and estimated CSI: $CS^p(T_u, Partial) = CS^e(T_u, Estimated) = KLMN$.

The details of the proposed MABUC scheme are summarized in Algorithm 5. At the beginning of every period $T$, i.e. $t \in \mathbb{T}_0$, we update the algorithm parameters $(T_u, f_u)$ that will be used for static frames by solving the problem (P5), then we use the full CSI and call dynamic algorithm to achieve the optimum clustering and beamforming. In the intermediate frames, we initialize the fixed cluster by the clustering solution of the last frame, and apply the static algorithm with the parameters $(T_u, f_u)$ solved in the last dynamic frame to obtain the maximum sum-rate.

The main feature of MABUC algorithm is its adaptive behavior in mobile environments. Aware of the users velocity variations, the period of alternating dynamic and static algorithms may be changed dynamically to adapt to the new environment conditions. Furthermore, the channel correlation is also adapted since the correlated coefficient $\lambda$ is chosen as a function of velocity $v$. The choices of CSI feedback schemes are then much more consistent to the channel environment dynamics, and that ensures a good performance at a reasonable cost.

### 4.5.2 MABUC performance evaluation

In this section, we numerically evaluate the performance of the proposed MABUC algorithm. We consider a 7-cell wrapped around two-tier H-CRAN. Each cell has a single macro-RRH and 3 pico-RRHs equally separated in space. The number of

**Algorithm 5:** Proposed Mobility Aware Beamforming and User Clustering Scheme

**initialize** *frame t, user mobility profile set* $\mathbb{U}$, $\mathbb{T}_0$ *set of dynamic frames (beginning frames of every period T), targeted throughput* $R^{target}$, *number of frames F*
$\mathbb{T} = \{1, 2, 3\}$
$\mathbb{F} = \{f, p, e\}$ *corresponding to full CSI, partial CSI and estimated CSI, respectively ;*
**repeat**
  **if** $t \in \mathbb{T}_0$ **then**
    *Update algorithm:* $(T_u, f_u) = \arg\min C_u(T_u, f_u)$
     *s.t.* $\sum_{k \in u, u \in \mathbb{U}} r_k(T_u, f_u) \geq R^{target}$ ;
    *Get full CSI:* $f_u^t = f, \forall k \in u, u \in \mathbb{U}$ ;
    *Call Dynamic Algorithm ;*
  **else**
    *Use CSI feedback scheme* $f_u$ *solved at frame* $t - mod(t, T_u)$;
    *Call Static Algorithm ;*
  **end**
  *Set clustering solution as the initial clusters for frame t+1 ;*
  *Move to next frame;*
**until** *convergence;*

mobile users is 10 users per macro cell. As previously, the users follow a Random Waypoint mobility model. The channel correlation coefficient $\lambda$ is computed following (4.5) in which carrier frequency $f$ and fronthaul delay $T_d$ are also set as 900 MHz and 2 ms, respectively. The fronthaul constraints for macro-RRH and pico-RRH are 683.1 Mbps and 106.5 Mbps, respectively [TBKM17]. The antennas used in simulations are antenna arrays for MIMO-LTE systems. All channels undergo Rayleigh small scale fading. The channel matrix is generated by Communications System Toolbox in Matlab. To solve the WMMSE problem we used CVX, a package for specifying and solving convex programs [GB14, GB08]. Other parameter settings are listed in Table 4.3.

#### 4.5.2.1 Empirical analysis

As mentioned previously, we consider three CSI feedback strategies: namely full CSI, partial CSI and estimated CSI, and we limit the period $T_u$ up to $T = 3$ frames due to the significant loss of performance for longer periods [TBKM17]. To solve the problem P5, we first reconsider the empirical analysis presented in section 4.4.2. These results were obtained when launching extensive simulations for the

| Simulation parameters | |
|---|---|
| Cellular layout | Hexagonal 7-cell wrapped-around |
| Channel bandwidth | 10MHz |
| Intercell distance | 0.8km |
| Number of macro RRHs, pico RRHs, users per macro-cell | (1,3,10) |
| TX power for macro/pico RRH | (43, 30) dBm |
| Antenna gain | 15 dBi |
| Background noise | -169 dBm/Hz |
| Path-loss from macro RRH to user | 128.1 + 37.6 log10(d) |
| Path-loss from pico RRH to user | 140.7 + 36.7 log10(d) |
| Log-normal shadowing | 8 dB |
| CSI error variance | -20 dB |

Table 4.3: Parameter settings for simulations

considered H-CRAN scenario to evaluate the performance of the ABUC algorithm [TBKM17] for different fixed values of $(T_u, f_u)$. The main objective is to analyse the performance of the scheme under different combinations of CSI feedback strategies and acquisition periodicity. From Fig. 4.7, which represents the maximum system sum-rate performance as function of channel correlation coefficient $\lambda$,

We can derive the sum-rate performance in descending order (from best performance to the worst) for different intervals of $\lambda$ and the corresponding mobility profiles (velocity intervals). For example, we observe that in the low mobility region, i.e. velocity between 0 and 18 km/h ($0.96 \leq \lambda \leq 1$), the algorithm with period $T = 2$ has better sum-rate than that with $T = 3$, also, the estimated CSI approaches the performance of full CSI and outperforms the partial CSI scheme. Such observation allow us to choose the best mechanism regarding the targeted performance-cost tradeoff for each interval of mobility.

#### 4.5.2.2 MABUC algorithm performance

We consider 5 intervals of user velocity that are determined in Table 4.4. For each interval, we derive from the empirical results of Fig. 4.7. the best $(T_u, f_u)$ values. The proposed MABUC algorithm is evaluated with different targeted sum-rates.

First, we show in Fig. 4.8 the average sum-rate convergence of the proposed MABUC algorithm with two targeted sum-rates: 200 and 220 Mbit/s. The purpose is to check how the proposed algorithm performs with the targets that are lower

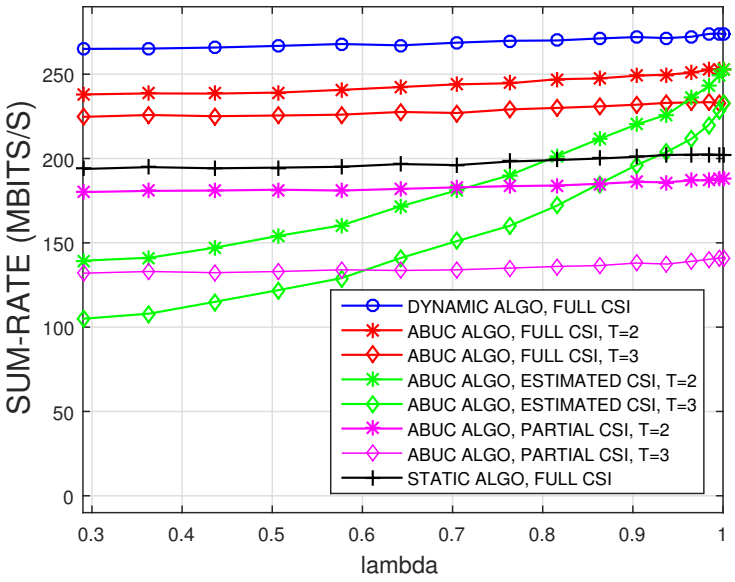


Figure 4.7: Sum-rate performance against lambda

than the maximum sum-rate achieved by ABUC which is seen as a benchmark algorithm [TBKM17]. The user velocity is selected randomly during the whole scheduling process. The results are compared to ABUC algorithm for the full CSI and partial CSI cases which are the superior and inferior bounds for sum-rate performance. On one hand, we observe that MABUC based on the parameters derived in Table 4.4, outperforms ABUC with partial CSI scheme, and on the other hand it approaches the performance of ABUC with Full CSI up to 85.02% and 95.95% respectively.

In Fig. 4.9, we compare the performance of the proposed MABUC algorithm to ABUC clustering solution in case of full CSI and partial CSI for different targeted sum-rate values. As we can see, our solution can always obtain an achievable rate that satisfies the data rate demand. Especially for the low mobility case, i.e 0-18 km/h, the algorithm can approach the performance of full CSI scheme.

| $\lambda$ | 0.96 - 1 | 0.86 - 0.96 | 0.7 - 0.86 | 0.6 - 0.7 | 0.3 - 0.6 |
|---|---|---|---|---|---|
| $v$ $[km/h]$ | 0 - 18 | 18 - 36 | 36 - 54 | 54 - 64 | 64 - 90 |
| | (2,f) | (2,f) | (2,f) | (2,f) | (2,f) |
| | (2,e) | (3,f) | (3,f) | (3,f) | (3,f) |
| | (3,f) | (2,e) | (2,e) | (2,p) | (2,p) |
| | (3,e) | (3,e) | (2,p) | (2,e) | (2,e) |
| | (2,p) | (2,p) | (3,e) | (3,e) | (3,p) |
| | (3,p) | (3,p) | (3,p) | (3,p) | (3,e) |

Table 4.4: Algorithm performance order for different user mobility profiles

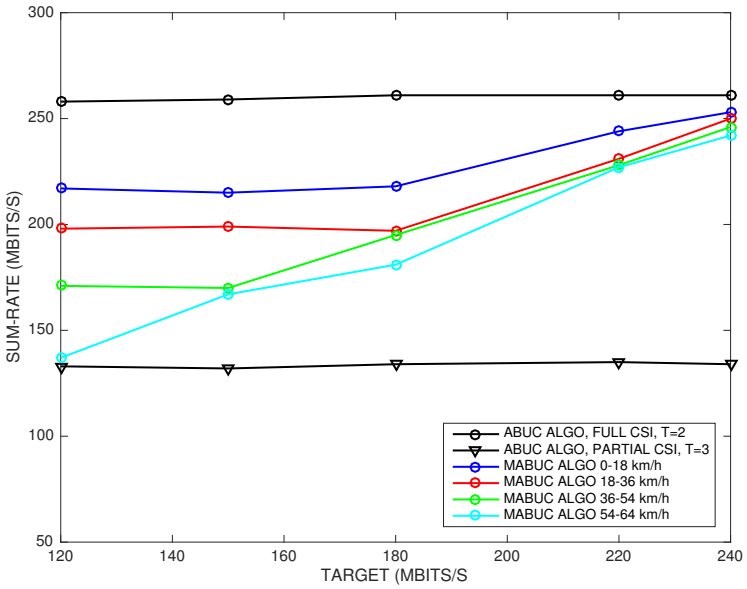


Figure 4.9: User data rate performance as function of targeted sum-rate

To evaluate the cost reduction of our proposed algorithm, we first plot in Fig. 4.10 the amount of CSI feedback overhead as a function of the number of users per macro-cell. The results show that MABUC algorithm provides an important reduction in CSI overhead compared to the Full CSI scheme (22−30% for high mobility and 33 − 36% for low mobility). We also observe that the CSI cost increases when the mobility is higher as more frequent CSI feedback is needed to track the highly variable channel.

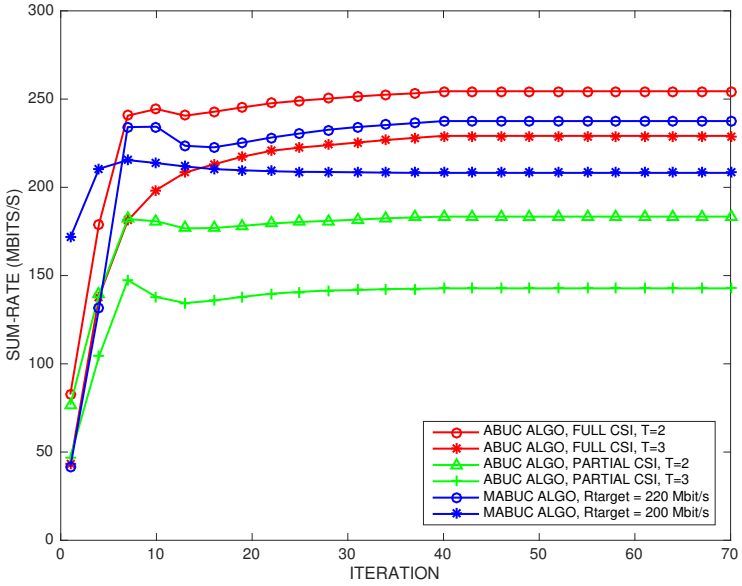


Figure 4.8: Average sum-rate convergence against number of iterations

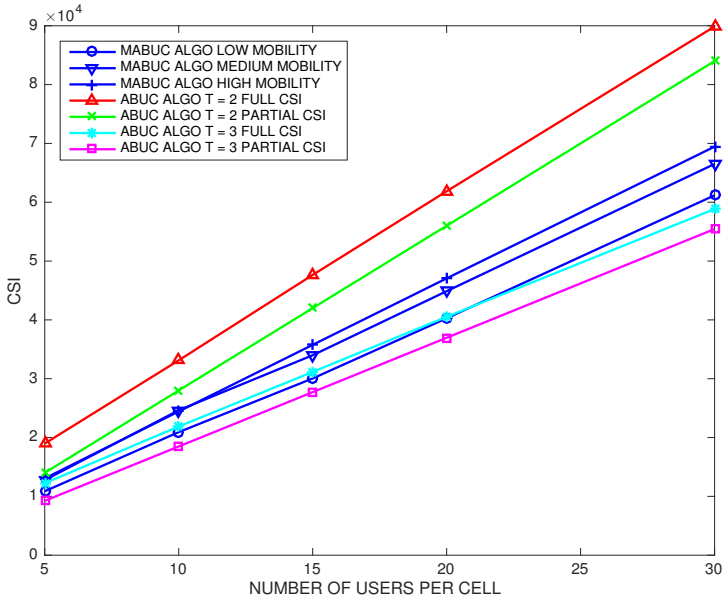


Figure 4.10: CSI overhead as function of number of users per macro-cell

Finally, in Fig. 4.11, we compare the computational complexity reduction achieved

by our proposed algorithm compared to ABUC with $T = 2$ and $T = 3$. The results prove that our scheme reduces drastically the complexity mainly thanks to the fact that the MABUC algorithm tends to select whenver possible longer periods, i.e. $T = 3$.

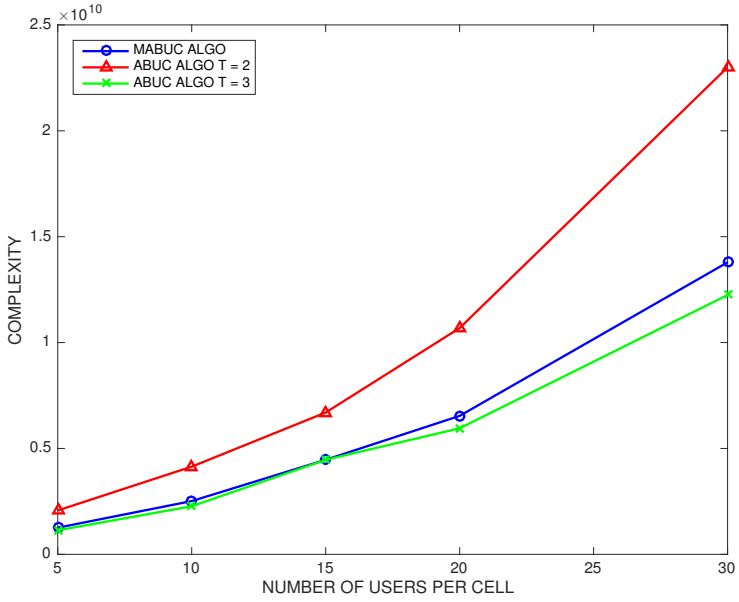


Figure 4.11: Algorithm complexity as function of number of users per macro-cell

To conclude, our numerical results prove that the proposed MABUC algorithm provides an appreciable performance-cost tradeoff under various mobility profiles. In comparison with ABUC algorithm as a benchmark in cases of full CSI and partial CSI, it guarantees the targeted sum-rate performance while enabling a significant reduction in CSI signaling and computational complexity costs.

## 4.6 Conclusion

In this chapter, we investigated the effect of users' mobility on the joint beamforming and user clustering problem in downlink H-CRAN. We first proposed ABUC, an evolved version of the Hybrid scheme that is aware of users mobility. The empirical analysis on ABUC scheme performance allows us to derive the best parameters values of the algorithm according to the users velocity. Then,

we proposed MABUC, an enhanced version of the scheme which automatically and adaptively activates dynamic and static clustering strategies to achieve a targeted sum-rate performance while maintaining the complexity and CSI signaling costs to a minimum. Compared to previous baseline schemes, our algorithm optimizes the allocation process over time (successive frames) rather than on a frame by frame basis. It also selects the appropriate values of the dynamic clustering periodicity $T$ as well as the CSI feedback strategy to meet the targeted sum-rate performance. This selection is done heuristically based on the empirical results obtained in the H-CAN scenario under different user mobility profiles. The numerical results show a good sum-rate performance while providing a considerable reduction in complexity and signaling costs. In the next chapter of this thesis, we aim to avoid the reliability of MABUC on the empirical results for parameters settings. To do so, we propose to consider a reinforcement learning approach to improve the algorithm parameters tuning process in accordance to the varying system dynamics (network, users mobility, channel variations, traffic load, etc.).

# Chapter 5

# A Deep Q-learning framework for mobility-aware CSI feedback for optimized beamforming and user clustering

## 5.1 Introduction

In this last chapter of the thesis, we aim to design a framework that is able to solve the problem of CSI feedback selection in a smart and flexible manner. The solution must adapt to a heterogeneous network with different types of user mobility when the users may change dynamically their velocity over time. To identify the best feedback parameters such as the type of CSI feedback and clustering period T, we first propose a Q-learning framework to optimize these feedback parameters on-the-fly, according to each user mobility profile mainly velocity [HBK+19]. The framework is able to adapt the feedback parameters to the changes of users velocity.

In a second step, to avoid the scalability issue of the Q-learning approach, we introduce a deep reinforcement learning approach (DRL) which is better suited for dealing with such intricate long-term resource allocation optimization, under highly varying wireless environments. Indeed, reinforcement learning is expected to handle tough situations that approach real-world complexity [MKS+15].

The DRL has been applied to several resource allocation problems in wireless networks. In [HZY+17], the authors consider the problem of cache-enabled opportunistic interference alignment (IA) in wireless networks. In [SPM19], a DRL based algorithm is proposed for joint problem of mode selection and resource management in Fog Radio Access Network (Fog-RAN). More specifically, in [XWT+17], a reinforcement learning technique is applied to dynamic resource allocation in CRAN. The authors present a DRL framework which is able to reach the objective of minimizing power consumption and meeting demands of wireless users over a long operational period.

The task of reinforcement learning can usually be described as a Markov Decision Process (MDP) without mandatory requirement of state space, explicit transition probability and reward function [OCH15]. In this work, we first express our joint beamforming and clustering problem as MDP model then reformulate it as a partially observable Markov decision process (POMDP) problem to solve it by making use of a recurrent neural network (RNN).

The rest of this chapter is organized as follows: Section 5.2 presents some basics on deep reinforcement learning. In section 5.3, we describe the system model and the problem formulation. We detail our proposed Q-learning algorithm when assuming an MDP problem in section 5.4 and prensent its simulation results in section 5.5. Then, in section 5.6, we introduce some backgrounds on deep Q-Learning and POMDP model. Section 5.7 reveals our ABUC's deep Q-Learning framework which is evaluated through extensive simulations in section 5.8. Finally, section 5.9 concludes the chapter.

## 5.2 Background on reinforcement learning

Reinforcement learning is an important branch of machine learning, where an agent makes interactions with an environment trying to control the environment to its optimal states that receive the maximal rewards. The task of RL can usually be described as a Markov decision process (MDP), however, state space, explicit transition probability and reward function are not necessarily required [OCH15]. In traditional RL, the problem spaces are very limited and the possible states in an environment are only few.

Reinforcement learning formalism is one way in which to learn to select actions which maximize a reward. In particular, it specifies that the reinforcement learner tries to infer an action-value function, i.e., a function which predicts the value (in terms of the reward that will be achieved) of each of the many actions an agent could take. Thus, if the approximation is good, the agent can choose the best action.

Q-learning is a reinforcement learning technique which goal is to learn a policy that informs an agent what action to take under what circumstances. It does not require a model of the environment and can handle problems with stochastic transitions and rewards, without requiring adaptations. The learning agent maximize its total (future) reward by adding the maximum reward attainable from future states to the reward for achieving its current state, effectively influencing the current action by the potential future reward. This potential reward is a weighted sum of the expected values of the rewards of all future steps starting from the current state.

In each decision epoch, the agent decides to make an action and observes the results from this action. Each action-state pair produces a Q-value that will be updated in a Q-table in which the columns and the rows represent the actions and the states, respectively. The updated value of $Q^*(s_t, a_t)$ is computed by the Bellman function as presented in [MKS+13]:

$$Q^*(s_t, a_t) = Q(s_t, a_t) + \alpha\left[\Gamma_t(s_t, a_t) + \gamma \max_{s_{t+1}} Q^{t+1}(s_{t+1}, a_{t+1}) - Q(s_t, a_t)\right] \quad (5.1)$$

where $Q(s_t, a_t)$ denotes the Q-value at state $s_t$ when executing action $a_t$ in time slot $t$, $\Gamma_t$ is the system reward at state $s_t$ and action $a_t$. $\alpha$ and $\gamma$ are learning rate and discount rate of the future expected reward, respectively.

## 5.3 System Model and Problem Formulation

In this chapter, we consider the same H-CRAN system model presented in the previous chapter and which consists of a BBU Pool, $L$ macro and pico RRHs and $K$ users.

$\mathbb{L} = \{1, 2, ..., L\}$ and $\mathbb{K} = \{1, 2, ..., K\}$ are the sets of RRHs and of users, respectively.

For a given user k, the same expression of $H_k$, $w_k$, $\text{SINR}_\text{k}$ and $r_k$ as given in chapter 3 remain valid to represent the downlink channel array, the transmit beamforming vector, the Signal-to-Interference-plus-Noise-Ratio and achievable rate of user k, respectively.

Of course, we consider the same weighted sum-rate maximization problem (P1) presented in chapter 3. The problem maximizes the weighted sum-rate of all users in the network under the fronthaul link capacity constraints and per-RRH power constraints. It is formulated as follows,

$$\begin{aligned} \max_{\{\mathbf{w}_{lk}, l\in\mathbb{L}, k\in\mathbb{K}\}} \quad & \textstyle\sum_{k=1}^{K} \alpha_k r_k & (1) \\ \text{s.t.} \quad & P_l = \sum_{k=1}^{K} \|\mathbf{w}_{lk}\|_2^2 \le P_l^{max} & (1a) \\ & \sum_{k=1}^{K} 1\{\|\mathbf{w}_{lk}\|_2^2\} r_k \le C_l^{max} & (1b) \end{aligned} \tag{P1}$$

## 5.4 Optimizing ABUC's feedback parameters using Q-learning

In this section, we design a reinforcement learning framework which enables the proposed ABUC algorithm (see Algorithm 4 - chapter 4) to optimize its scheduling parameters on-the-fly, given each user mobility profile.

We propose the following Q-learning model by defining the state, action spaces and reward function as follows:

*1) System State:* The current system state $s_t$ is jointly determined by the states of all K users. Due to the relationship of the received SINR and the channel coefficient, we model the channel coefficient, $|h_{lk}|^2$, as a Markov random variable. We partition and quantize the range of $|h_{lk}|^2$ into N levels. Each level corresponds to a state of the Markov channel. Each user k state is defined as the quantized CSI level $n_k^t$, where $1 \le n_t^k \le N$, $n_t^k \in \mathbb{N}$. The system state at time slot $t$ is defined as,

$$s_t = \{n_t^1, n_t^2, \ldots, n_t^k\}$$

*2) System Action*: In the system, the central scheduler has to decide which feedback parameters to be selected. Let $\mathbf{T} = \{T_1, \ldots, T_p, \ldots, T_P\}$ and $\mathbf{F} = \{f_1, \ldots, f_q, \ldots, f_Q\}$ denote the set of possible values of $T$ and CSI feedback schemes, respectively, in which $P \in \mathbb{N}$ and $Q$ represents the set dimension of all possible CSI feedback

strategies.

The current composite action $a_t$ is denoted by

$$a_t = \{a_t^1, a_t^2, \ldots, a_t^k\}$$

where $a_k^t = (T_t^k, f_t^k)$ represents the feedback parameters of user $k$ at time slot $t$, where period $T_t^k \in \mathbf{T}$ and CSI feedback type $f_t^k \in \mathbf{F}$.

*3) Reward Function*: The system reward needs to represent the optimization objective, that is to simultaneously reduce the system cost and satisfy the sum-rate demands. Here, we define the overall system reward at state $s_t$ and action $a_t$ as

$$\Gamma_t(s_t, a_t) = \rho_1 \sum_{k=1}^{K} r_k(s_t, a_t) - \rho_2 \sum_{k=1}^{K} C_k(s_t, a_t) \tag{5.2}$$

where the first term is the system achieved sum-rate at state $s_t$ and action $a_t$, and the second one denotes the CSI signaling overhead induced by the same state and action, $\rho_1$ and $\rho_2$ are weighting parameters representing the trade-off between the sum-rate and the cost, and $\rho_1 + \rho_2 = 1$.

Given the current action of user $k$, $a_t = (T_k, f_k)$, the CSI overhead cost of each user $k$ can be expressed as $C_k(s_t, a_t) = C_k(s_t, T_k, f_k)$, $f_k \in \{f, p, e\}$, in which $C_k(s_t, T_k, f_k)$ is computed over $T_k$ frames and can be expressed as follows:

- If Full CSI: $C_k(s_t, T_k, f) = \frac{1}{T_k}\Big[\big[L + (T_k - 1)L_k\big]MN\Big]$
- If partial or Estimated CSI : $C_k(s_t, T_k, p) = C_k(s_t, T_k, e) = \frac{LMN}{T_k}$

The Q-learning based framework uses an $\epsilon$-greedy strategy [RPMD14] in which the amount of exploration is globally controlled by the parameter $\epsilon$, that determines the randomness in action selections. In the $\epsilon$-greedy method, the agent selects a random action with a fixed probability $\epsilon$, $0 \leq \epsilon \leq 1$. At first, this rate must be initiated to its highest value, i.e. $\epsilon = 1$, as we don't have any knowledge about the values in the Q-table. At each time step, a uniform random number $\xi$ is drawn, where $\xi \in [0, 1]$. If $\xi > \epsilon$, the action that gives the greatest value in the Q-table will be chosen, otherwise we select greedily one of the learned actions in the action set. We reduce $\epsilon$ progressively as the agent becomes more confident at estimating Q-values. The Q-learning framework is detailed in Algorithm 6.

**Algorithm 6:** Proposed ABUC's Q-learning framework

**initialize** user mobility profile set $\mathbb{U}$
$F_{max}$: number of learning episodes
$F_0$: number of frames for each learning episode
$\epsilon$: exploration rate, $\epsilon \leftarrow 1$
**for** *episode i = 1:* $F_{max}$ **do**
  **if** *i = 1* **then**
    With probability $\epsilon$, randomly select an action
  **else**
    Randomly generate a probability $\xi$
    **if** $\xi \leq \epsilon$ **then**
      randomly select an action
    **else**
      choose action $a_i = arg\max Q(s_i, a_i)$
    **end**
  **end**
  **for** *frame t=1:*$F_0$ **do**
    *Execute ABUC with* $a_k^i$ *parameter*
    *Obtain beamforming and clustering solutions for each frame t*
    *Compute average sum-rate of episode i over all* $F_0$ *frames*
  **end**
  *Compute the reward* $\Gamma_i$ *using* (5.2) *and observe the new state* $s_{i+1}$
  *Update entry* $(s_i, a_i)$ *of Q-table using* (5.1)
  *Update CSI quantization state* $\{n_i^k\}$
  *Reduce exploration rate* $\epsilon$ *by 0.1 %*
**end**

## 5.5 Simulation results of ABUC's Q-learning framework

In this section, we present the performance results of the proposed ABUC's Q-learning feedback parameter selection framework on a H-CRAN network. We consider a two-tier H-CRAN which consists of a single macro-RRH and 3 pico-RRHs equally separated in space. The number of mobile users is 10, uniformly distributed over the macro cell. We assume a Random Waypoint model to represent users' movements. The fronthaul constraints for macro-RRH and pico-RRH are 683.1 Mbps and 106.5 Mbps, respectively [DY15]. All channels undergo Rayleigh small scale fading and log-normal shadowing. The other parameter settings can be found in Table 5.1.

| Simulation parameters | |
|---|---|
| Cellular layout | Hexagonal two-tier H-CRAN network |
| Channel bandwidth | 10MHz |
| Intercell distance | 0.8km |
| TX power for macro/pico RRH | (43, 30) dBm |
| Antenna gain | 15 dBi |
| Background noise | -169 dBm/Hz |
| Path-loss from macro RRH to user | 128.1 + 37.6 log10(d) |
| Path-loss from pico RRH to user | 140.7 + 36.7 log10(d) |
| Log-normal shadowing | 8 dB |
| CSI error variance | -20 dB |
| Scheduling frame | 10 ms |
| User priority weights $\alpha_k$ | 1 $\forall k$ |

Table 5.1: Parameter settings for simulations

To evaluate the algorithm's behavior with regards to user mobility, we consider different mobility profiles represented by the parameter $\lambda$ which is a function of velocity. We set the carrier frequency $f$ and the fronthaul delay $T_{dl}$ for all RRH $l$ as 900 MHz and 2 ms [3GP14], respectively.

Our goal in this section is to derive some preliminary performance results of the proposed ABUC's Q-learning based framework on a simple network which consists of 1 macro-RRH and 3 pico-RRHs and 3 users. The agent will learn over

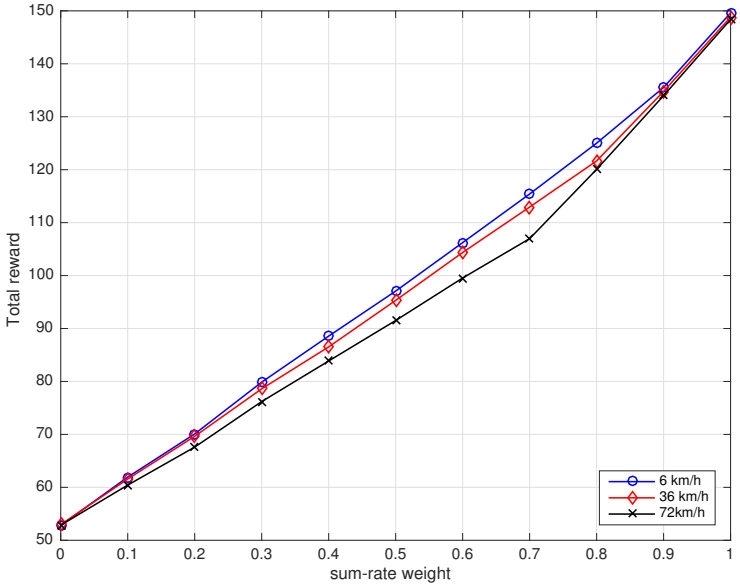


Figure 5.1: Converged total reward as function of weight $\rho_1$

1200 episodes for a state space of 64 states, corresponding to 4 states of CSI quantization for each user, i.e. the value of channel coefficients $|h_{lk}|^2$ are quantized into 4 ranges which are bounded by the following values: $6 \times 10^{-6}, 1.8 \times 10^{-5}$ and $8 \times 10^{-5}$. The action set for each user consists of 4 actions: T=1 with Full CSI and T=2 with Full CSI, Partial CSI and Estimated CSI, resulting in a Q-table of size 64 $\times$ 64.

We consider two different scenarios: in the first one, all users have the same velocity while in the second, each user has its own individual velocity.

Firstly, we evaluated the proposed algorithm in the first scenario where all users undergo the same velocity which is varied over the three mobility profiles, namely: low, medium and high mobility corresponding respectively to 6 km/h, 36 km/h and 72 km/h. We plot in Fig. 5.1 the converged value of the total reward against different values of sum-rate weight $\rho_1$ which varies between 0 and 1. We observe that when $\rho_1$ approaches 1, the reward tends toward the sum-rate and all users whatever their velocity converge to take the same optimal action ($T = 1$, Full CSI). Inversely, when $\rho_1$ approaches 0, the CSI cost factor becomes more dominating on the reward value, then the users choose the optimal action

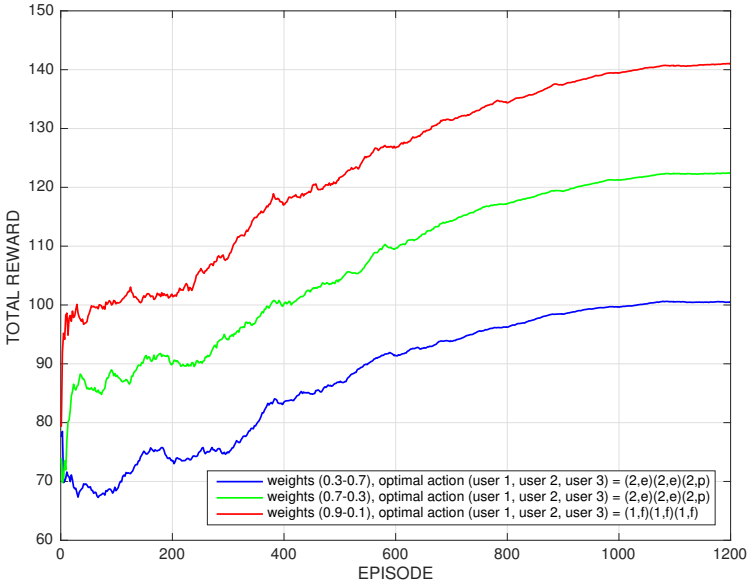


Figure 5.2: Total reward convergence over the learning episodes for different values of weights $(\rho_1, \rho_2)$; Individual velocities: user 1 = 6 km/h, user 2 = 36 km/h, user 3 = 72 km/h

that minimizes the CSI cost, i.e. ($T = 2$, Estimated CSI) for low and medium velocities, and ($T = 2$, Partial CSI) for high velocities. In addition, we also observe that the reward slightly decreases as the mobility becomes higher due to the CSI degradation.

We vary the value of weights $(\rho_1, \rho_2)$ to three cases (0.3, 0.7), (0.7, 0.3) and (0.9, 0.1) representing different situations of tradeoff between the sum-rate and the induced costs. We can see in Fig. 5.2 that the three users having different velocities converge individually to different optimal actions which are highly dependant on their respective velocities. We observe that for weight $\rho_1 = 0.3$ or $\rho_1 = 0.7$, the users with low and medium velocity take the action ($T = 2$, Estimated CSI), while the user with high mobility converges to ($T = 2$, Partial CSI). The selection of these actions confirms the effectiveness of the learning algorithm. Indeed, in case of low and medium mobility, the CSI estimation is accurate enough to be used when $\rho_1 = 0.3$ and $\rho_1 = 0.7$ for a balanced trade-off between sum-rate and cost, while the high mobility user no longer maintains an acceptable CSI estimation and then prefers selecting Partial CSI. Moreover, coupled with the fact that $T = 2$ is very effective for cost reduction, the users converge to $T = 2$ instead of $T = 1$. Finally, in

case of $\rho_1 = 0.9$ which corresponds to a predominant sum-rate performance, the learning algorithm wisely converges to ($T = 1$, Full CSI) action regardless the user velocity as Full CSI and dynamic clustering at all frame presents the best action for sum-rate maximization.

We can see that our proposed Q-learning algorithm works well in solving the optimal feedback strategy in both cases of homogeneous and heterogeneous mobility profile. However, the algorithm's efficiency and convergence are only confirmed in a small network scenario with a small number of users per cell and a limted number of SINR states. The reason is that Q-learning is not appropriate for solving problems with a large space of actions and states. Therefore, we propose to improve this framework by using a Deep Q-learning approach that will be described in the following section. Moreover, this proposed method is based on an MDP model where the states are given by quantized CSI levels which are different from real SINR states due to feedback delay, feedback strategy (partial and estimated especially for $T_k > 1$). Therefore, in the next section, we propose to use the partially observable Markov decision process (POMDP) model which better suits our targeted problem.

## 5.6 Basics on deep Q-learning for partially observable Markov decision process (POMDP)

### 5.6.1 Background on POMDP

In an ideal case of MDP, the agent must know the full state of the system for its further decisions. However, this is rarely true in a real world environment. The full state of the system cannot be provided or even determined. To deal with this issue, Partially Observable Markov Decision Process (POMDP), which models the lack of knowledge of the true underlying state by a probability distribution over the set of possible states, was introduced in [HS15]. Generally, a POMDP is described as a 6-tuple (S, A, P, R, O, Ω) where S,A,P, and R are the states, actions, transitions, and rewards as the same as an MDP, as shown in Fig. 5.3. The difference now is the introduction of the observation space O and its probability distribution Ω. The agent, instead of having the true system state s, receives an observation $o \in O$ according to the probability distribution $o \sim \Omega(s)$.


(a) MDP

(b) POMDP

Figure 5.3: MDP and POMDP

For that reason, and as we cannot observe the full state of SINR, our problem should be modeled as a POMDP problem. Indeed, as represented in SINR formula in Chapter 3, the value of SINR of user $k$, $\text{SINR}_\text{k}$, is a function of channel $H_k$. Hence, the quantized state of $\text{SINR}_\text{k}$ depends completely on the CSI feedback strategy chosen at each time slot.

### 5.6.2 Deep Q-learning

Deep reinforcement learning (DRL) is the combination of deep learning and reinforcement learning, and the Deep Q-learning (DQL) is one of the most known DRL techniques. With DQL we can program Artificial Intelligence (AI) agents that can operate in environments with discrete action spaces.

In each decision epoch, the agent decides to make an action and observes the results from this action. Each action-state pair produces a Q-value that is updated by the Bellman function as presented in Equation (5.1).

In order to logically represent and train the Deep Q-Network (DQN), we need to express the loss function that indicates how far our prediction is from the actual target. We want to decrease this gap between the prediction and the target. We will define our loss function as follows [MKS+15]:

$$L(s_t, a_t) = (\Gamma_{\text{Tot}}(s_t, a_t) + \gamma \max_{a'} \hat{Q}(s_t, a'_t) - Q(s_t, a_t))^2 \tag{5.3}$$

where $\Gamma_\text{t}$ is the system total reward, $\Gamma_{\text{Tot}}(s_t, a_t) + \gamma \max_{a'} \hat{Q}(s_t, a'_t)$ is the target of Q-value and $Q(s_t, a_t)$ is the current prediction of DQN.

As said previously, in POMDP the decision is made based on the history of the observed states. Therefore, a specific Recurrent Neural Network (RNN) layer,

especially Long Short Term Memory (LSTM) is employed in front of the feature to memorize information from previous observations [TVLC18, HS15]. The LSTM network is considered as one of the most successful RNNs because it overcomes the problem of training a recurrent network and in turn has been used in a wide range of applications. The action history is explicitly processed by an LSTM layer and fed as input to a Q-network. Particularly, its recurrent structure is able to integrate an arbitrarily long history to better estimate the current state instead of utilizing a fixed-length history as in DQNs [ZLP17].

## 5.7 ABUC's Deep Q-learning framework

In this section, we detail the a deep Q-learning framework which enables the proposed ABUC algorithm to optimize its scheduling parameters on-the-fly when assuming a large number of users having different mobility profiles.

First, we define the action space and reward functions in the Deep Q-learning model. In addition, as we consider the problem as a POMDP model, the system observation state will be defined instead of the system state.

*1) System Observation State:* The system observation state $o_t$ is jointly determined by the states of all K users. We partition and quantize the range of $|SINR_k|$ into N levels. Each level corresponds to a state of the Markov channel. Each user k state is defined as the quantized SINR level $n_k^t$, where $1 \leq n_t^k \leq N, n_t^k \in \mathbb{N}$. The system state at time slot $t$ is defined as,

$$o_t = \{n_t^1, n_t^2, \ldots, n_t^k\}$$

*2) System Action*: In the DQL, we maintain the same definition of action as in our Q-learning model. However, we can consider more actions than in previous Q-learning framework thanks to the strength of DNN.

*3) Reward Function*: The reward function is the same as in Q-learning framework.

Similar to the Q-learning approach, our Deep Q-learning algorithm uses an $\epsilon$-greedy strategy [RPMD14] in which the amount of exploration is controlled by the parameter $\epsilon$, that randomly selects the action. The agent selects a random action with a fixed probability $\epsilon$, $0 \leq \epsilon \leq 1$. At first, this rate must be initiated to a sufficient high value, i.e. $\epsilon = 1$, and then be decayed progressively after each

super-frame when it get more knowledge about the environment.

We also define a super-frame as a number of $F_0$ successive scheduling frames in which the same action is executed. The obtained reward for the corresponding action is averaged over every single frame in a super-frame.

Different to Q-learning approach, the agent do not have the global knowledge about the expected reward value for each action-state pair, but it is learned by experience. A method that trains the neural network with experiences in the memory is called *replay()*.

Experience replay is what lets neural networks work well with reinforcement learning. Each experience (consisting of the current state, action, reward, and next state) the agent gets is stored in what is called the experience replay memory. Instead of training the neural network on whatever it is seeing at the current moment, a random number of history is sampled from the replay memory to train the network.

To do this, we sample some experiences from the memory and call this method by *minibatch*. By using the *replay*, the experiences used to train the DQN come from many different points in time. This smooths out learning and avoids catastrophic failure.

The details of the proposed ABUC's Deep Q-learning framework are given in

Algorithm 7.

**Algorithm 7:** Proposed ABUC's Deep Q-learning framework

**initialization** initialize replay memory
$F_{max}$: number of super-frames
$F_0$: number of frames for each super-frame
$\epsilon$: exploration rate, $\epsilon \leftarrow 1$
$\xi$ : exploration decay
$minibatch$ : number of randomly sampled elements of the memory for replay
**for** *episode i = 1:* $F_{max}$ **do**
  **if** *i = 1* **then**
    With probability $\epsilon$, randomly select an action
  **else**
    Randomly generate a probability $\xi$
    **if** $\xi \leq \epsilon$ **then**
      randomly select an action
    **else**
      choose action $a_i = arg\max Q(o_i, a_i)$
    **end**
  **end**
  **for** *frame t=1:*$F_0$ **do**
    *Execute ABUC with* $a_i^k$ *parameter*
    *Obtain beamforming and clustering solutions for each frame t*
    *Compute average sum-rate of episode* $i$ *over all* $F_0$ *frames*
  **end**
  *Compute the reward* $\Gamma_i$ *using* (5.2) *and observe the new state* $o_{i+1} = \{n_i^k\}$
  *Store transition* $(o_i, a_i, o_{i+1})$ *in replay memory.*
  *Reduce exploration rate* $\epsilon = \epsilon * \xi$
  *Get* $minibatch$ *samples from memory for training the neural network*
  *Call replay function*
**end**

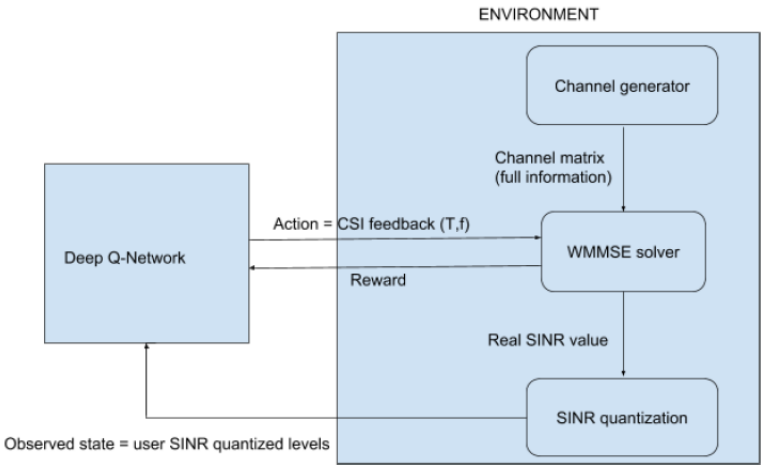


Figure 5.4: Deep Q-learning framework

## 5.8 Simulation results of ABUC with DQL

To evaluate the performance of our proposed learning framework, we developed a simulation environment composed of Matlab code to simulate user mobility, the radio environment and resource allocation along with a Python program which simulates the learning network. We consider a two-tier H-CRAN which consists of a single macro-RRH and 3 pico-RRHs equally separated in space. 10 mobile users are randomly generated and uniformly distributed over the macro-cell area. We assume a Random Waypoint model to represent users' movements.

The other parameter settings of the H-CRAN network are the same as presented in Q-learning (see Table 5.1).

In Fig. 5.4, we present the simulation components of the DQL framework. The input channel are generated by Rayleigh Fading Channel in Matlab. The WMMSE algorithm for solving joint beamforming and clustering will output the sum-rate, CSI cost and observation SINR state and send them to the Deep Q-Network (in Python). The Neural Network and LSTM layer are built in Keras. The convergence of action is identified whenever the action is maintained during 30 consecutive super-frames. The number of single frames in each super-frame is set to 10.

We implement the DNN structure as presented in Fig. 5.5, the LSTM layers are inserted after three dense hidden layers. We also apply a Dropout layer to the input which can help prevent over-fitting.

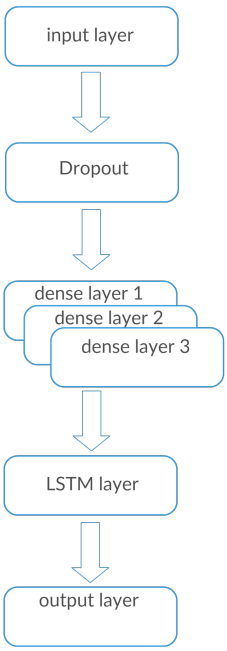


Figure 5.5: Deep Neural Network design

The agent will learn over super-frames for a state space of $6^K$ states, corresponding to the 6 SINR quantization levels of each user. The action set for each user consists of 7 actions: T=1 with Full CSI (1,f), T=2 with Full CSI (2,f), T=3 with Full CSI (3,f), T=2 with Estimated CSI (2,e), T=3 with Estimated CSI (3,e), T=2 with Partial CSI (2,p) and T=3 with Partial CSI (3,p), giving the state space size of $6^K$.

We consider two scenarios: homogeneous and heterogeneous scenarios in terms of user velocity. In the first one, all users have the same velocity while in the second, each user has its own individual velocity.

### 5.8.1 Deep Q-learning performance in homogeneous mobility scenario

Firstly, we evaluate the proposed algorithm in a H-CRAN network where 9 users undergo the same velocity which is varied over the three mobility profiles, namely: low, medium and high mobility corresponding respectively to 5 km/h, 40 km/h and 80 km/h. We vary the value of weights $(\rho_1, \rho_2)$ to five cases (0.1, 0.9) (0.3, 0.7), (0.5, 0.5), (0.7, 0.3) and (0.9, 0.1) representing different situations of trade-off between the sum-rate and the induced costs.

Fig. 5.6 shows the convergence of the average of overall reward over superframes with the optimal action of the corresponding value of weights. First of all, we can see that the reward increases with the weight $\rho_1$ as the value of the sum-rate is dominant on the reward value. We observe that when $\rho_1$ approaches 0, e.g. $\rho_1 = 0.1$ in Fig. 5.6(a), the sum-rate factor is much less prevailing than that of CSI cost on the reward function, then users choose the action that minimizes as much as possible their cost by extending the period to $T = 3$ and avoid to use Full CSI feedback. In this case, as the channel estimation has a good quality for low and medium mobility, (3,e) is chosen as optimal action. While in case of high mobility, (3,p) is used instead because CSI estimation worsens. Inversely, when $\rho_1$ approaches 1, e.g. $\rho_1 = 0.9$ in Fig. 5.6(e), the reward tends very nearly toward the sum-rate and all users whatever their velocity converge to take the Full CSI with T=1 for the best possible performance in terms of achievable rate.

For the other values of $\rho_1$, we still find a reasonable optimized trade-off at convergence. In Fig. 5.6(b), although the users maintain the same converged actions as in Fig. 5.6(a) as $\rho_1$ is still low, the reward gap between low mobility and the two others mobility profiles is enlarged. We can observe the highest difference between the reward of low mobility compared to medium and high mobility in Fig. 5.6(c), which is mainly due to the actions adopted by the users in this case. When low mobility users still use Estimated CSI, the rest have to apply Full CSI to avoid the sum-rate degradation, but suffer a much higher CSI overhead. In Fig. 5.6(d), as the sum-rate begins to overcome CSI cost in weight, i.e. $(\rho_1, \rho_2) = (0.7, 0.3)$, all users tend to guarantee a better sum-rate by reducing their period to T=2.

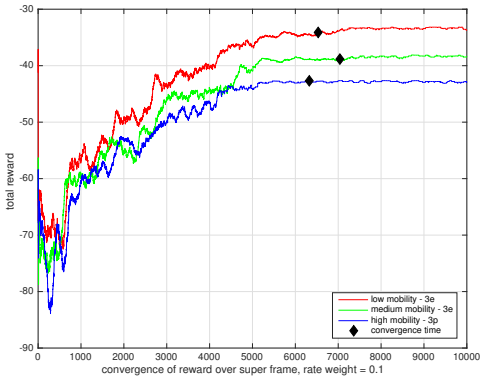


(a) (0.1, 0.9)

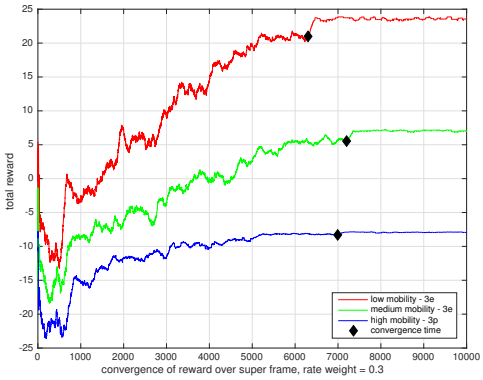


(b) (0.3, 0.7)

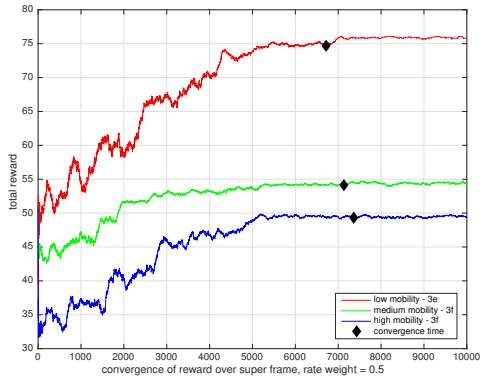


(c) (0.5, 0.5)

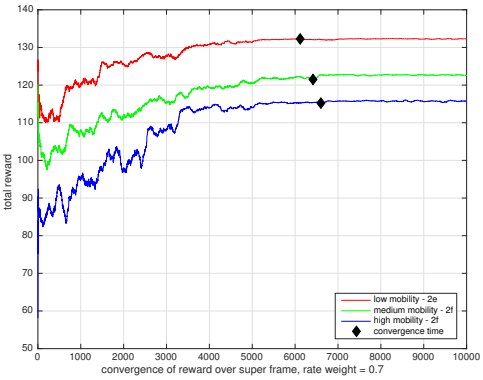


(d) (0.7, 0.3)

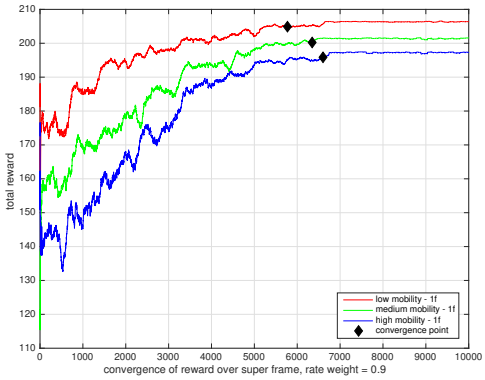


(e) (0.9, 0.1)

Figure 5.6: Total reward convergence in homogeneous mobility scenario

| Mobility | $\rho_1 = 0.1$ | $\rho_1 = 0.3$ | $\rho_1 = 0.5$ | $\rho_1 = 0.7$ | $\rho_1 = 0.9$ |
|---|---|---|---|---|---|
| Low | (3,e) | (3,e) | (3,e) | (2,e) | (1,f) |
| Medium | (3,e) | (3,e) | (3,f) | (2,f) | (1,f) |
| High | (3,p) | (3,p) | (3,f) | (2,f) | (1,f) |

Table 5.2: Synopsis of optimal actions

To conclude, regarding the action and the reward, we can observe that low velocity users can afford an estimation of CSI rather than using partial or full knowledge of CSI (except for $\rho_1 = 0.9$. The reason is that the channel quality is expected to be more stable in low velocity case and the CSI estimation performs with accurate precision according to Eq. (4.3). While in higher velocity, the CSI estimation is no longer accurate and the sum-rate performance degrades significantly. As well, for the same mobility profile, when the sum-rate weight $\rho_1$ increases, the users tend to switch from estimated and Partial CSI to Full CSI to get a better sum-rate, when at the same time reduce their period T to limit the loss of performance in static frames. The optimal actions are summarized in the Table (5.2).

### 5.8.2 Deep Q-learning performance in heterogeneous mobility scenario

In this scenario, we also consider the same H-CRAN network including 9 users displaying three different mobility profiles. Users 1-2-3 have low velocity, users 4-5-6 show a medium velocity and the rest of users have high velocity. We vary the sum-rate rate coefficient $\rho_1$ over three values: 0.1, 0.5 and 0.9. The initial positions of users are plotted in Fig. 5.7.

In Fig. 5.8, we present the convergence of individual reward, rate and CSI cost for $\rho_1 = 0.1$. As for the homogeneous scenario, we can see that the users converge to the same optimal action based on their own individual profile. The group of low mobility always obtain the highest values of reward thanks to the most accurate and stable quality of CSI feedback. Meanwhile, the groups of higher velocity often suffer more degradation in terms of sum-rate and also pay higher CSI cost to get more accurate information from Partial CSI and Full CSI feedback.

The others results of converged reward, rate and action of individual users for $\rho_1 = 0.5$ and $\rho_1 = 0.9$ are given in Table 5.3 and Table 5.4, respectively. Again, we observe the same tendency in terms of converged action as in homogeneous scenario.

As the low mobility users did not move much according to Fig. 5.7 and the

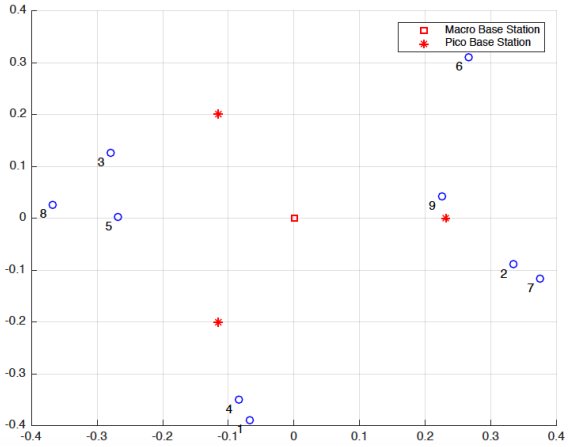


Figure 5.7: Initial positions of users

| User | 1 | 2 | 3 | 4 | 5 | 6 | 7 | 8 | 9 |
|---|---|---|---|---|---|---|---|---|---|
| Reward | 7.52 | 7.61 | 6.76 | 5.39 | 4.79 | 5.27 | 5.10 | 5.03 | 5.65 |
| Sum-rate | 21.00 | 22.32 | 21.18 | 22.20 | 21.84 | 21.49 | 21.96 | 21.16 | 22.89 |
| Action | (3,e) | (3,e) | (3,e) | (3,f) | (3,f) | (3,f) | (3,f) | (3,f) | (3,f) |

Table 5.3: Converged individual reward, rate and action per user for $\rho_1 = 0.5$

| User | 1 | 2 | 3 | 4 | 5 | 6 | 7 | 8 | 9 |
|---|---|---|---|---|---|---|---|---|---|
| Reward | 21.74 | 22.39 | 21.00 | 20.85 | 20.20 | 20.08 | 21.05 | 20.51 | 22.91 |
| Sum-rate | 26.38 | 27.10 | 25.55 | 25.39 | 24.67 | 24.54 | 25.61 | 25.01 | 27.68 |
| Action | (1,f) | (1,f) | (1,f) | (1,f) | (1,f) | (1,f) | (1,f) | (1,f) | (1,f) |

Table 5.4: Converged individual reward, rate and action per user for $\rho_1 = 0.9$

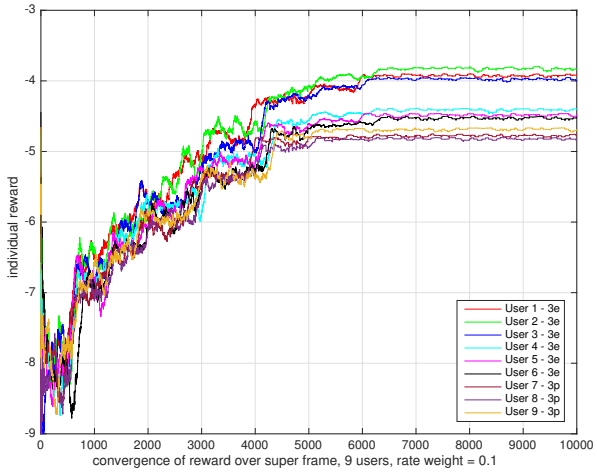


(a) Individual reward

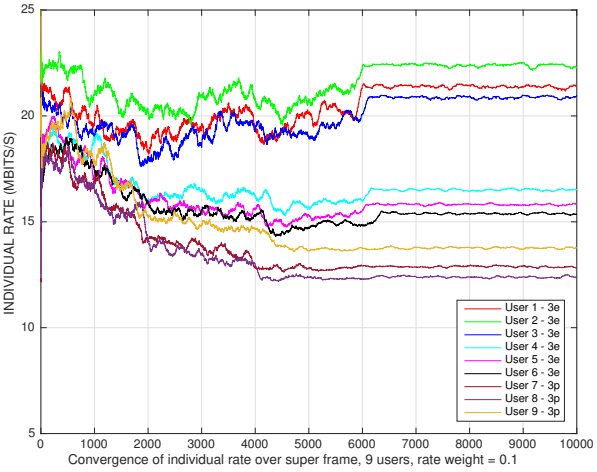


(b) Individual rate (Mbit/s)

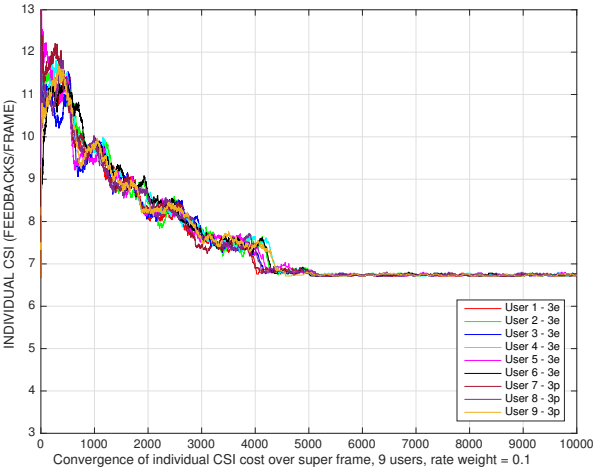


(c) Individual CSI cost (feedback/frame)

Figure 5.8: Individual convergence of reward, rate and CSI cost in heterogeneous mobility scenario, $\rho_1 = 0.1$

logged positions derived during the experiments, we can observe in Fig. 5.8(b) that the initial position may somewhat have influence on the individual rate performance. For example, user 2 has clearly a better rate than that of users 1 and 3 thanks to a more favorable position over the scheduling time, as users with the best channel conditions are more likely to be served more often by the sum-rate maximization scheduler. In Fig. 5.8(c), all users converge to the same CSI cost value as both actions (3,e) and (3,p) induce the same cost.

In Fig. 5.9, we present the convergence of the individual CSI overhead cost obtained for two others values of $\rho_1$. In Fig 5.9(a), the users from 4 to 9 who adopt action (3,f) naturally converge all to a higher cost value than that of low mobility users, as action (3,e) generates less CSI feedback owing to the CSI estimation strategy. In Fig 5.9(b), once again all users converge to same value of CSI cost as all of them undertake the same action (1,f) at the convergence.

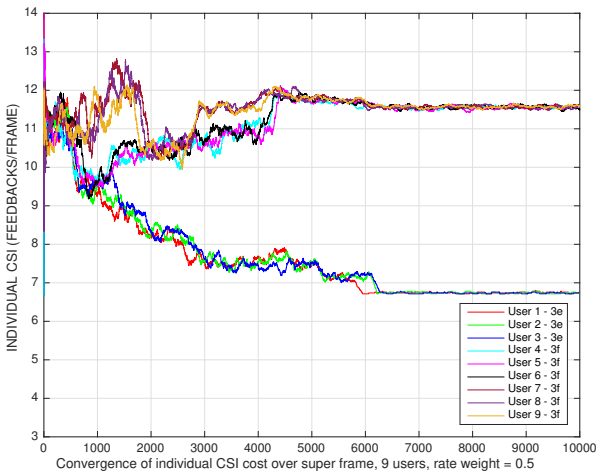


(a) (0.5, 0.5)

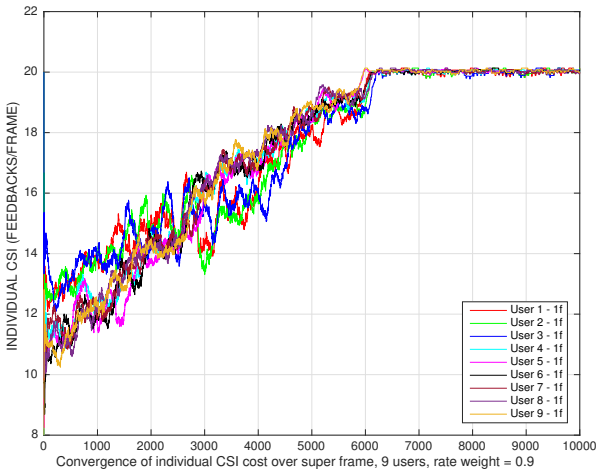


(b) (0.9, 0.1)

Figure 5.9: Individual CSI cost convergence in heterogeneous mobility scenario

### 5.8.3 Optimal action and convergence time against different number of users

To examine whether and how the number of users may influence the converged action and the convergence time, we carried this set of experiments by varying the number of users from 6, 9 to 12 users in a heterogeneous mobility case with

$\rho_1 = 0.1$. The results are presented in Fig. 5.10.

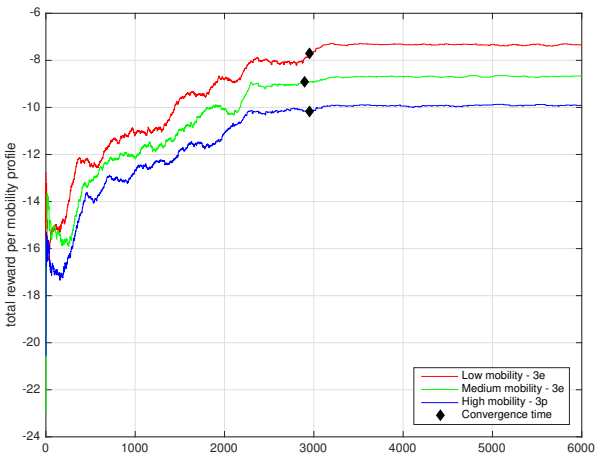


(a) 6 users

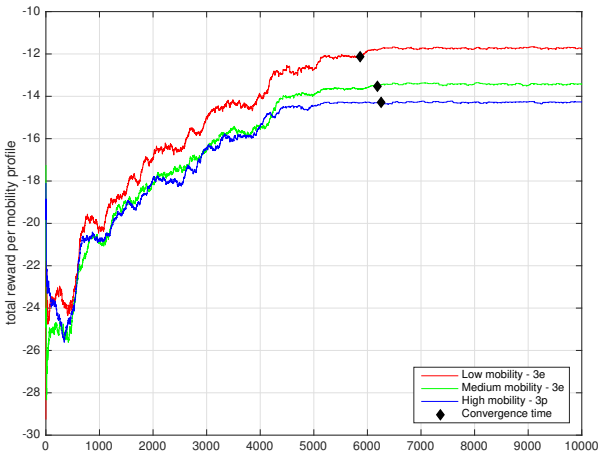


(b) 9 users

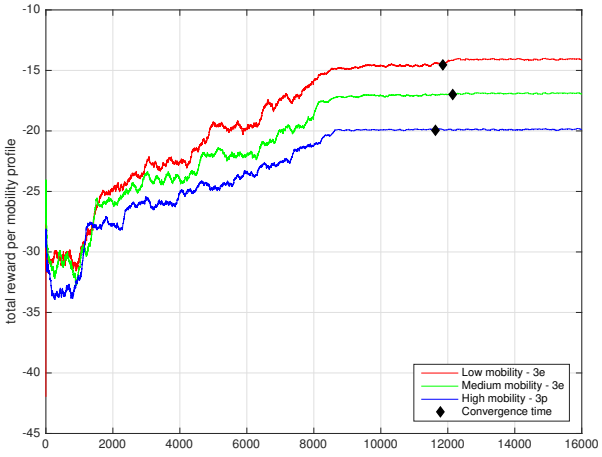


(c) 12 users

Figure 5.10: Reward convergence per mobility profile in heterogeneous mobility scenario

Table 5.5 summarizes additional results concerning the convergence time, optimal action and total user rate per mobility profile as function of the number of users. We can see from Table 5.5 and Fig. 5.8 that the convergence time increases with the number of users, as the state space and action space grow exponentially as a function of the number of users $K$. Hence, the algorithm takes more time to explore all possible actions to finally converge to the optimal ones. However, it is important to notice that whatever the value of K, the optimal actions remain the same for each mobility profile.

| Mobility | 6 | | | 9 | | | 12 | | |
|---|---|---|---|---|---|---|---|---|---|
| | CV | action | SR | CV | action | SR | CV | action | SR |
| Low | 2958 | (3,e) | 46.96 | 5862 | (3,e) | 63.83 | 11866 | (3,e) | 101.48 |
| Medium | 2901 | (3,e) | 34.09 | 6198 | (3,e) | 47.44 | 12152 | (3,e) | 72.97 |
| High | 2954 | (3,p) | 21.83 | 6264 | (3,p) | 37.81 | 11625 | (3,p) | 44.17 |

Table 5.5: Convergence per mobility profile, CV = convergence time, SR = sum-rate

### 5.8.4 Distribution of selected actions

In order to analyze how each action is picked during the whole scheduling process until the convergence, we plot in Fig. 5.11 the percentage of the actions' selection before the convergence of the algorithm is reached for each type of user mobility.

In these figures, we can observe that the optimal action in each case is always the most selected. In addition, looking at the most frequently selected action, we can notice that the choices are coherent with the sum-rate-CSI trade-off, i.e. the values of $(\rho_1, \rho_2)$. For example, when observing the results for $\rho_1 = 0.1$ (blue bars), the two best actions are always (3,e) and (3,p) regardless of the velocity, that is because at the lowest value of $\rho_1$, the users prefer the largest period T=3 with Estimated CSI and Partial CSI. Therefore, every option with Full CSI, i.e. $\{1,2,3\}$ or $\{(1,f),(2,f),(3,f)\}$ must be quickly eliminated from the candidate action set.

In Fig. 5.11(a), for $\rho_1 = 0.5$ (green bars), the most frequent actions for low mobility users are still that of Estimated CSI and Partial CSI, but in this case, the two best ones are (2,e) and (3,e) because they offer the better sum-rate at low velocity compared to Partial CSI. For the same weight in Fig. 5.11(b) and Fig. 5.11(c), (2,f) and (3,f) are the most selected actions since the estimation of CSI becomes less

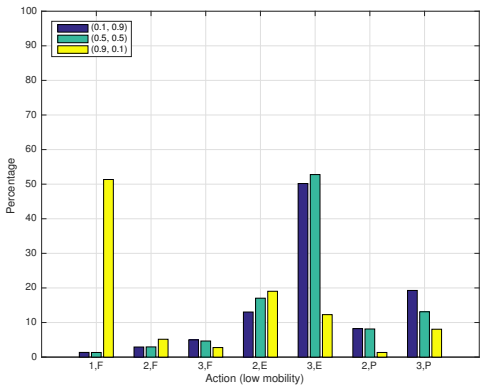


(a) Low mobility users 1-3

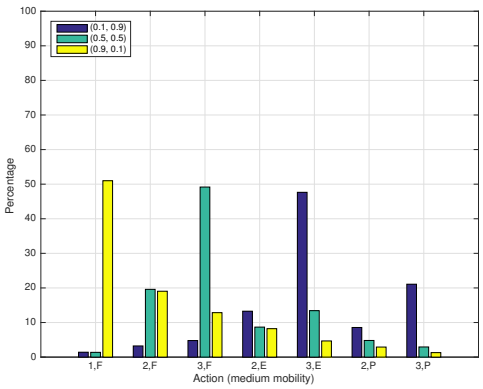


(b) Medium mobility users 4-6

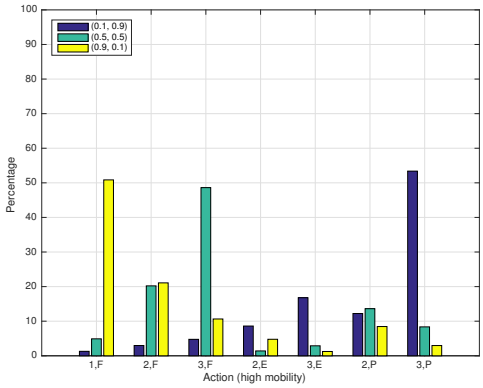


(c) High mobility users 7-9

Figure 5.11: Percentage of action's selection for different mobility profiles

| User | 1 | 2 | 3 | 4 | 5 | 6 | 7 | 8 | 9 |
|---|---|---|---|---|---|---|---|---|---|
| $\rho_1 = 0.1$ | 5860 | 5862 | 4342 | 5188 | 5664 | 6198 | 5190 | 5334 | 6264 |
| $\rho_1 = 0.5$ | 5837 | 5244 | 6004 | 5837 | 6018 | 5658 | 5922 | 5905 | 5242 |
| $\rho_1 = 0.9$ | 5497 | 4884 | 5634 | 5982 | 5837 | 5188 | 5922 | 5982 | 5712 |

Table 5.6: Synopsis of convergence time (expressed in number of super-frames) in case of heterogeneous mobility users

accurate.

For $\rho_1 = 0.9$ (yellow bars), as the sum-rate almost dominates over the total reward function, (1,f) is always the best choice for all mobility profiles. Somehow, we can see that Estimated CSI is still competitive in Fig. 5.11(a) at low mobility thank to a good estimation quality. This action is much less selected in case of higher velocities as shown in Figs. 5.11(b) and Fig. 5.11(c).

The convergence times of individual users are summarized in Table 5.6. We observe almost similar convergence time intervals that are around 5000-6000 super-frames even with different initial positions and user velocities. Such observation consolidates the conclusion that the convergence time is mainly impacted by the number of user K and not in the least by the individual characteristic of users.

### 5.8.5 Adaptivity of the online-learning in dynamic environments

In real networks, the user mobility can vary in real-time and the current agent's knowledge about the environment cannot be applicable anymore in solving the optimal action. Therefore, it is necessary for the system to adapt to the environment's changes and rapidly re-learn the optimal policy.

In Fig. 5.12, we present the short moving average of total reward in a network of 3 users having different velocities (5,40,80) km/h at the beginning of the experiment. The current scenario setting achieves a convergence after 443 super-frames with optimal actions (3e, 3e, 3p). At super-frame 800, user 1 who at first has a low mobility (5 km/h) switches its velocity to 80 km/h. This sudden acceleration makes an important degradation on the total reward because the quality of CSI estimation is drastically deteriorated as user 1 is selecting an action (T=3, Estimated CSI) which is no more appropriate to the real experienced channels.

At super-frame 851, the agent detects the change of mobility by recognizing a drop of 5% of the moving average of converged reward (phase 1). At this point,

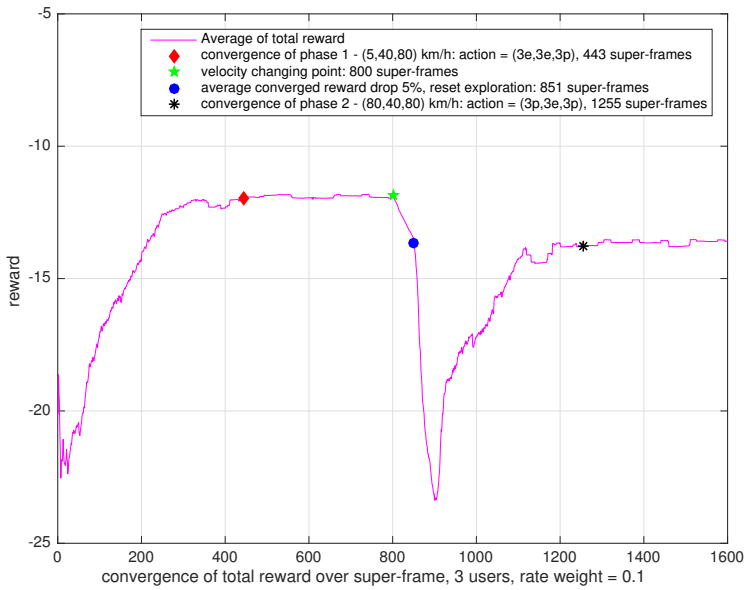


Figure 5.12: Reward convergence over the super-frames in case of online-learning

the exploration rate $\epsilon$ is reset to allow the agent start learning the new behavior of users. As we can see in the figure, the new convergence is established at super-frame 1225 with new optimal actions (3p, 3e, 3p), that better adapt to the individual change of user 1.

This result shows the good behavior of the online-learning of our framework to adapt in real-time network operation. The time of adaptation can be adjusted by acting on the parameter of change detection (e.g. reward drop $\leq 5\%$) for a better reactivity.

## 5.9 Conclusion

In this last chapter of the thesis, we designed two reinforcement learning frameworks which enable our proposed ABUC algorithm to optimize its scheduling parameters on-the-fly, given each user mobility profile. We proposed a first model based on a Q-learning approach that was able to learn about the system dynamics and predict the best parameter set to apply for each user depending on its individual mobility behavior. Nevertheless, despite the encouraging results of

the Q-learning approach, this method reaches its limits when dealing with large scale problems (large space of actions and states) due to the lack of computational memory. Therefore, we proposed a deep Q-learning algorithm based on an POMDP model to better tackle the scalability issue of our targeted problem.

More specifically, we have shown that our proposed DQL framework can achieve attractive results in terms of converged action and obtained reward in both homogeneous and heterogeneous mobility scenarios. The experiments prove that the convergence time is mainly impacted by the number of users in the network. They also demonstrated the online-learning ability of the framework to rapidly adapt the changes of the users mobility.

# Chapter 6

# Conclusions

## 6.1 Summary of contributions

5G and beyond systems are expected to address unprecedented challenges to cope with a high degree of heterogeneity in terms of deployment types (macro and small cells), environments (low-density to ultra-dense urban areas) and mobility scenarios (static to high-speed transport). Internet of Things (IoT) is envisionned to be a major communication scenario in such systems and in which many interconnected fixed or mobile end-user devices or sensors will contribute to the concept of network densification. New traffic generated from various devices such as in smart grid, smart homes and cities, and e-health scenarios with different communications characteristics, will need intelligent management requirements. To achieve the goals of such scenarios, the combination of advanced radio access technologies such as cloud computing, MIMO and beamforming with a hetregeneous and dense deployment infrastructures would provide seamless coverage, on-demand resource processing, delay-aware storage, and high network capacity wherever needed.

In this thesis, we addressed the problem of resource allocation and sum-rate maximization in the downlink communications of H-CRANs. Our research effort was mostly focused on the joint beamforming and user clustering optimization. Most reference solutions in the literature dealing with such problem have provided either optimal or heuristic solutions mainly for fixed-mobility scenarios and for a given scheduling frame. These works have neglected one or several

requirements in terms of algorithmic complexity, signalling overhead, CSI imperfectness, and user mobility. To overcome such limitations, we proposed in this thesis a new class of algorithms which fulfill the problem of sum-rate optimization while being aware of users mobility. More specifically, our solutions through a joint beamforming and user clustering optimization offer an attractive trade-off between system performance expressed in terms of sum-rate against the cost incurred during the scheduling, beamforming and clustering process.

Another important contribution of our work is the in-depth analysis we produced on the effect of user mobility on the algorithms' parameters and performance. We proposed to take into account users' mobility in the channel estimation model to mirror the stochastic dynamics of the communication channel which is highly dependent on users mobility. Our proposed solutions are also able to dynamically tune their parameters in accordance to users mobility profile (mainly velocity) to achieve the best performance. Another originality of our work is that we proposed a CSI feedback scheduling strategy. Our algorithms with their CSI periodicity and strategy parameters offer to the system a smart and adaptive user-dependent CQI feedback allocation which, to the best of our knowledge, constitutes a real novelty. Hereafter, we summarize in detail our main contributions.

The first contribution investigates the performance-cost trade-off of joint beamforming and user clustering problem in H-CRANs. We proposed a simple yet effective Hybrid algorithm that periodically activates dynamic and static clustering schemes to balance between the optimality of the beamforming and association solutions while being aware of practical system constraints (complexity and signaling overhead). The key benefit of the proposed Hybrid algorithm is to take into account the temporal dimension of the allocation process while being aware of practical system operation metrics. The numerical results show that the proposed solution narrows significantly the performance gap with the optimal dynamic solution, while greatly reducing the required computational complexity, CSI feedback and re-association signaling overhead when taking into consideration the user scheduling process over several frames.

In the second contribution, we delved deeper into the effect of users' mobility on the joint beamforming and user clustering problem in downlink H-CRAN. We first proposed ABUC, an evolved version of the Hybrid scheme that is aware of users mobility. The empirical analysis on ABUC scheme performance lets us to

derive the most suitable parameter values of the algorithm according to the users velocity. Then, we proposed MABUC, an enhanced version of the scheme which automatically and adaptively activates dynamic and static clustering strategies to achieve a targeted sum-rate performance while maintaining the complexity and CSI signaling costs to a minimum. Compared to the baseline schemes, MABUC optimizes the allocation process over time (successive frames) rather than on a frame-by-frame basis. It also selects the appropriate values of the dynamic clustering periodicity $T$ as well as the CSI feedback strategy to meet the targeted sum-rate performance. This selection is done heuristically based on the empirical results obtained in the H-CAN scenario under different user mobility profiles. The numerical results show a good sum-rate performance while providing a considerable reduction in complexity and signaling costs.

In our last contribution, we designed two reinforcement learning frameworks which enable our proposed ABUC algorithm to optimize its scheduling parameters on-the-fly, given each user mobility profile. Firstly, we proposed a model based on a Q-learning algorithm that was able to learn about the system dynamics and predict the best parameter set to apply for each user depending on its individual mobility behavior. Secondly, to overcome the scalability limitation of the Q-learning approach, we proposed a deep Q-learning framework based on an POMDP model. The simulation results shown the good performane of the DQL framework in terms of converged actions and rewards for both homogeneous and heterogeneous mobility scenarios. We also showed the online-learning feature of the framework which offers rapid adaptation to sudden changes in users mobility.

## 6.2 Future work

As a short-term planned work, we aim to consolidate our proposals by taking into account additional system performance objectives in the optimization problem such as energy efficiency. Hence, it is necessary to integrate a comprehensive power consumption model at the macro/pico-RRH sides including different components such as digital baseband (BB), power amplifier (PA) or analog RF [EAR].

Other system constraints such as fronthaul delay can also be integrated into problem formulation. Indeed, the fronthaul delay has an important role on the

estimation model of CSI as shown in Equation (4.4). Therefore, it would be interesting to evaluate and examine closely the impact of the fronthaul delay on the outdated CSI and on our feedback scheduling parameters in particular. Another direction of improvement might be to address the sum-rate degradation caused by large periods of CSI (T>=4).

Concerning the reinforcement learning part, the deep learning model can be still improved by choosing carefully some parameters such as the number of hidden layers, learning rate and mini-batch size in the algorithm. As well, the convergence time can be sped up by implementing the core WMMSE algorithm in another optimization tool such as CVXPY. To improve the detection time and response time of the online-learning in case of real-time environment changes, further studies are required.

Another interesting open issue is to consider the beamforming and user clustering problem in the context of Edge computing, e.g., Fog-RAN or MEC (Mobile Edge Computing). In that case, we take advantage of local computing and storage capabilities at edge base stations to avoid heavy communication overhead and large latency caused by backhaul/fronthaul transmission and centralized processing. It would be worth solving user association function in a centralized manner at the BBU side while the CSI-sensitive beamforming function closer to the users in a distributed manner at the edge RRH side. To solve these problems, we can also rely on DRL approaches.

Finally, it would be greatly interesting to pay attention to the Fog/Edge Computing-based IoT scenarios, in which several constraints and requirements specific to IoT applications should be considered such as network low data rate, low latency or resource-constrained devices.

## 6.3 Publications

This section sums up the results of our work that have been published in international conferences and journals.

**Journal:**

- *Under preparation:* Duc Thang Ha et al., "Optimized joint beamforming and user clustering under mobility and CSI imperfectness: a Deep Q-learning approach". To be submitted to IEEE Transactions on Vehicular Technology.

- Duc Thang Ha, Lila Boukhatem, Megumi Kaneko, Nhan Nguyen-Thanh, and Steven Martin. "Adaptive beamforming and user association in heterogeneous cloud radio access networks: A mobility-aware performance-cost trade-off". Elsevier Computer Networks, 160:130 – 143, Sep 2019.

**Conferences:**

- Duc Thang Ha, Lila Boukhatem, Megumi Kaneko and Steven Martin. "Performance-cost trade-off of joint beamforming and user clustering in cloud radio access networks." In 2017 IEEE 28th Annual International Symposiumon Personal, Indoor, and Mobile Radio Communications (PIMRC), pages 1–5, Oct 2017.

- Duc Thang Ha, Lila Boukhatem, Megumi Kaneko, and Steven Martin. "An advanced mobility-aware algorithm for joint beamforming and clustering in heterogeneous cloud radio access network." In Proceedings of the 21st ACM International Conference on Modeling, Analysis and Simulation of Wireless and Mobile Systems, MSWIM '18, pages 199–206, New York, NY, USA, 2018. ACM.

# Bibliography


[3GP14] 3GPP. Technical specification group services and system aspects, quality of service (QoS) concept and architecture (release 12). *Report TS 23.107, V12.0.0*, Sep 2014.

[AAD+16] B. Al-Oquibi, O. Amin, H. Dahrouj, T. Y. Al-Naffouri, and M. Alouini. Energy efficiency for cloud-radio access networks with imperfect channel state information. In *2016 IEEE 27th Annual International Symposium on Personal, Indoor, and Mobile Radio Communications (PIMRC)*, pages 1–5, Sep. 2016.

[AoCHC15] R. Al-obaidi, A. Checko, H. Holm, and H. Christiansen. Optimizing Cloud-RAN deployments in real-life scenarios using microwave radio. In *Networks and Communications (EuCNC), 2015 European Conference on*, pages 159–163, June 2015.

[ARN+17] M. Ali, Q. Rabbani, M. Naeem, S. Qaisar, and F. Qamar. Joint user association, power allocation, and throughput maximization in 5G H-CRAN networks. *IEEE Transactions on Vehicular Technology*, 66(10):9254–9262, Oct 2017.

[AWA11] Mohammad abdul AWAL. *Efficace utilisation des ressources de CQI Feedback pour les systèmes sans fil multi-utilisateur multi-porteuse*. Theses, Université Paris Sud - Paris XI, October 2011.

[BG06] M. Biguesh and A. B. Gershman. Training-based MIMO channel estimation: a study of estimator tradeoffs and optimal training signals. *IEEE Transactions on Signal Processing*, 54(3):884–893, March 2006.

[BLM+14] N. Bhushan, J. Li, D. Malladi, R. Gilmore, D. Brenner, A. Damnjanovic, R. T. Sukhavasi, C. Patel, and S. Geirhofer. Network densification: the dominant theme for wireless evolution into 5G. *IEEE Communications Magazine*, 52(2):82–89, February 2014.

[BMSP12] S. Barbera, P. H. Michaelsen, M. Säily, and K. Pedersen. Mobility performance of LTE co-channel deployment of macro and pico cells. In *2012 IEEE Wireless Communications and Networking Conference (WCNC)*, pages 2863–2868, April 2012.

[CCY+15] A. Checko, H. L. Christiansen, Y. Yan, L. Scolari, G. Kardaras, M. S. Berger, and L. Dittmann. Cloud RAN for mobile networks - a technology overview. *IEEE Communications Surveys Tutorials*, 17(1):405–426, 2015.

[CJL+14] L. Chen, H. Jin, H. Li, J. Seo, Q. Guo, and V. Leung. An energy efficient implementation of C-RAN in HetNet. In *2014 IEEE 80th Vehicular Technology Conference (VTC2014-Fall)*, pages 1–5, Sep. 2014.

[CRZK17] N. Chen, B. Rong, X. Zhang, and M. Kadoch. Scalable and flexible massive MIMO precoding for 5G H-CRAN. *IEEE Wireless Communications*, 24(1):46–52, February 2017.

[DDD+15] H. Dahrouj, A. Douik, O. Dhifallah, T. Y. Al-Naffouri, and M. S. Alouini. Resource allocation in heterogeneous cloud radio access networks: advances and challenges. *IEEE Wireless Communications*, 22(3):66–73, June 2015.

[DDR+15] H. Dahrouj, A. Douik, F. Rayal, T. Y. Al-Naffouri, and M. Alouini. Cost-effective hybrid RF/FSO backhaul solution for next generation wireless systems. *IEEE Wireless Communications*, 22(5):98–104, October 2015.

[DMW+11] A. Damnjanovic, J. Montojo, Y. Wei, T. Ji, T. Luo, M. Vajapeyam, T. Yoo, O. Song, and D. Malladi. A survey on 3GPP heterogeneous networks. *IEEE Wireless Communications*, 18(3):10–21, June 2011.

[DY14] B. Dai and W. Yu. Sparse beamforming and user-centric clustering for downlink cloud radio access network. *IEEE Access*, 2:1326–1339, 2014.

[DY15] B. Dai and W. Yu. Backhaul-aware multicell beamforming for downlink cloud radio access network. In *2015 IEEE International Conference on Communication Workshop (ICCW)*, pages 2689–2694, June 2015.

[DYTB11] H. Dahrouj, W. Yu, T. Tang, and S. Beaudin. Power spectrum optimization for interference mitigation via iterative function evaluation. In *2011 IEEE GLOBECOM Workshops (GC Wkshps)*, pages 162–166, Dec 2011.

[EAN11] NEC Corporation Alcatel Lucent Ericsson AB, Huawei Technologies and Nokia Siemens Networks. Common public radio interface CPRI; interface specification. *CPRI specification*, v5.0, Sep 2011.

[EAR] Earth project infso-ict-247733 earth deliverable d2.3.

[GB08] Michael Grant and Stephen Boyd. Graph implementations for nonsmooth convex programs. In V. Blondel, S. Boyd, and H. Kimura, editors, *Recent Advances in Learning and Control*, Lecture Notes in Control and Information Sciences, pages 95–110. Springer-Verlag Limited, 2008. `http://stanford.edu/~boyd/graph_dcp.html`.

[GB14] Michael Grant and Stephen Boyd. CVX: Matlab software for disciplined convex programming, version 2.1. `http://cvxr.com/cvx`, March 2014.

[GH17] Zeineb Guizani and Noureddine Hamdi. CRAN, H-CRAN, and F-RAN for 5G systems: Key capabilities and recent advances. *Int. Journal of Network Management*, 27, 2017.

[GJ15] A. Gupta and R. K. Jha. A survey of 5G network: Architecture and emerging technologies. *IEEE Access*, 3:1206–1232, 2015.

[HBK+19] Duc Thang Ha, Lila Boukhatem, Megumi Kaneko, Nhan Nguyen-Thanh, and Steven Martin. Adaptive beamforming and user association in heterogeneous cloud radio access networks: A mobility-aware performance-cost trade-off. *Computer Networks*, 160:130 – 143, 2019.

[HBKM18] Duc Thang Ha, Lila Boukhatem, Megumi Kaneko, and Steven Martin. An advanced mobility-aware algorithm for joint beamforming and clustering in heterogeneous cloud radio access network. In *Proceedings of the 21st ACM International Conference on Modeling, Analysis and Simulation of Wireless and Mobile Systems*, MSWIM '18, pages 199–206, New York, NY, USA, 2018. ACM.

[HHLC15] S. C. Hung, H. Hsu, S. Y. Lien, and K. C. Chen. Architecture harmonization between cloud radio access networks and fog networks. *IEEE Access*, 3:3019–3034, 2015.

[HS15] Matthew J. Hausknecht and Peter Stone. Deep recurrent Q-learning for partially observable MDPs. *CoRR*, abs/1507.06527, 2015.

[HYA13] K. Hosseini, W. Yu, and R. S. Adve. Cluster based coordinated beamforming and power allocation for MIMO heterogeneous networks. In *2013 13th Canadian Workshop on Information Theory*, pages 96–101, June 2013.

[HZY+17] Y. He, Z. Zhang, F. R. Yu, N. Zhao, H. Yin, V. C. M. Leung, and Y. Zhang. Deep-reinforcement-learning-based optimization for cache-enabled opportunistic interference alignment wireless networks. *IEEE Transactions on Vehicular Technology*, 66(11):10433–10445, Nov 2017.

[IHD+14] C. L. I, J. Huang, R. Duan, C. Cui, J. Jiang, and L. Li. Recent progress on C-RAN centralization and cloudification. *IEEE Access*, 2:1030–1039, 2014.

[LAL16] M. Y. Lyazidi, N. Aitsaadi, and R. Langar. Dynamic resource allocation for Cloud-RAN in LTE with real-time BBU/RRH assignment. In *2016 IEEE International Conference on Communications (ICC)*, pages 1–6, May 2016.

[LCWW12] J. Li, D. Chen, Y. Wang, and J. Wu. Performance evaluation of cloud-ran system with carrier frequency offset. In *2012 IEEE Globecom Workshops*, pages 222–226, Dec 2012.

[LGX12] D. López-Pérez, İ. Güvenç, and Xiaoli Chu. Mobility enhancements for heterogeneous networks through interference coordination. In

*2012 IEEE Wireless Communications and Networking Conference Workshops (WCNCW)*, pages 69–74, April 2012.

[LSDL07] Y. Li, A. C. K. Soong, Y. Du, and J. Lu. Beamforming with imperfect CSI. In *2007 IEEE Wireless Communications and Networking Conference*, pages 1156–1160, March 2007.

[LSZ+10] Y. Lin, L. Shao, Z. Zhu, Q. Wang, and R. K. Sabhikhi. Wireless network cloud: Architecture and system requirements. *IBM Journal of Research and Development*, 54(1):4:1–4:12, January 2010.

[MAA18] A. M. Mahmood, A. Al-Yasiri, and O. Y. K. Alani. A new processing approach for reducing computational complexity in Cloud-RAN mobile networks. *IEEE Access*, 6:6927–6946, 2018.

[MKGM+15] M. A. Marotta, N. Kaminski, I. Gomez-Miguelez, L. Z. Granville, J. Rochol, L. DaSilva, and C. B. Both. Resource sharing in heterogeneous cloud radio access networks. *IEEE Wireless Communications*, 22(3):74–82, June 2015.

[MKS+13] Volodymyr Mnih, Koray Kavukcuoglu, David Silver, Alex Graves, Ioannis Antonoglou, Daan Wierstra, and Martin A. Riedmiller. Playing Atari with deep reinforcement learning. *CoRR*, abs/1312.5602, 2013.

[MKS+15] Volodymyr Mnih, Koray Kavukcuoglu, David Silver, Andrei A. Rusu, Joel Veness, Marc G. Bellemare, Alex Graves, Martin Riedmiller, Andreas K. Fidjeland, Georg Ostrovski, Stig Petersen, Charles Beattie, Amir Sadik, Ioannis Antonoglou, Helen King, Dharshan Kumaran, Daan Wierstra, Shane Legg, and Demis Hassabis. Human-level control through deep reinforcement learning. *Nature*, 518(7540):529–533, February 2015.

[Mob11] China Mobile. C-RAN: the road towards green RAN. *White Paper, ver*, 2, 2011.

[MSKS12] D. S. Michalopoulos, H. A. Suraweera, G. K. Karagiannidis, and R. Schober. Amplify-and-forward relay selection with outdated channel estimates. *IEEE Transactions on Communications*, 60(5):1278–1290, May 2012.

[MZC+17] X. Mao, B. Zhang, Y. Chen, J. Yu, and Z. Han. Matching game based resource allocation for 5G H-CRAN networks with device-to-device communication. In *2017 IEEE 28th Annual International Symposium on Personal, Indoor, and Mobile Radio Communications (PIMRC)*, pages 1–6, Oct 2017.

[NGM15] Ltd. NGMN. Further study on critical C-RAN technologies. *Technical report, NGMN alliance*, 2015.

[OBB+14] A. Osseiran, F. Boccardi, V. Braun, K. Kusume, P. Marsch, M. Maternia, O. Queseth, M. Schellmann, H. Schotten, H. Taoka, H. Tullberg, M. A. Uusitalo, B. Timus, and M. Fallgren. Scenarios for 5G mobile and wireless communications: the vision of the METIS project. *IEEE Communications Magazine*, 52(5):26–35, May 2014.

[OCH15] Hao Yi Ong, Kevin Chavez, and Augustus Hong. Distributed deep Q-learning. *CoRR*, abs/1508.04186, 2015.

[PBS+12] F. Pantisano, M. Bennis, W. Saad, R. Verdone, and M. Latva-aho. On the dynamic formation of cooperative multipoint transmissions in small cell networks. In *2012 IEEE Globecom Workshops*, pages 1139–1144, Dec 2012.

[PCB15] S. Park, C. Chae, and S. Bahk. Large-scale antenna operation in heterogeneous cloud radio access networks: a partial centralization approach. *IEEE Wireless Communications*, 22(3):32–40, June 2015.

[PEW+18] C. Pan, M. Elkashlan, J. Wang, J. Yuan, and L. Hanzo. User-centric C-RAN architecture for ultra-dense 5G networks: Challenges and methodologies. *IEEE Communications Magazine*, 56(6):14–20, June 2018.

[PLJ+14] M. Peng, Y. Li, J. Jiang, J. Li, and C. Wang. Heterogeneous cloud radio access networks: a new perspective for enhancing spectral and energy efficiencies. *IEEE Wireless Communications*, 21(6):126–135, December 2014.

[PLW+11] M. Peng, Y. Liu, D. Wei, W. Wang, and H. Chen. Hierarchical cooperative relay based heterogeneous networks. *IEEE Wireless Communications*, 18(3):48–56, June 2011.

[PLZW15] M. Peng, Y. Li, Z. Zhao, and C. Wang. System architecture and key technologies for 5G heterogeneous cloud radio access networks. *IEEE Network*, 29(2):6–14, March 2015.

[PSL+16] M. Peng, Y. Sun, X. Li, Z. Mao, and C. Wang. Recent advances in cloud radio access networks: System architectures, key techniques, and open issues. *IEEE Communications Surveys Tutorials*, 18(3):2282–2308, thirdquarter 2016.

[PSSS13] S. H. Park, O. Simeone, O. Sahin, and S. Shamai. Joint precoding and multivariate backhaul compression for the downlink of cloud radio access networks. *IEEE Transactions on Signal Processing*, 61(22):5646–5658, Nov 2013.

[PXC+15] M. Peng, H. Xiang, Y. Cheng, S. Yan, and H. V. Poor. Inter-tier interference suppression in heterogeneous cloud radio access networks. *IEEE Access*, 3:2441–2455, 2015.

[PXH+15] M. Peng, X. Xie, Q. Hu, J. Zhang, and H. V. Poor. Contract-based interference coordination in heterogeneous cloud radio access networks. *IEEE Journal on Selected Areas in Communications*, 33(6):1140–1153, June 2015.

[PYP14] Mugen Peng, Shi Yan, and H. V. Poor. Ergodic capacity analysis of remote radio head associations in cloud radio access networks. *IEEE Wireless Communications Letters*, 3(4):365–368, Aug 2014.

[PYXP16] M. Peng, Y. Yu, H. Xiang, and H. V. Poor. Energy-efficient resource allocation optimization for multimedia heterogeneous cloud radio access networks. *IEEE Transactions on Multimedia*, 18(5):879–892, May 2016.

[RGIG15] M. M. U. Rahman, H. Ghauch, S. Imtiaz, and J. Gross. RRH clustering and transmit precoding for interference-limited 5G CRAN downlink. In *2015 IEEE Globecom Workshops (GC Wkshps)*, pages 1–7, Dec 2015.

[RHL13] Meisam Razaviyayn, Mingyi Hong, and Zhi-Quan Luo. A unified convergence analysis of block successive minimization methods for nonsmooth optimization. *SIAM Journal on Optimization*, 23(2):1126–1153, 2013.

[RL14] Xiongbin Rao and Vincent K. N. Lau. Interference alignment with partial CSI feedback in MIMO cellular networks. *CoRR*, abs/1403.3740, 2014.

[RMVT15] P. Rost, A. Maeder, M. C. Valenti, and S. Talarico. Computationally aware sum-rate optimal scheduling for centralized radio access networks. In *2015 IEEE Global Communications Conference (GLOBECOM)*, pages 1–6, Dec 2015.

[RPMD14] Milos Rovcanin, Eli De Poorter, Ingrid Moerman, and Piet Demeester. A reinforcement learning based solution for cognitive network cooperation between co-located, heterogeneous wireless sensor networks. *Ad Hoc Networks*, 17:98–113, 2014.

[RTV15] P. Rost, S. Talarico, and M. C. Valenti. The complexity–rate tradeoff of centralized radio access networks. *IEEE Transactions on Wireless Communications*, 14(11):6164–6176, Nov 2015.

[Sal16] T. Salman. Cloud RAN: Basics, advances and challenges,. *Wireless and Mobile Networking*, April 2016.

[SPM19] Y. Sun, M. Peng, and S. Mao. Deep reinforcement learning based mode selection and resource management for green fog radio access networks. *IEEE Internet of Things Journal*, pages 1–1, 2019.

[SRB+15] D. Sabella, P. Rost, A. Banchs, V. Savin, M. Consonni, M. Di Girolamo, M. Lalam, A. Maeder, and I. Berberana. Benefits and challenges of cloud technologies for 5G architecture. In *2015 IEEE 81st Vehicular Technology Conference (VTC Spring)*, pages 1–5, May 2015.

[SRLH11] Q. Shi, M. Razaviyayn, Z. Q. Luo, and C. He. An iteratively weighted MMSE approach to distributed sum-utility maximization for a MIMO interfering broadcast channel. *IEEE Transactions on Signal Processing*, 59(9):4331–4340, Sept 2011.

[SZL13] Yuanming Shi, Jun Zhang, and Khaled Ben Letaief. Group sparse beamforming for green Cloud-RAN. *CoRR*, abs/1310.0234, 2013.

[TBKM17] H. D. Thang, L. Boukhatem, M. Kaneko, and S. Martin. Performance-cost trade-off of joint beamforming and user clustering in cloud radio access networks. In *2017 IEEE 28th Annual International Symposium on Personal, Indoor, and Mobile Radio Communications (PIMRC)*, pages 1–5, Oct 2017.

[TBKNT19] Ha Duc Thang, Lila Boukhatem, Megumi Kaneko, and Nhan Nguyen-Thanh. Adaptive beamforming and user association in heterogeneous cloud radio access networks: a mobility-aware performance-cost trade-off. *Computer Networks*, 2019.

[TCP+15] T. Taleb, M. Corici, C. Parada, A. Jamakovic, S. Ruffino, G. Karagiannis, and T. Magedanz. EASE: EPC as a service to ease mobile core network deployment over cloud. *IEEE Network*, 29(2):78–88, March 2015.

[TVLC18] Le Pham Tuyen, Ngo Anh Vien, Md. Abu Layek, and Tae Choong Chung. Deep hierarchical reinforcement learning algorithm in partially observable markov decision processes. *CoRR*, abs/1805.04419, 2018.

[TZY17] F. Tian, P. Zhang, and Z. Yan. A survey on C-RAN security. *IEEE Access*, 5:13372–13386, 2017.

[VTR14] M. C. Valenti, S. Talarico, and P. Rost. The role of computational outage in dense cloud-based centralized radio access networks. In *2014 IEEE Global Communications Conference*, pages 1466–1472, Dec 2014.

[WZHW15] J. Wu, Z. Zhang, Y. Hong, and Y. Wen. Cloud radio access network (C-RAN): a primer. *IEEE Network*, 29(1):35–41, Jan 2015.

[XWT+17] Z. Xu, Y. Wang, J. Tang, J. Wang, and M. C. Gursoy. A deep reinforcement learning based framework for power-efficient resource allocation in cloud RANs. In *2017 IEEE International Conference on Communications (ICC)*, pages 1–6, May 2017.

[ZLP17] Pengfei Zhu, Xin Li, and Pascal Poupart. On improving deep reinforcement learning for POMDPs. *CoRR*, abs/1704.07978, 2017.

université PARIS-SACLAY
ÉCOLE DOCTORALE
Sciences et technologies de l'information et de la communication (STIC)

**Titre :** Allocation de ressources et association utilisateur/cellule optimisées pour les futurs réseaux denses

**Mots clés :** H-CRAN, formation de faisceau, association utilisateur à cellule, CSI imparfait, mobilité, apprentissage par renforcement

**Résumé :** Depuis plusieurs années, les opérateurs de téléphonie mobile sont confrontés à une croissance considérable du trafic de données mobiles. Dans un tel contexte, la technologie Cloud Radio Access Network (CRAN) qui intègre les solutions de Cloud Computing aux réseaux d'accès radio est considérée comme une nouvelle architecture pour les futures générations de réseaux 5G. L'approche CRAN permet une optimisation globale des fonctions de traitement en bande de base du signal et de la gestion des ressources radio pour l'ensemble des RRH et des utilisateurs.
Parallèlement, les réseaux hétérogènes (HetNets) ont été proposés pour augmenter efficacement la capacité et la couverture du réseau 5G tout en réduisant la consommation énergétique. En combinant les avantages du Cloud avec ceux des réseaux HetNets, le concept de réseaux H-CRAN (Heterogeneous Cloud Radio Access Networks) est né et est considéré comme l'une des architectures les plus prometteuses pour répondre aux exigences des futurs systèmes.
Plus particulièrement, nous abordons le problème important de l'optimisation jointe de l'association utilisateur-RRH et de la solution de beamforming sur la liaison descendante d'un système H-CRAN. Nous formulons un problème de maximisation du débit total du système sous des contraintes de mobilité et d'imperfection de CSI (Channel State Information). Notre principal défi consiste à concevoir une solution capable de maximiser le débit tout en permettant, contrairement aux autres solutions de référence, de réduire la complexité de calcul, et les coûts de signalisation et de feedback CSI dans divers environnements.
Notre étude commence par proposer un algorithme Hybride, qui active périodiquement des schémas de clustering dynamiques et statiques pour aboutir à un compromis satisfaisant entre optimalité et le coût en complexité et signalisation CSI et réassociation. L'originalité de l'algorithme Hybride réside aussi dans sa prise en compte de la dimension temporelle du processus d'allocation sur plusieurs trames successives plutôt que son optimalité (ou sous-optimalité) pour la seule trame d'ordonnancement courante. De plus, nous développons une analyse des coûts de l'algorithme en fonction de plusieurs critères afin de mieux appréhender le compromis entre les nombreux paramètres impliqués.
La deuxième contribution de la thèse s'intéresse au problème sous la perspective de la mobilité utilisateur. Deux variantes améliorées de l'algorithme Hybride sont proposées : ABUC (Adaptive Beamforming et User Clustering), une version adaptée à la mobilité des utilisateurs et aux variations du canal radio, et MABUC (Mobility-Aware Beamforming et User Clustering), une version améliorée qui règle dynamiquement les paramètres de feedback du CSI (périodicité et type de CSI) en fonction de la vitesse de l'utilisateur. L'algorithme MABUC offre de très bonnes performances en termes de débit cible tout en réduisant efficacement la complexité et les coûts de signalisation CSI.
Dans la dernière contribution de la thèse, nous approfondissons l'étude en explorant l'optimisation automatique des paramètres d'ordonnancement du CSI. Pour ce faire, nous exploitons l'outil de l'apprentissage par renforcement afin d'optimiser les paramètres de feedback CSI en fonction du profil de mobilité individuelle des utilisateurs. Plus spécifiquement, nous proposons deux modèles d'apprentissage. Le premier modèle basé sur un algorithme Q-learning a permis de démontrer l'efficacité de l'approche dans un scénario à taille réduite. Le second modèle, plus scalable car basé sur une approche Deep Q-learning, a été formulé sous la forme d'un processus de type POMDP (Partially observable Markov decision process). Les résultats montrent l'efficacité des solutions qui permettent de sélectionner les paramètres de feedback les plus adaptés à chaque profil de mobilité, même dans le cas complexe où chaque utilisateur possède un profil de mobilité différent et variable dans le temps.

**Title :** Optimized resource allocation and user/cell association for future dense networks

**Keywords :** H-CRAN, beamforming, user-to-cell association, imperfect CSI, mobility, reinforcement learning

**Abstract :** Recently, mobile operators have been challenged by a tremendous growth in mobile data traffic. In such a context, Cloud Radio Access Network (CRAN) has been considered as a novel architecture for future wireless networks. The radio frequency signals from geographically distributed antennas are collected by Remote Radio Heads (RRHs) and transmitted to the cloud-centralized Baseband Units (BBUs) pool through fronthaul links. This centralized architecture enables a global optimization of joint baseband signal processing and radio resource management functions for all RRHs and users.

At the same time, Heterogeneous Networks (HetNets) have emerged as another core feature for 5G network to enhance the capacity/coverage while saving energy consumption. Small cells deployment helps to shorten the wireless links to end-users and thereby improving the link quality in terms of spectrum efficiency (SE) as well as energy efficiency (EE). Therefore, combining both cloud computing and HetNet advantages results in the so-called Heterogeneous-Cloud Radio Access Networks (H-CRAN) which is regarded as one of the most promising network architectures to meet 5G and beyond system requirements.

In this context, we address the crucial issue of beamforming and user-to-RRH association (user clustering) in the downlink of H-CRANs. We formulate this problem as a sum-rate maximization problem under the assumption of mobility and CSI (Channel State Information) imperfectness. Our main challenge is to design a framework that can achieve sum-rate maximization while, unlike other traditional reference solutions, being able to alleviate the computational complexity, CSI feedback and reassociation signaling costs under various mobility environments. Such gain helps in reducing the control and feedback overhead and in turn improve the uplink throughput.

Our study begins by proposing a simple yet effective algorithm baptized Hybrid algorithm that periodically activates dynamic and static clustering schemes to balance between the optimality of the beamforming and association solutions while being aware of practical system constraints (complexity and signaling overhead). Hybrid algorithm considers time dimension of the allocation and scheduling process rather than its optimality (or suboptimality) for the sole current scheduling frame. Moreover, we provide a cost analysis of the algorithm in terms of several parameters to better comprehend the trade-off among the numerous dimensions involved in the allocation process.

The second key contribution of our thesis is to tackle the beamforming and clustering problem from a mobility perspective. Two enhanced variants of the Hybrid algorithm are proposed: ABUC (Adaptve Beamforming and User Clustering), a mobility-aware version that is fit to the distinctive features of channel variations, and MABUC (Mobility-Aware Beamforming and User Clustering), an advanced version of the algorithm that tunes dynamically the feedback scheduling parameters (CSI feedback type and periodicity) in accordance with individual user velocity. MABUC algorithm achieves a targeted sum-rate performance while supporting the complexity and CSI signaling costs to a minimum.

In our last contribution, we propose to go further in the optimization of the CSI feedback scheduling parameters. To do so, we take leverage of reinforcement learning (RL) tool to optimize on-the-fly the feedback scheduling parameters according to each user mobility profile. More specifically, we propose two RL models, one based on Q-learning and a second based on Deep Q-learning algorithm formulated as a POMDP (Partially observable Markov decision process). Simulation results show the effectiveness of our proposed framework, as it enables to select the best feedback parameters tailored to each user mobility profile, even in the difficult case where each user has a different mobility profile.

**Université Paris-Saclay**
Espace Technologique / Immeuble Discovery
Route de l'Orme aux Merisiers RD 128 / 91190 Saint-Aubin, France